

Hydrogeological Investigations at Diamond Y Springs and Surrounding Area,  
Pecos County, Texas

by

Radu Boghici, B.S.

Thesis

Presented to the Faculty of the Graduate School

of The University of Texas at Austin

in Partial Fulfillment

of the Requirements

for the Degree of

Master of Arts

The University of Texas at Austin

August, 1997

Hydrogeological Investigations at Diamond Y Springs and Surrounding Area,  
Pecos County, Texas

APPROVED BY

SUPERVISING COMMITTEE:

---

John M. Sharp, Jr.

---

Philip C. Bennett

---

Brenda Kirkland George

In memoriam:

David J. Disney (1955 - 1995)

## ACKNOWLEDGEMENTS

This work was supported by a grant from The Nature Conservancy of Texas. The Geology Foundation financed my first trip into the field.

I would like to thank Dr. Jack Sharp, my supervisor, for the opportunity to work on the Diamond Y project, and for his guidance during the phases of this investigation.

I give many thanks to Dr. Phil Bennett and Dr. Brenda Kirkland George, the others members of my committee, for taking the time to read and review this thesis. Dr. Bennett's suggestions greatly improved my understanding of the springs' chemistry. I am indebted to Dr. Lynton Land for analyzing my water samples for Oxygen-18 free of charge. John Karges is commended for his help during my visits to Fort Stockton. The springs' monitoring program could not have been implemented without his cooperation.

This research greatly benefited from in-depth discussions with Norm van Broekhoven, Robert Mace, Ian Jones, Barry Hibbs, and my wife, Erika. I am grateful to John Ashworth for his help during the initial stages of my research.

Finally, a big thanks to Erika and son Vlad for their moral support and willingness to deal with my moods during all this time.

May 1997

## ABSTRACT

Hydrogeological Investigations at Diamond Y Springs and Surrounding Area,

Pecos County, Texas

by

Radu Boghici, M.A.

The University of Texas at Austin, 1996

SUPERVISOR: John M. Sharp, Jr.

This study presents the results of local hydrogeologic investigations at Diamond Y Springs and vicinity, a 660 mi<sup>2</sup> (1710 km<sup>2</sup>) area of north-central Pecos County, Texas. The data confirm the hypothesis of Rustler aquifer waters as the chief source of flow at Diamond Y Springs today. Dissolution of halite and gypsum, base exchange, evaporation, and mixing of the two hydrochemical facies of the Rustler with recent local waters can explain the water chemistry and isotopic composition. The main controls on the regional flow pattern are: (1) the permeability contrast between the Belding-Coyanosa trough fill and the Edwards Formation, (2) the amount of cross-formational flow recharging the Edwards-Trinity (Plateau) aquifer through the Belding fault system, (3) the amount of recharge from the Rustler aquifer, and (4) the amount of groundwater pumped in the Belding-Fort Stockton and Coyanosa irrigation districts.

## TABLE OF CONTENTS

TABLE OF CONTENTS.....	vi
LIST OF FIGURES.....	ix
LIST OF TABLES.....	xi
1. INTRODUCTION.....	1
A. Statement of the Problem.....	1
B. Objectives of Study.....	1
C. General Nature of the Study Area.....	3
D. Previous Investigations.....	6
E. Climate.....	6
2. PHYSIOGRAPHY AND DRAINAGE.....	11
A. Physiography.....	11
B. Drainage.....	13
3. GEOLOGY.....	15
A. Stratigraphy.....	15
Upper Guadalupe Series.....	20
Ochoan Series.....	25
Triassic Rocks.....	30
Cretaceous Rocks.....	31
Quaternary.....	37

<b>B. Structural Geology.....</b>	<b>35</b>
<b>4. HYDROGEOLOGY.....</b>	<b>38</b>
<b>A. Capitan Limestone Aquifer.....</b>	<b>38</b>
<b>B. Rustler Aquifer.....</b>	<b>39</b>
<b>C. Edwards-Trinity (Plateau) Aquifer.....</b>	<b>41</b>
<b>D. Diamond Y Springs.....</b>	<b>49</b>
<b>5. GROUNDWATER CHEMISTRY AND ISOTOPY.....</b>	<b>61</b>
<b>A. Methods.....</b>	<b>61</b>
<b>B. Results and Interpretation.....</b>	<b>63</b>
<b>Chemical Processes Responsible for the</b>	
<b>Composition of Diamond Y Springs.....</b>	<b>67</b>
<b>C. Isotopic Analyses.....</b>	<b>71</b>
<b>D. Origin of Solutes.....</b>	<b>77</b>
<b>6. FLOW SYSTEM MODELING.....</b>	<b>87</b>
<b>A. Methods.....</b>	<b>87</b>
<b>Boundary and Initial Conditions.....</b>	<b>87</b>
<b>Finite-Difference Methods.....</b>	<b>88</b>

**B. Groundwater Flow Modeling in the**

**Diamond Y Springs Region..... 89**

**Model Setup..... 90**

**Calibration..... 97**

**Model Results and Discussion..... 99**

**Model Limitations.....105**

**7. CONCLUSIONS.....107**

**8. REFERENCES.....109**

**9. APPENDIX.....114**

**VITA.....120**

## LIST OF FIGURES

Figure 1. Location of study area.....	4
Figure 2. Surface drainage features in Pecos County.....	14
Figure 3. Strike-oriented geologic cross-section through Pecos County.....	16
Figure 4. Dip-oriented geologic cross-section through Pecos County.....	17
Figure 5. Generalized geologic map of Pecos County.....	18
Figure 6. Regional Permian structure.....	36
Figure 7. Generalized potentiometric map of Rustler aquifer.....	40
Figure 8. Piper plot showing Rustler water chemical composition.....	42
Figure 9. Map showing the areal extent and the basal structure of the Edwards-Trinity aquifer.....	43
Figure 10. Conceptual groundwater flow model for the Edwards-Trinity aquifer.....	47
Figure 11. Piper plot showing Edwards-Trinity aquifer water composition.....	48
Figure 12. Map showing Diamond Y springs and sampling locations.....	51
Figure 13. Diamond Y Springs system hydrograph, May 1990-July 1991.....	54
Figure 14. Piper plot showing Diamond Y springwater composition.....	55
Figure 15. Diamond Y Springs system conductivity, May-August 1990.....	56
Figure 16. Diamond Y Springs system pH, May-August 1990.....	58



## LIST OF TABLES

Table 1 Temperature and precipitation at Fort Stockton, 1859-1990.....	7
Table 2. Freeze dates in spring and fall at Fort Stockton.....	8
Table 3. The Permian-Quaternary hydrostratigraphy.....	19
Table 4. Results of tritium analyses.....	76
Table 5. Water balance over the whole model domain (steady-state calibration runs).....	99
Table 6. Pumping rates used in the transient flow simulations.....	101

## **1. INTRODUCTION**

### **A. Statement of the Problem**

Groundwater development in the Fort Stockton area, Pecos County led to lowering of potentiometric surface and to discharge cessation at several local springs, including the well-known Comanche Springs. Diamond Y Springs, which are the focus of this project, feed little ponds which are the host of a federally listed endangered species of fish (*Cyprinodon Bovinus*). Continued groundwater withdrawal in the area could result in flow decline at Diamond Y, thus threatening the protected species.

### **B. Objectives of Study**

A preliminary search for information regarding the hydrogeology of Fort Stockton area shows an abundance of data (water-level measurements, water quality analyses, pumping records), but a lack of previous interpretation. The objective of the study is to characterize of the hydrogeology of the Fort Stockton and surrounding areas using an integrated hydrochemical and numerical modeling approach. The study employs well-established hydrological, hydrochemical, and isotopic methods to delineate the boundaries of the regional and local groundwater systems, to trace local, intermediate, and regional

flowpaths, to describe the distribution of groundwater facies, and to account for groundwater origins. Basic data are used to develop a conceptual hydrologic model over the study region. A numerical groundwater flow model is developed and calibrated to estimate the amount of recharge, and hydraulic conductivity field. The results of the study should (1) advance our knowledge of the hydrogeologic controls on the spring-aquifer interactions in a complex carbonate-aquifer system, and (2) provide information needed for managing portions of the aquifer system.

As the study area undergoes residential, commercial, and industrial development, it is clear that understanding how aquifer parameters and pumping wells affect spring discharge will be more important in the allocation of water resources and drought contingency plans of the local water authority. The eventual goal is to obtain both a scientific and utilitarian understanding of this complex, dynamic stream-aquifer system. This research is a first step toward that realization.

### **C. General Nature of the Study Area**

The area encompassed by this study lies in central Pecos County, Texas (figure 1). The city of Fort Stockton is in the southern part of the study area, approximately 240 mi (405.6 km) east of El Paso, along Interstate Highway 10. The Diamond Y Springs are located on a 15 mi<sup>2</sup> (38.9 km<sup>2</sup>) nature preserve owned by the Nature Conservancy of Texas (TNCT), about 10 mi (16.1 km) north of Fort Stockton, Pecos County, Texas. The investigation, however, is not confined to the TNCT preserve area, but covers 660 mi<sup>2</sup> (1,710 km<sup>2</sup>) around Fort Stockton (roughly, about 12 USGS 7.5 minute topographic quadrangles).

Pecos County was created in 1871 from a part of Presidio County. It was named for the Pecos River, which borders the county to the north. The county is about 88 mi (142 km) from north to south, and about 108 mi (173.8 km) from east to west. It is the second largest county in Texas. Fort Stockton, the county seat, was established in 1845 and 9 years later a U.S. Army fort was established here. It served as refuge for travelers on the Old Spanish Trail. Perhaps the most important justification for a fort at this location was Comanche Springs, which flowed at about 60 million gallons of water per day (226,000 m<sup>3</sup>/day) in 1869 (Annie Riggs Museum Archives, Fort Stockton). However, largely because of

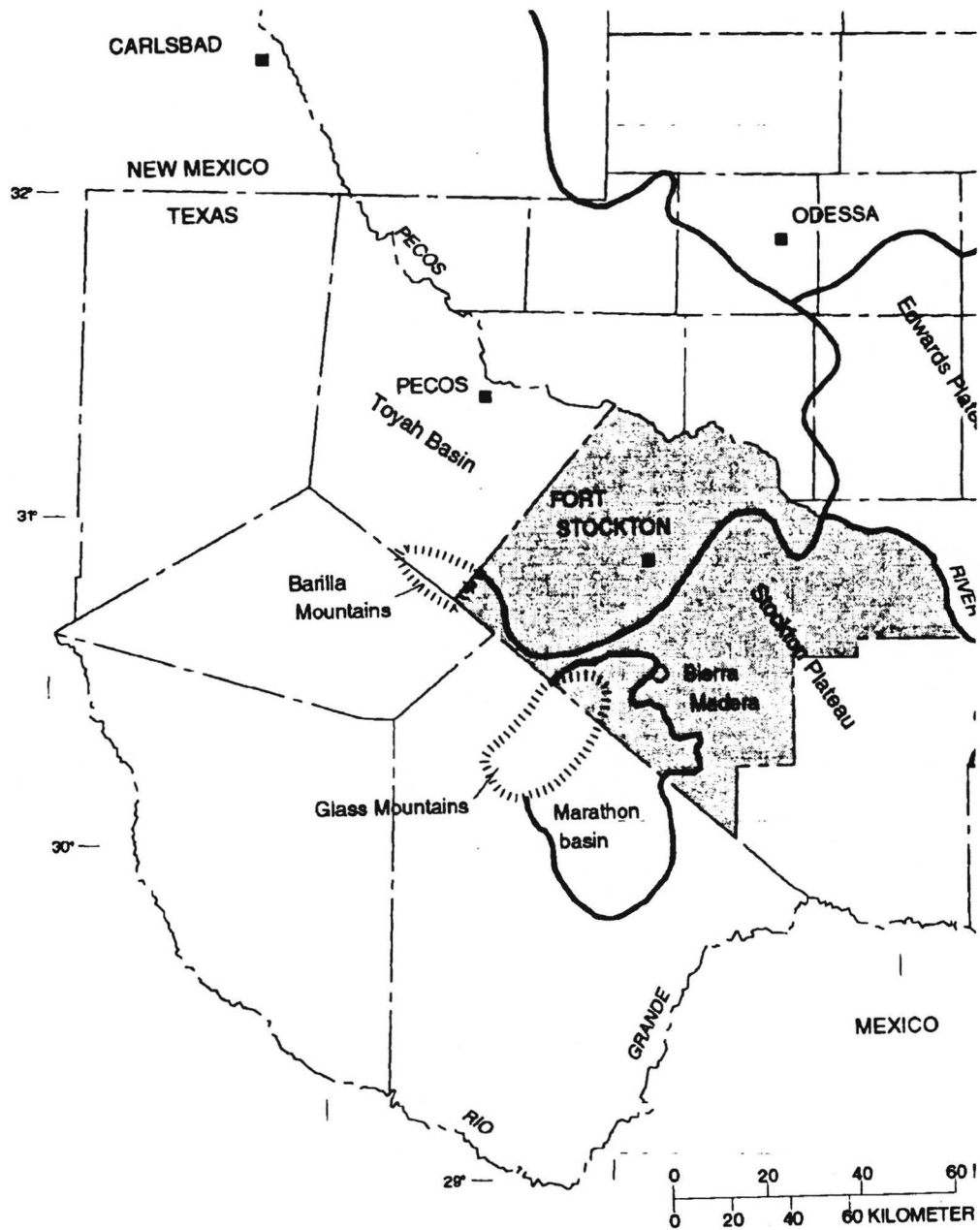


Figure 1. Location of study area

pumping of groundwater for irrigation, Comanche Springs ceased flowing in 1952. In 1990 the county had a population of 14,675, while Fort Stockton was inhabited by 9,518 people. Ranching and irrigated farming are the most important economic activities in the county. Based on the Conservation Needs Inventory (1967), 67,674 acres (274 km<sup>2</sup>) was irrigated cropland, 2,759,563 acres (11,168 km<sup>2</sup>) was rangeland, 1,920 acres (7.7 km<sup>2</sup>) was water, and 12,119 acres (49 km<sup>2</sup>) was urban areas. The irrigated area declined to 25,000 acres (101 km<sup>2</sup>) (USDA, 1976). The ranching stock in Pecos County consists of beef cattle and sheep, while cotton, grain sorghum, barley, alfalfa, cantaloupe, onions, peppers, pecans, and cabbage are the main cultivated crops. Petroleum production, sulphur mining, and the automotive testing grounds are also significant in the local economy.

#### **D. Previous Investigations**

Adkins (1927) reported discharge figures for Comanche Springs and water chemistry data for several wells and for Comanche Springs, but did not comment on Diamond Y springs. Armstrong and McMillion (1961) were the first to refer to Diamond Y springs; they provided some discharge and chemistry data. Audsley's (1956) investigation focused on the hydrogeology of the Fort Stockton area. Rees and Buckner (1980) investigated the Edwards-Trinity aquifer in the Trans-Pecos of Texas on a large scale. Brune (1975) presented some discharge data on Diamond Y and a history of the springs. Small and Ozuna (1993) published an assessment of the groundwater conditions for Pecos County. Finally, Veni (1991) centered his work exclusively on Diamond Y; he was the first to give a detailed account on the hydrogeology of these springs.

#### **E. Climate**

The climate of the study area is semi-arid and is characterized by hot summers and cool winters. Table 1 gives temperature and precipitation data recorded at Fort Stockton the period 1859 to 1990. Table 2 gives probable dates for the first freeze in fall and the last freeze in spring.

TABLE 1. TEMPERATURE AND PRECIPITATION <sup>1)</sup>

(Recorded in the period 1859-1990 at Fort Stockton, Texas)

MONTH	AVERAGE MONTHLY TEMPERATURES (°F)			AVERAGE MONTHLY PRECIPITATION (in)	
	High	Low	Mean	Rainfall	Snowfall
January	62.5	31.3	46.4	0.53	0.40
February	67.0	34.6	50.7	0.52	0.70
March	74.2	40.4	57.3	0.49	0.10
April	82.6	48.9	65.5	0.73	0.00
May	89.4	57.4	73.5	1.66	0.00
June	95.6	65.3	80.3	1.64	0.00
July	96.1	67.4	81.6	1.68	0.00
August	95.5	66.4	80.6	1.89	0.00
September	89.7	61.0	74.9	2.49	0.00
October	81.4	50.9	65.9	1.34	0.00
November	70.9	39.4	54.6	0.70	0.40
December	63.5	32.6	47.7	0.68	0.20

<sup>1)</sup>Data from the National Oceanic and Atmospheric Administration

TABLE 2 FREEZE DATES IN SPRING AND FALL <sup>1)</sup>

(Recorded in the period 1955-1975 at Fort Stockton, Texas)

PROBABILITY	TEMPERATURE		
	24° F or lower	28° F or lower	32° F or lower
Last freezing temperature in spring:			
1 year in 10 later than	March 27	April 8	April 13
2 years in 10 later than	March 18	April 1	April 8
5 years in 10 later than	March 2	March 18	March 29
First freezing temperature in the fall:			
1 year in 10 earlier than	November 10	November 2	October 26
2 years in 10 earlier than	November 17	November 7	November 1
5 years in 10 earlier than	November 30	November 17	November 11

<sup>1)</sup>After Rives (1980).

In winter the average temperature is 47 °F (8.3 °C), and the average daily minimum temperature is 32 °F (0 °C). The lowest temperature ever recorded in the study area was 4 °F (-15.5 °C) and occurred on January, 5, 1972. During summer the average temperature is 80 °F (26.7 °C), and the average daily maximum temperature is 94 °F (34.4 °C). The highest recorded temperature at Fort Stockton was 110 °F (43.3 °C) on June, 22, 1969.

The average annual precipitation in the study area is 12 in (305 mm). Of this, 8 in (203 mm) or 65 percent falls from April through September. The heaviest one-day rainfall during the period of record was 3.38 in (85.9 mm) at Fort Stockton on May, 27, 1957. An average of 40 days per year have thunderstorms. Most of them occur during summer. Snowfall in the Fort Stockton area is rare. About half the winters have no measurable snowfall. In 25 percent of the winters the snowfall measures more than 3 in (76.2 mm) and is largely a short-duration event. Also, it only takes two to three days for the accumulated snow to dissipate. The heaviest one-day snowfall was more than 4 in (101.6 mm).

The average relative humidity in midafternoon is about 40 percent, and increases later in the day. The average humidity at dawn is about 70 percent. The sun shines 80 percent of the time during summer and 75 percent of the time during winter. The dominant wind blows from the south-southeast, with a high speed of 13 mi/h (21 km/h) in April.

Evaporation has been monitored by the National Weather Service between 1940 and 1961 (Dougherty, 1975). The potential annual evaporation is about 109 in (2769 mm). The monthly evaporation ranges between

4 in (102 mm) in January and 12-14 in (305-356 mm) in summer when the crop demand for water is highest (Armstrong and McMillion, 1961).

The following chapters of the study describe the physiography and the drainage of the study area (chapter 2), and its general geology and structure (chapter 3). Chapter 4 familiarizes the reader with the hydrogeology of Pecos County and the Diamond Y Springs, while the next two chapters discuss the springs' hydrochemistry and isotopy (chapter 5), and the development of a groundwater flow model for the study area (chapter 6). Chapter 7 presents the conclusions of this research.

## **2. PHYSIOGRAPHY AND DRAINAGE**

The surface of Pecos County is nearly level to gently undulating in the northern half and hilly to mountainous in the southern half. A network of creeks occasionally transmits surface water to the Pecos River, county's main draining feature

### **A. Physiography**

The study area is in the Stockton Plateau (figure 1, p. 4), an extension of the Edwards Plateau of Central Texas. The Stockton Plateau is a plain of degradation (Adkins, 1927, p.13) where the formerly continuous limestone tablelands are being eroded. The altitude of the Plateau around Fort Stockton ranges between 2000 ft (600 m) and 3000 ft (900 m) above sea level. Relief of 200 to 300 ft (60 to 90 m) is common in the larger creeks.

In the northern part of the area the Stockton Plateau is completely eroded, exposing soft shales, red beds, and evaporites. The dominant features of this region are: a flat land surface, gravel fills, and steppes vegetation. The southern part of the study area is a stripped plain of Cretaceous limestone (Adkins, 1927), presently in a stage of immature dissection. It consists of a large number of flat-top hills or mesas, whose summits lie on the same stratigraphic

level so that the slope of the region is that of the rock beds, (i.e., towards E and NE). Surrounding the mesas are graded slopes and pediments. The mesas are the result of the selective erosion of about 600 ft (180 m) of soft shales and limestones. Three interspersed, more resistant limestone intervals (called "*caprocks*" by Adkins, 1927) control the local relief: the lower, middle, and upper Caprock. The lower Caprock (Upper Fredericksburg) is mostly buried under valley fill. The upper Caprock (Upper Washita) is commonly eroded, therefore the middle Caprock (Middle Washita) is dominant, and produces that "one-story" flat top profile, characteristic to the area.

Although not located within the study area, the Glass Mountains serve as potential recharge areas for the Edwards-Trinity aquifer in Pecos County. The Glass Mountains are in southern Pecos County and occupy there an area of about 75 mi<sup>2</sup> (28.9 km<sup>2</sup>). Their elevation ranges between 4,000 to 6,000 ft (1220 to 1824 m), and are made of intensely eroded and faulted limestone and dolomite. Deep creeks with thick deposits of boulders and gravel cut through the mountains.

## **B. Drainage**

The main drainage feature is Pecos River which receives surface water from a number of creeks (see figure 2). All the tributaries in Pecos County are ephemeral, the most important of which are: Coyanosa Draw, Courtney Creek, Leon Creek (which unites with the Diamond Y Draw in the study area), Sixshooter Draw, and Comanche Creek. In rare occasions these creeks flow directly to the Pecos River. Usually, the high evapotranspiration rate and the streambed configuration combine to limit runoff to Pecos River.

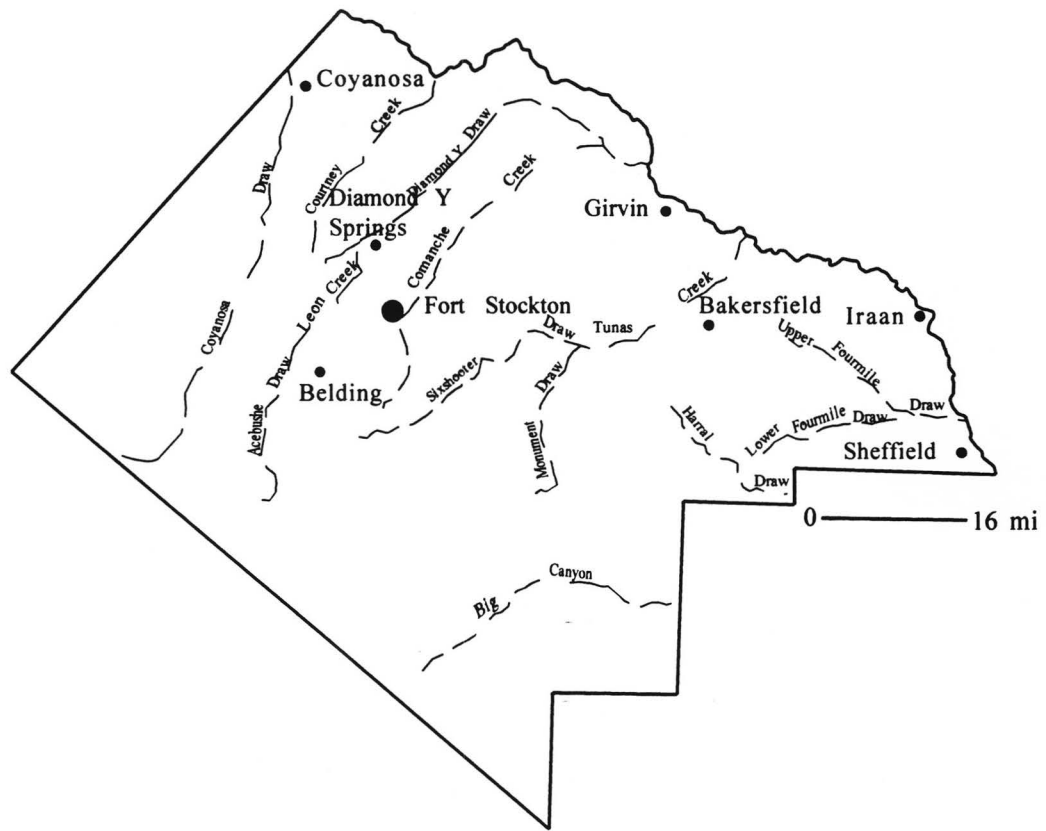


Figure 2. Surface drainage features over Pecos County

### **3. GEOLOGY**

This chapter presents the stratigraphy of the Permian and Cretaceous rocks under the study area, and discusses how regional structure controls the groundwater flow.

#### **A. Stratigraphy**

Several formations have an impact on the groundwater flow and chemistry in the study area. The Permian-Quaternary succession is summarized in table 3, and the spatial relationship between the stratigraphic members are shown in figures 3 and 4. The surface geology is shown in figure 5. Geologic units under the area of interest that contain ground water range in age from early Paleozoic to Holocene. Pre-Permian (Ordovician, Silurian, and Devonian) rocks yield water as a by-product of petroleum production activities. Head and chemistry data for these units are very limited.

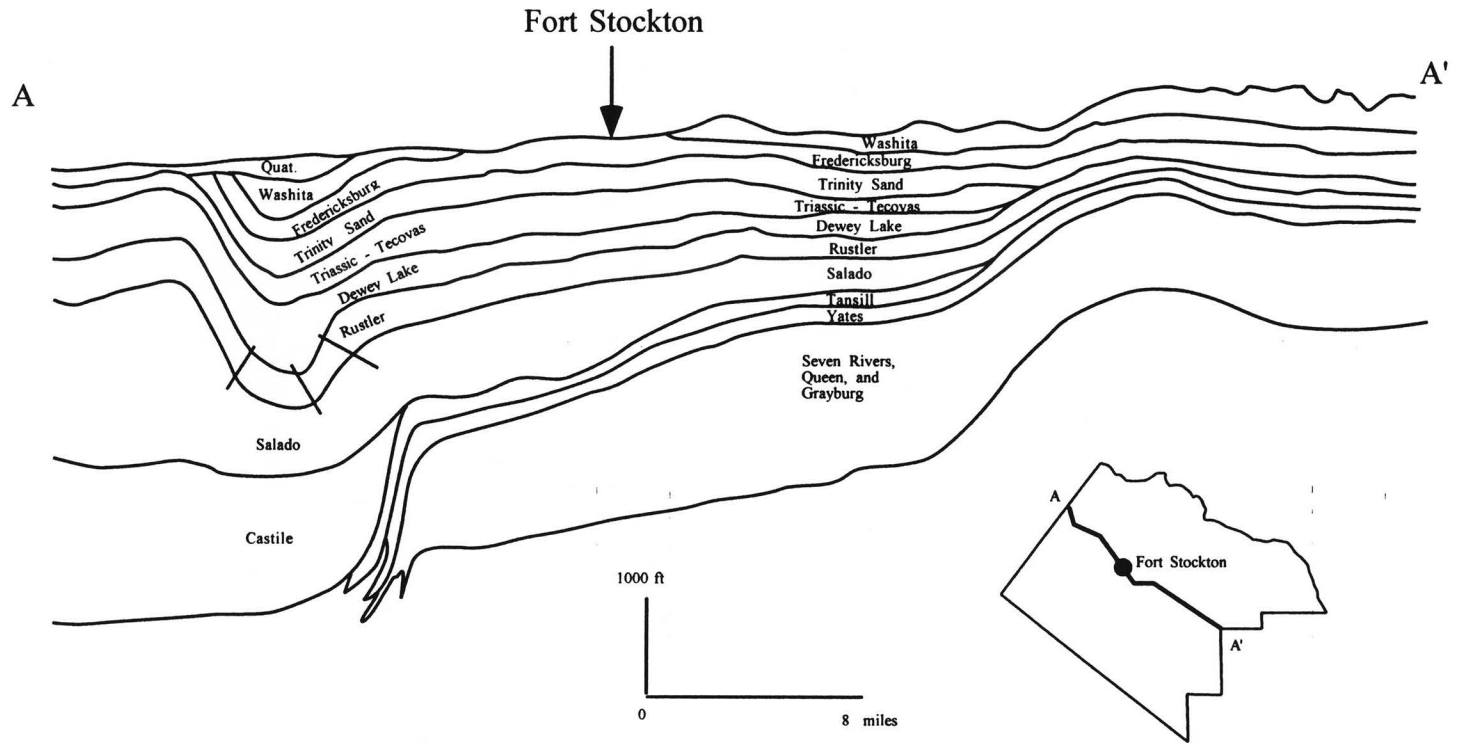


Figure 3. Strike - oriented geologic cross - section through Pecos County (Modified from WTGS, 1962)

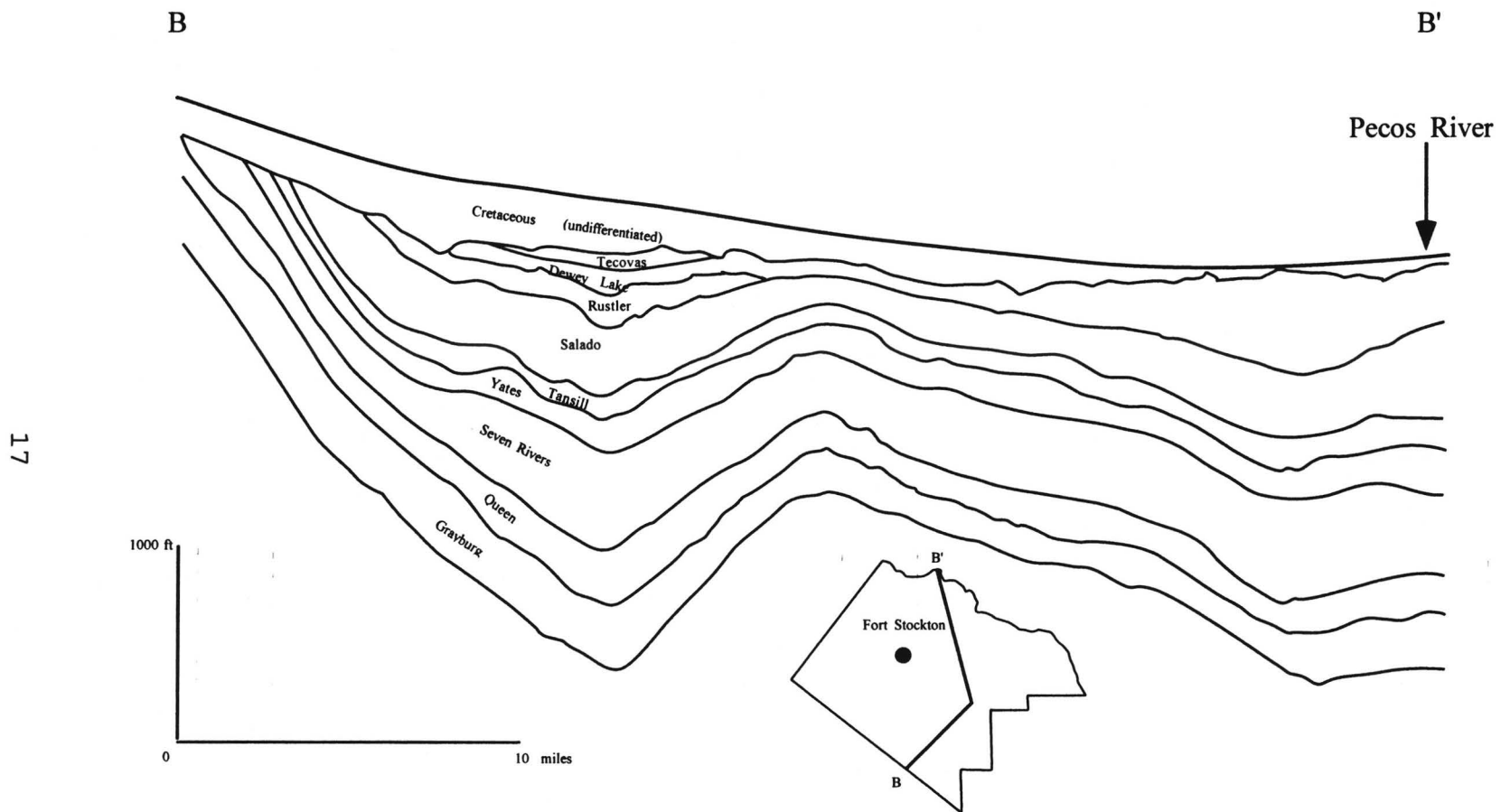


Figure 4. Dip - oriented geologic cross - section through Pecos County (modified after WTGS, 1951)



TABLE 3. STRATIGRAPHIC UNITS AND THEIR WATER-YIELDING PROPERTIES<sup>1)</sup>

SYSTEM	SERIES OR GROUP	UNIT	LITHOLOGY	WATER-YIELDING PROPERTIES	AQUIFER
Quaternary and Tertiary		Alluvium	Unconsolidated silt, sand, gravel, clay, caliche, gypsum	Small to large yield of fresh to brackish water	Cenozoic Alluvium
Cretaceous	Washita Group	Buda Limestone <i>"upper caprock"</i>	Soft nodular limestone, marl, hard limestone	Not known to yield water	Edwards-Trinity
		Boracho Formation <i>"middle caprock"</i>	Hard, massive limestone and thin-bedded limestone with some clay	Yields small quantities of water.	
		University Mesa Marl	Soft, nodular limestone, marl, and hard limestone.	Small yield of brackish water	
	Fredericksburg Group	Finlay Formation <i>"lower caprock"</i>	Massive, ledge-forming limestone and soft, nodular limestone	Yields small to moderate quantities of fresh to brackish water	
	Trinity Group	Maxon Sandstone	Fine- to coarse-grained quartz sand with silt, and limestone	Small to moderate yield of fresh to brackish water	
		Glen Rose Formation	White, marly limestone, yellow marl	Small yield of water	

Triassic	Dockum Group	Santa Rosa	Reddish arkosic, sandstone	Small to moderate yield brackish water	Santa Rosa
		Tecovas	Red shale, silt and sandstone	Not known to yield water	
Permian	Ochoan Series	Dewey Lake Redbeds	Sand, shale, gypsum, and anhydrite	Not known to yield water	
		Rustler Formation	Dolomite, anhydrite, halite, shale, sandstone, and limestone	Small to large yield of fresh to saline water	Rustler
		Salado Formation	Halite, anhydrite, and dolomite	Not known to yield water	
		Castile Formation	Calcareous anhydrite, halite, and limestone	Not known to yield water	
	Guadalupe Series	Upper Guadalupe, undivided	Dolomite, limestone, shale	Small to moderate yield of brackish water	
		Capitan Limestone	Dolomite, limestone, anhydrite, and sandstone	Moderate to large yield of brackish water	Capitan Limestone

<sup>1)</sup> Compiled from Armstrong and McMillion (1961) and Small and Ozuna (1993).

## UPPER GUADALUPE SERIES

### Capitan Limestone

The Capitan Limestone is a sequence of carbonate rocks deposited as a reef and a reef talus. It can be as thick as 1800 ft (549 m) and consists of massive dolomitic limestone, alternating with siliceous shales, and thin-bedded limestones. The Capitan is an arcuate belt of rocks paralleling the east side of the

Delaware Basin. Adams and Frenzel (1950) estimated the width of the reef at no more than 5 mi (8 km). In the northern part of Pecos County the depth to the Capitan is greater than 4000 ft (1219 m), while towards southwest its equivalent, the Gilliam limestone, crops out in the Glass Mountains. Towards the east the Capitan is continued into the Whitehorse Group, and in the Delaware Basin it is interfingering with the upper segment of the Delaware Mountain Group (Armstrong and McMillion, 1961)

### **Whitehorse Group**

The Whitehorse Group consists of five formations: the Grayburg Formation, Queen Formation, Seven Rivers Formation, Yates Sandstone, and Tansill Formation. These are back-reef time equivalents of the Capitan Limestone.

### **Grayburg Formation**

The Grayburg Formation is the basal sequence of the Whitehorse Group. Under the study area the Grayburg is about 350 ft (107 m) thick, and consists of dolomite, sandy dolomite, and limestone with sandstone intercalations (Armstrong and McMillion, 1961). The top of the formation is sometimes

marked by a brown limestone layer. Anhydrite may be present, and is common near Bakersfield (figure 5). The depth to the Grayburg Formation ranges between 1300 to 2800 ft (396 to 853 m) (Armstrong and McMillion, 1961).

### **Queen Formation**

The Queen Formation overlies the Grayburg Formation, and both display similar lithologies: dolomite interbedded with red and grey sandstone and anhydrite. The Queen usually contains more anhydrite than its neighbour below and is known to be about 400 ft (122 m) thick (Armstrong and McMillion, 1961).

### **Seven Rivers Formation**

The Seven Rivers Formation is present throughout the Delaware Basin and adjacent Northwestern Shelf and Central Basin Platform (Page and Adams, 1940; King, 1942; Tait and others, 1962; Hills, 1972). It ranges from approximately 800 ft (244 m) thick in the Midland Basin to 370 ft (113 m) or less on the Central Basin Platform.

The Seven Rivers Formation exhibits regional lithologic variations. The Seven Rivers is up to two thirds halite within the northeastern Delaware Basin. On the Central Basin Platform, it is mainly anhydrite and gypsum (King, 1942),

which were deposited in a restricted back-reef area of the Capitan complex. In the reef area and at the southern edge of the Central Basin Platform, the unit is primarily dolomite (Mear and Yarbrough, 1961; Hills, 1972). The formation is described by McNeal and Hemenway (1972) as tan, brown, and gray fractured, microcrystalline dolomite layered with thin beds of gray, shaly siltstone, dark brown to black shale, and streaks of white to gray, finely crystalline gypsum.

### **Yates Formation**

Conformably overlying the Seven Rivers Formation, the Yates, occurs throughout the eastern Delaware Basin and on the Central Basin Platform (Page and Adams, 1940; Tait and others, 1962). The formation was originally described as the Yates Sandstone, an 80- (24 m) to 125-ft (38 m)-thick sandstone bed in the Yates oil field of Pecos County (Gester and Hawley, 1929). However, this bed does not everywhere include all strata between the Seven Rivers and Tansill Formations. Mear and Yarbrough (1961) formally proposed that the Yates Formation be expanded to include the entire interval.

The Yates is thickest (340 ft [104 m]) near the western edge of of the Central Basin Platform in Ward County, and thinnest (80 ft [24 m]) at the southeastern edge of the platform, in northeastern Pecos County. The Yates Formation displays a marked lithologic heterogeneity. For instance, within the

inner shelf, the Yates is primarily fine red sandstone with minor shale, anhydrite, and halite interbeds; however, the southern edge of the platform the formation contains mostly dolomite and subordinate amounts of sandstone and anhydrite/gypsum.

### **Tansill Formation**

This uppermost formation of the Guadalupian Series in West Texas was deposited throughout the study area. The Tansill rests conformably on the underlying Yates Formation (Page and Adams, 1940). Within the Delaware Basin the Tansill is typically 100 to 150 ft (30.5 to 45.5 m) thick and it grades into the massive reef facies of the Capitan limestone (DeFord and Riggs, 1941). Although "Tansill" has been used in subsurface terminology since the 1920's, DeFord and Riggs (1941) formally defined the unit and provided a description of the type section located near Carlsbad, New Mexico.

In the Delaware Basin, the Tansill Formation contains varying amounts of anhydrite/gypsum, dolomite, halite, and sandstone (Page and Adams, 1940). On the western edge of the Platform, underlying the Diamond Y area of interest, the Tansill is gray to brown microcrystalline dolomite with anhydrite inclusions. Eastward, away from the reef, the formation becomes progressively more anhydritic (Mear and Yarbrough, 1961).

## **OCHOAN SERIES**

Ochoan strata are represented by four formations (in ascending sequence): Castile, Salado, and Rustler Formations and Dewey Lake Redbeds.

### **Castile Formation**

The Castile was named by Richardson (1904) from exposures at Castile Springs in northern Culberson County, Texas. As mapped by Dietrich and others (1983), the Castile Formation in Texas forms a broad, east-dipping, north to south outcrop belt (Gypsum Plain) extending from the Apache Mountains in the south to the Texas-New Mexico border north of Culberson County, Texas. The overlying Salado Formation is exposed in the eastern part of this outcrop belt, but because of the pervasive hydration of anhydrite and dissolution of gypsum and halite in the near-surface zone, the two formations cannot be easily differentiated. The Castile Formation, 1000 to 2100 ft (305 to 640 m) thick, extends throughout the Delaware basin (King, 1942; Bachman, 1984). In the eastern part of the basin, the formation thins to a few feet of basal strata, grading laterally into uppermost Capitan reef carbonates, deposited along the Central Basin Platform (Hills, 1972). The Castile Formation is composed of rhythmically interlaminated salts of different solubilities (mostly calcite-

anhydrite, but also anhydrite-halite interlaminae) and beds of anhydrite/gypsum, halite, limestone, and minor amounts of very fine terrigenous clastics. The Castile is easily identifiable by its distinctive alternating laminae of calcite and anhydrite. In core, individual lamina pairs have been correlated as far as 70 mi (113 km) across the basin and are interpreted to represent nonglacial varves (Snider, 1966; Anderson and others, 1972). Other rock types are also present in the Castile Formation. Halite beds, the principal large-scale marker beds of the formation are present only in the northern and the eastern parts of the Delaware Basin.

### **Salado Formation**

The Salado Formation crops out in the eastern part of the Gypsum Plain. King (1942) and Adams (1944) suggest that although some Salado rocks are exposed, most of the formation is truncated by an angular unconformity at the base of the overlying Rustler Formation. They noted that the Salado thickens downdip to the east. Kroenlein (1939) suggested that the present westernmost extent of the formation approximates its original depositional limits. Lang (1935) originally defined the formation and named it after Salado Wash in northern Loving County, Texas.

Ranging from 380 to 700 ft (91.5 to 213.5 m) thick, the Salado

Formation was deposited both in the Delaware Basin and on bordering shelf areas. King (1942) estimated the formation's minimum original thickness to be up to 1000 ft (305 m) near the basin margins, and as thick as 2000 ft (609.5 m) in the east-central part of the Delaware Basin. Snider (1966) noted a maximum thickness of 2530 ft (716.5 m) in the eastern part of this basin. Progressive eastward (from outcrop) dissolution of thick Salado halite beds and truncation of the upper Salado Formation in the western and west-central parts of the Delaware Basin probably account for most regional thickness variations (Anderson *et al.*, 1978).

The Salado Formation is a more diverse assemblage of rock types than is the Castile. In the study area, the Salado Formation is predominantly halite with lesser amounts of anhydrite, dolomite, sandstone, and siltstone. Locally in the northern part of the Delaware Basin, potash salts, such as polyhalite occur (Adams, 1944). Terrigenous clastics occur mostly in the lower part of the formation. The greatest differences between the Salado and Castile Formations in west-central Delaware Basin are (1) absence in the Salado of thick intervals of interlaminated calcite and anhydrite, (2) occurrence in the Salado of dolomite, and (3) greater abundance of terrigenous clastics in the Salado (Hentz *et al.*, 1989).

### **Rustler Formation**

The Rustler Hills and the adjacent plains to the east of Culberson and western Reeves Counties compose the outcrop belt of the east-dipping Rustler Formation (Dietrich et al., 1983). The north-to-south-trending outcrop belt ranges from 5 to 12 mi (8 to 19.5 km) wide and extends from the Apache Mountains in the south to southeastern New Mexico in the north.

The Rustler Formation (Richardson, 1904) is the youngest unit of the Ochoan Series that contains bedded evaporites. The Rustler ranges from 250 to 670 ft (76 to 204 m) thick, and is distributed throughout the Delaware Basin and adjacent shelf areas (King, 1942). The Rustler thickens to the south (Snider, 1966). Where the lower part of the Rustler Formation crops out in the Rustler Hills, it is composed of dolomite, dolomitic limestone, limestone breccia, gypsum, and mudstone with minor siltstone and sandstone near the base (Hall, 1952; Tunnell, 1952). The complete Rustler section, preserved in the subsurface, can be divided into an upper 150- to 175-ft (45.5 m to 53.5 m) unit of anhydrite/gypsum and a lower dolomite, anhydrite, sandstone, and shale unit (Adams, 1944). In the eastern part of the basin, dolomite decreases in abundance. Halite replaces some anhydrite in the upper and lower divisions at the northeastern edge of the basin.

Dissolution of anhydrite/gypsum-bearing members and concurrent collapse of overlying beds produced brecciated strata that disrupted the Rustler succession. An average of up to 30 percent of the original thickness has been lost through dissolution (Hentz et al., 1989).

### **Dewey Lake Redbeds**

This formation lies conformably atop the Rustler (Page and Adams, 1940; Tait et al., 1962), but is exposed in only a few isolated areas between the Rustler Hills and the western limit of Quaternary surficial deposits that cover most of Reeves County. Eifler (1976) and Dietrich (1983) mapped a few outcrops of the Dewey Lake in the westernmost Reeves County and along the Pecos River to the north. Page and Adams (1940) first described the unit from a subsurface section located near Dewey Lake, an alkali lake in northern Glasscock County, Texas.

The Dewey Lake Redbeds are at the top of the Permian section throughout the Delaware Basin. The overlying Upper Triassic Dockum Group rests unconformably on the Dewey Lake in some areas, but elsewhere the contact is gradational, suggesting that Lower and Middle Triassic deposits are included in the Dewey Lake (McGowen et al., 1979). The Dewey Lake is thickest in

structurally low areas along the eastern and southern edges of the Delaware Basin (Adams, 1944), and thins towards the west. Bachman (1984) noted that the formation attains a maximum thickness of 560 ft (170.7 m) in the north-central part of the basin. The Dewey Lake Redbeds are a homogenous reddish-brown mudstone and siltstone that commonly display gray reduction spots (Eager, 1983). Minor gypsum is locally present as cement, secondary crystals and vein fills.

### **TRIASSIC ROCKS**

The Triassic of Delaware Basin was described by Cummins (1890) as Dockum Beds from the type locality at Dockum in western Dickens County. Adkins (1927) partitions the Dockum strata into two members: a lower one (known as the Tecovas Formation) and an upper one (the Santa Rosa Sandstone). The total thickness of the Triassic in Pecos County ranges between 0 and 1550 ft (0 and 472.4 m) (Armstrong and McMillion, 1961).

The Tecovas Formation is a fine-grained clastic sequence composed of red shale, silt, and sandstone. The Tecovas underlies much of the western part of Pecos County. Its eastern boundary is roughly described by a north-south-trending line, passing between Grandfalls and Fort Stockton. The Santa Rosa Sandstone overlies the Tecovas Formation. The Santa Rosa is a reddish-brown, arkosic, micaceous, and conglomeratic sandstone.

Armstrong and McMillion (1961) add a third, uppermost member to the Dockum succession which they consider as "the exact equivalent of the Chinle Formation of the Colorado Plateau region". It is constituted of fine-grained clastic deposits, and locally overlays the Santa Rosa Sandstone.

## **CRETACEOUS ROCKS**

The Cretaceous in the study area is represented by clastic and carbonatic rocks of the Trinity, Fredericksburg, Washita, and Terlingua Groups.

### **Trinity Group**

The Trinity is divided into the Glen Rose Formation and the Maxon Sandstone.

#### **Glen Rose Formation**

The Glen Rose is composed primarily of thin-bedded, marly, white limestone ledges and yellowish-brown, partly sandy soft marl. It overlaps Permian strata, and it is 200 to 400 ft (61 to 122 m) thick.

#### **Maxon Sandstone**

This sequence is also known as the "Trinity Sand", which is a widely used term by well drillers, geologists, and most well owners in Pecos County. Armstrong and McMillion (1961) include the Maxon in the "Trinity Sand"

together with the "Basement Sands" (King, 1930) and with the "Basal Cretaceous Sandstone" (Adkins, 1927).

The Maxon Sandstone is a fine-grained, brown or yellowish-brown sandstone and sand with limestone fragments. A conglomerate layer about 8 in (20.5 cm) thick crops out at the base of the Maxon 30 mi (48.5 km) south of Fort Stockton (Armstrong and McMillion, 1961). The Maxon sandy member is present throughout Pecos County, and the total thickness of the formation averages 90 ft (27.5 m).

### **Fredericksburg Group**

The Fredericksburg Group is represented in the study area by the carbonatic Finlay Formation.

### **Finlay Formation**

The Finlay Formation consists of massive, coarse-grained limestone and sandstone about 40 ft (13 m) thick. In the vicinity of Glass Mountains, the Finlay is truncated, and that area the overlying Washita Group rests directly atop of Maxon.

### **Washita Group**

In Pecos County the Washita Group is divided into three members: the University Mesa Marl, Boracho Formation, and Buda Limestone. Rocks of the Washita Group crop out extensively throughout northern and eastern Pecos County, forming the typical mesa relief in the area.

#### **University Mesa Marl**

The University Mesa Marl is about 200 ft (60 m) thick and consists of soft, nodular limestone, marl, and hard massive-ledge forming limestone (Small and Ozuna, 1993).

#### **Boracho Formation**

The Boracho Formation, about 150 to 200 ft (45 to 50 m) thick, conformably overlies the University Mesa Marl in Pecos County. It consists of hard massive limestone, thin-bedded limestone and soft, nodular limestone with some clay.

#### **Buda Formation**

Buda Formation totals about 140 ft (40 m), and is represented by very hard, thin to thick bedded limestone in its upper third, a middle argillaceous thin to thick bedded sequence, and a bioclastic, coquinoid interval.

## **Terlingua Group**

### **Boquillas Limestone and Gulfian Rocks, Undivided**

The lowest unit of the Upper Cretaceous is the Boquillas Limestone which consists of limestone, marl and shale, flaggy, light gray, grayish-orange in colour. Armstrong and McMillion (1961) report a 250-ft (76 m) thickness for this interval. The uppermost Cretaceous rocks in the study area are approximately 300 ft (91.5 m) of marl, shale, and argillaceous limestone. Barnes (1983) suggests a possible correlation with units of Central Texas: Taylor, Austin, and upper part of Eagle Ford.

## **QUATERNARY**

### **Cenozoic Alluvium**

The Cenozoic alluvium consists of unconsolidated gravel, sand, silt, clay, and caliche. Its thickness varies from 10 ft (3.5 m) in the creeks near Glass Mountains, to more than 1000 ft (350 m) in the Coyanosa area, where the alluvium fills a deep trough (Armstrong and McMillion, 1961).

## **B. Structural Geology**

The most prominent structural features under the Pecos region are the Delaware Basin and the Central Basin Platform (figure 6). The Diamond Y area lies on the eastern edge of the Delaware Basin, at the hinge with the Central Basin Platform.

Armstrong and McMillion (1961) noted that the structure of the Cretaceous rocks in Pecos County closely reflects the structure of the older beds. Generally, Cretaceous rocks dip away from the center of the Marathon thrust belt at a rate of 5 to 10 ft / mile (1 to 2 m / km). North and northeast of the Glass Mountains rocks dip towards the northeast, whereas east of the Glass Mountains they dip eastward. In the Diamond Y area the Cretaceous beds dip to the north at a rate of about 30 ft / mile (18.5 m / km), and strike roughly east-west (Veni, 1991).

Dissolution of Ochoan evaporites by Cretaceous seawater caused the Permian beds to collapse and form a deep north-south trough located 2-3 mi (3.5-5 km) west of Fort Stockton (figure 5). Cretaceous, Tertiary, and Quaternary rock and sediments gradually filled the trough, and underwent subsidence, faulting and folding. The troughward tilt of the basal Cretaceous beds indicates that the trough was deepened by post-Cretaceous movements.

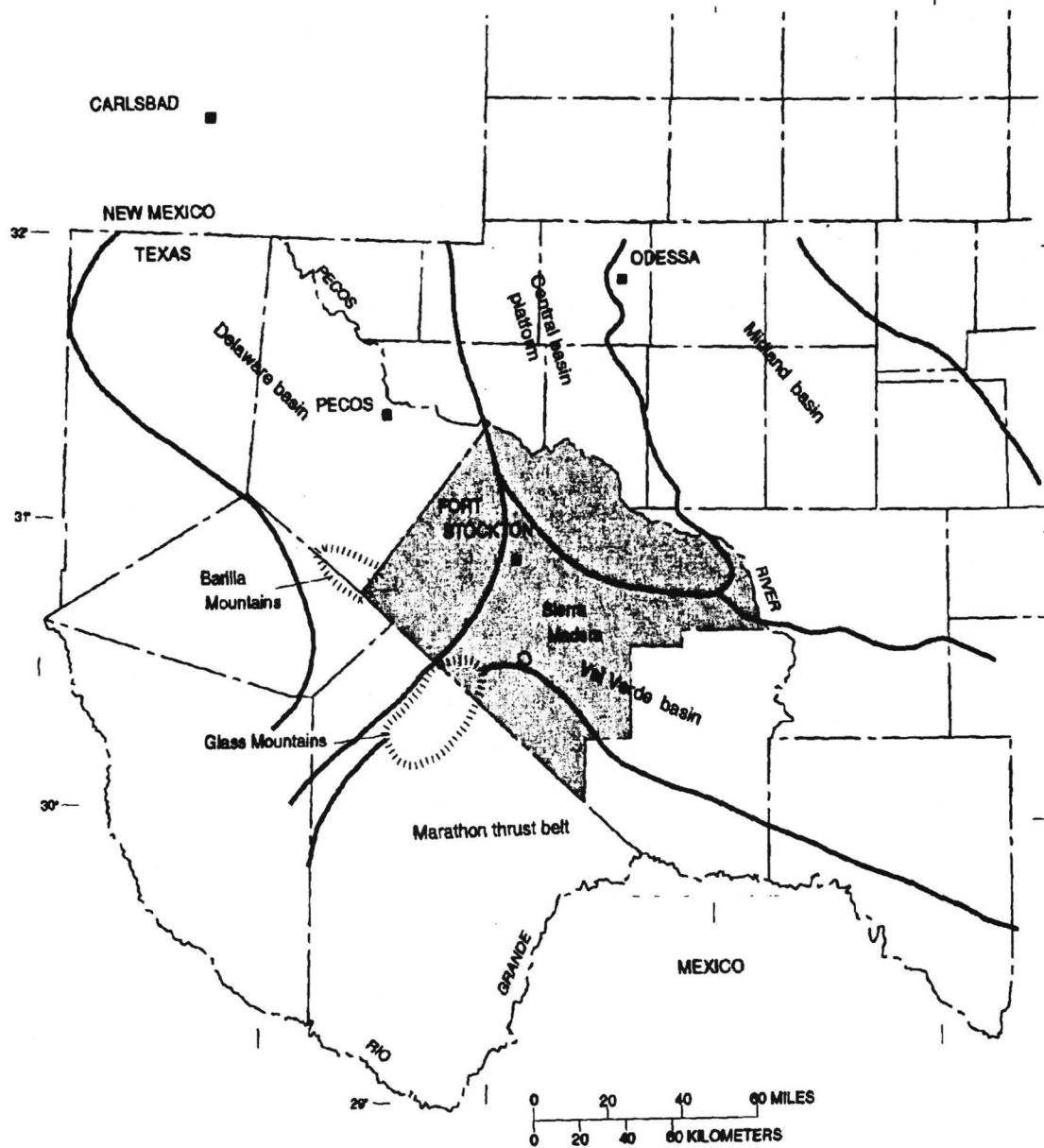


Figure 6. Regional Permian structure (after Small and Ozuna, 1993)

Armstrong and McMillion, (1961). state the relatively undisturbed conditions suggest that post-Cretaceous folding is not related to earlier tectonic events. They report post-Cretaceous faulting and describe the Belding fault system (figure 5) located 14 miles (23.5 km) southwest of Fort Stockton. No studies have discussed the region's fracture patterns but, according to Veni (1991), joints and other faults in the study area have a primary N20-30E orientation and a secondary east-west trend. In addition, the interpretation of two seismic sections shot in the Diamond Y area suggests at least two other fault systems. They are located right under the Diamond Y Springs Preserve (figure 5) and affect both Permian and Cretaceous strata.

## **4. HYDROGEOLOGY**

The main aquifers in the study area are: Capitan Limestone, Rustler, and Edwards-Trinity (Plateau). Several pre-Permian formations yield water as a by-product of oil and gas exploitation activities. They are not discussed here.

### **A. Capitan Limestone Aquifer**

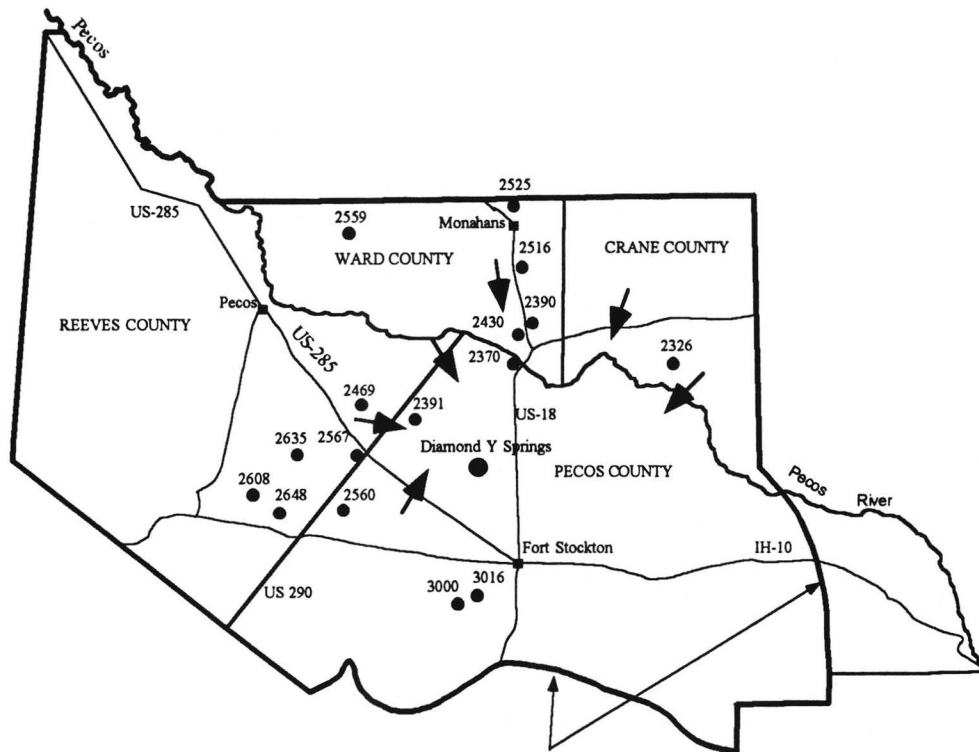
The confined Capitan Limestone aquifer is hosted by the vuggy carbonates of the Capitan Limestone. The aquifer parallels the edge of the Delaware Basin in an arcuate strip along its eastern and northern margins, from the Guadalupe Mountains (southeastern New Mexico) to the Glass Mountains (southwest of Fort Stockton). The depth to the aquifer in Pecos County is about 4000 ft (1200 m), which explains why it remains largely undeveloped in the area.

In Pecos County only two wells penetrate the aquifer. One of them flows about 1000 gallons per minute (3890 l/min) from a producing interval of about 3200 to 3600 ft (975.5 to 1097 m) below land surface. The owner of the well states that the casing ruptured soon after completion, thus making possible contamination with water from the Rustler aquifer. The other well, located in southern Pecos County, is plugged.

## **B. Rustler Aquifer**

The Rustler aquifer, both confined and unconfined in the study area is in the carbonates and evaporites of the Rustler Formation. It yields brackish to saline water to stock, irrigation, and oil recovery wells. Groundwater in the Rustler aquifer occurs under artesian conditions in northern, western, and southern Pecos County. In all these areas, the Triassic Tecovas Formation is the overlying confining layer for the Rustler aquifer. In northeast Pecos County, the Tecovas is truncated by Cretaceous rocks. Here the Rustler is unconfined. Most production in the county's 31 Rustler wells comes from solution openings or fractures in the Rustler dolomite (Armstrong and McMillion, 1961). Wells that do not tap into the solution cavities are acidized to increase yield.

Recharge to the Rustler aquifer is by precipitation on its outcrop in Culberson County, and on the Rustler-equivalent formations that crop out in the Glass Mountains (Armstrong and McMillion, 1961). Figure 7 depicts heads in the Rustler in Pecos County and neighboring areas. The arrows represent flowlines inferred from head distribution, and show a centripetal pattern: flowlines originating in the recharge areas converge to Diamond Y Springs. Discharge from the Rustler takes place mainly through wells (some of which



Modified from Richey, 1985

Approximate extent of Rustler aquifer

0 20 MILES

EXPLANATION

- 3587 Well location and water level elevation (feet above sea-level)
- ➔ General direction of groundwater flow in the Rustler aquifer

Figure 7. Selected wells, water levels and inferred flow directions in the Rustler aquifer, Pecos, Reeves, Ward, and Crane counties

have been flowing for years) and by upward leakage into the Edwards-Trinity (Plateau) aquifer.

Rustler water quality is variable in the study area. In the Leon-Belding irrigation area wells yield a brackish (TDS=1500 mg/l), water, as opposed to the saline waters (TDS as high as 80,000 mg/l) issuing in wells in northeastern Pecos County. The few uniform characteristics of this water include a high calcium concentration (>500 mg/l), and low bicarbonate (<200 mg/l). Hydrogen sulfide is also present. Piper plots showing the Rustler water chemical composition are shown in figure 8. A detailed discussion of the Rustler hydrochemistry is given in Chapter 5.

### **C. Edwards-Trinity (Plateau) Aquifer**

The Edwards-Trinity is the most important aquifer in the study area. It underlies most of Pecos County, as well as a portion of Reeves County and small parts of Culberson and Jeff Davis Counties (figure 9). The more permeable units in the Edwards-Trinity are the lower Cretaceous sands and limestones which are hydraulically connected with the overlying Cenozoic alluvium. Therefore, the Edwards-Trinity and the Cenozoic alluvium are commonly treated as a single, unconfined aquifer.

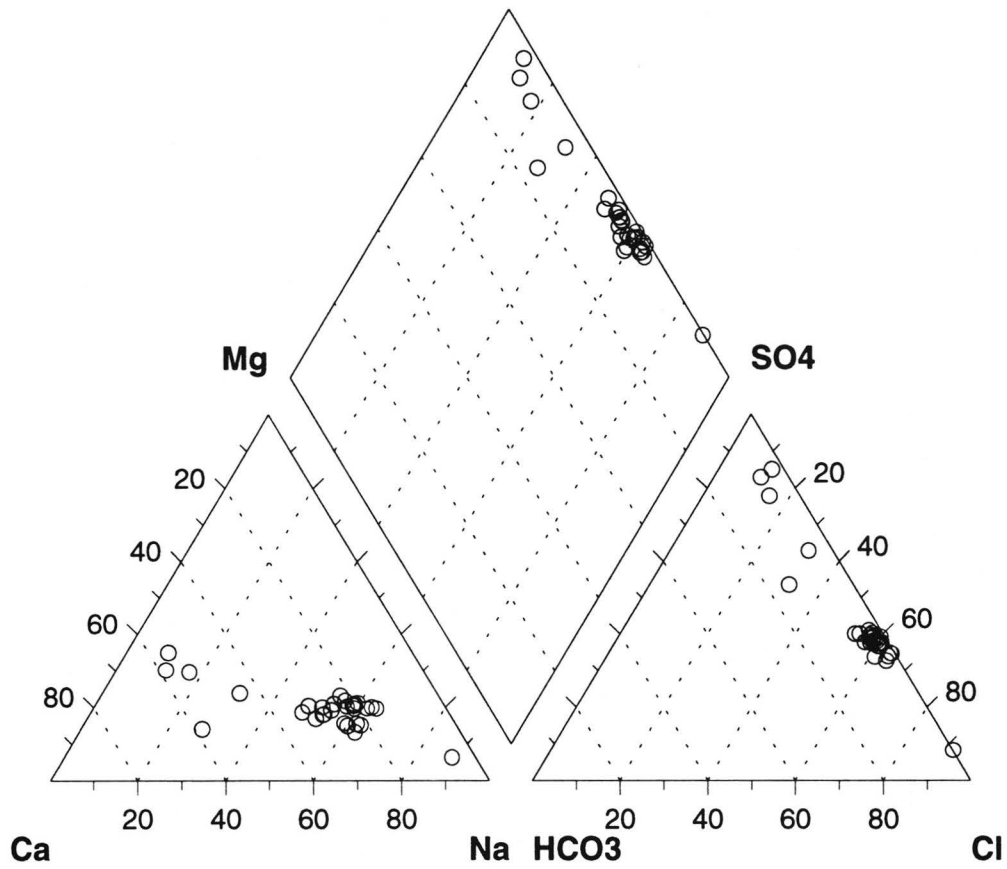
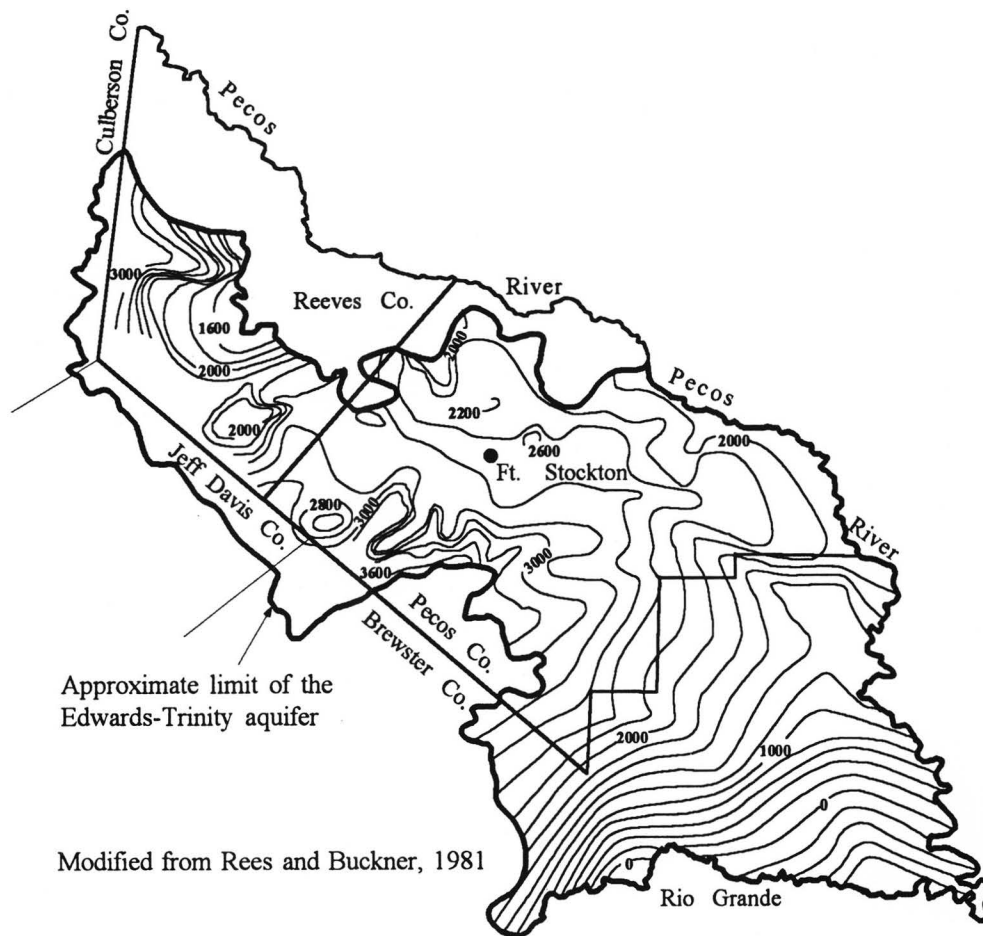


Figure 8. Piper plot showing Rustler water chemical composition



Approximate limit of the  
Edwards-Trinity aquifer

Modified from Rees and Buckner, 1981

0 — 30 miles

EXPLANATION

— 1000 — Base of the Edwards-Trinity  
aquifer, in feet above sea level

Figure 9 . Areal extent and basal structure of the Edwards-Trinity aquifer,  
Trans-Pecos, Texas.

The spatial relationships of the Cretaceous with the older Permian strata are shown in figure 3 (p. 16) and figure 4 (p. 17). In much of western and southern Pecos County the Cretaceous rests upon Permian and Triassic red beds. The shaly Tecovas Formation (Triassic) is a semi-pervious layer which limits flow between the Edwards-Trinity aquifer and the deeper, artesian, brackish-to-saline Rustler aquifer. East of the meridian passing through Fort Stockton and Grandfalls, the Tecovas is truncated, and the Edwards-Trinity directly overlies the Rustler. As stated above, dissolution of Ochoan evaporites during Gulfian time produced a collapse feature (trough) west of Fort Stockton which runs northward. It is filled with permeable alluvium, limestone, dolomite, and evaporite rubble. This produces a permeability contrast between the trough fill and the adjoining rocks to the east and west, and has an important impact on the flow system configuration.

Direct recharge to the Edwards-Trinity aquifer by precipitation and return flow is very small because of the high potential evapotranspiration (Armstrong and McMillion, 1961). Recharge by precipitation only occurs after periods of steady rainfall and during winter when evapotranspiration is low. This inference is also supported by water chemistry data from the Texas Water Development Board files and by data collected for this study.

Water samples from wells located in fertilized agricultural areas show no traces of nitrate. Much of the precipitation falling over the mountainous areas becomes runoff. In creeks and ravines it reaches faulted Cretaceous rocks or karstic features (such as the sinkholes on the M.R. Gonzales property east of Fort Stockton) and infiltrates. Armstrong and McMillion (1961, their plate 14) show a spectacular photograph of the now dry Comanche Creek Reservoir running into a sinkhole. Cross-formational flow is perhaps the largest contribution to the aquifer's recharge budget. Computer simulations of flow suggest at least 75,000 acre-ft ( $9.25 \cdot 10^7 \text{ m}^3$ ) water recharge the Edwards-Trinity (Plateau) aquifer from deeper sources every year. This recharge occurs principally near or through the Belding and Diamond Y fault systems.

Intensive development of the Edwards-Trinity aquifer for irrigation started in 1940. Previously, the groundwater flow system was essentially at steady-state (discharge approximately equaling recharge). Prior to irrigation, discharge occurred through springs, by evapotranspiration in areas of shallow water table, and by baseflow to the Pecos River. The average flow at Comanche Springs was 31,000 acre-ft ( $3.82 \cdot 10^7 \text{ m}^3$ ) a year between March 1941 and February 1948 (U.S. Bureau of Reclamation, 1956). The combined flow of other

springs in Pecos County was estimated to have been 17,500 acre-ft ( $2.15 \cdot 10^7 \text{ m}^3$ ) a year (U.S. Bureau of Reclamation, 1956). Based on the same source of information, baseflow to the Pecos River was in the order of 30,000 acre-ft ( $3.7 \cdot 10^7 \text{ m}^3$ ) a year as the flow of the Pecos River gained about or 36,000 acre-ft ( $4.44 \cdot 10^7 \text{ m}^3$ ) per year while passing Pecos County. The water issuing out of the springs usually evaporated, or evapotranspired, or seeped into the ground, so that runoff of springflow to the Pecos was (and is) negligible (Armstrong and McMillion, 1961).

After 1940, discharge through wells became important in the aquifer budget. In 1958, the total discharge from the aquifer was estimated to be 3 to 4 times the average annual recharge with about 120,000 acre-ft ( $1.48 \cdot 10^8 \text{ m}^3$ ) being yielded to wells (Armstrong and McMillion, 1961). The quantity of water pumped for irrigation, stock, and municipal use went down to about 77,000 acre-ft ( $9.5 \cdot 10^7 \text{ m}^3$ ) in 1974 (Rees and Buckner, 1980).

The conceptual model for groundwater flow within the Edwards-Trinity aquifer is illustrated in figure 10. Groundwater in the western part of Pecos County flows towards the north-northeast, in the central part it flows toward northeast, and in the eastern part of the county it flows towards the east. Much of the recharge is “funneled” through the trough towards the Pecos River.

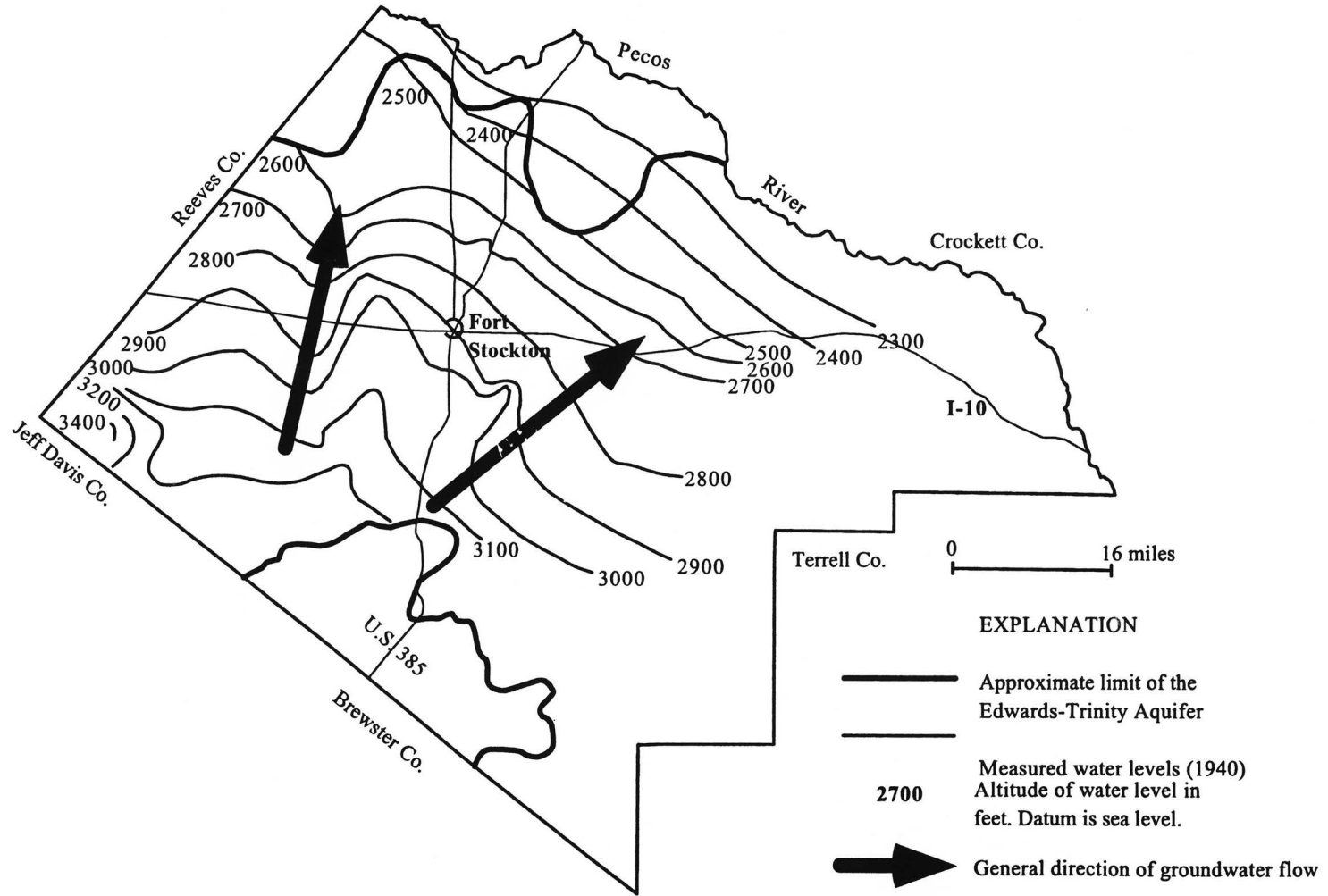


Figure 10. Conceptual groundwater flow model for the Edwards - Trinity aquifer in the study area

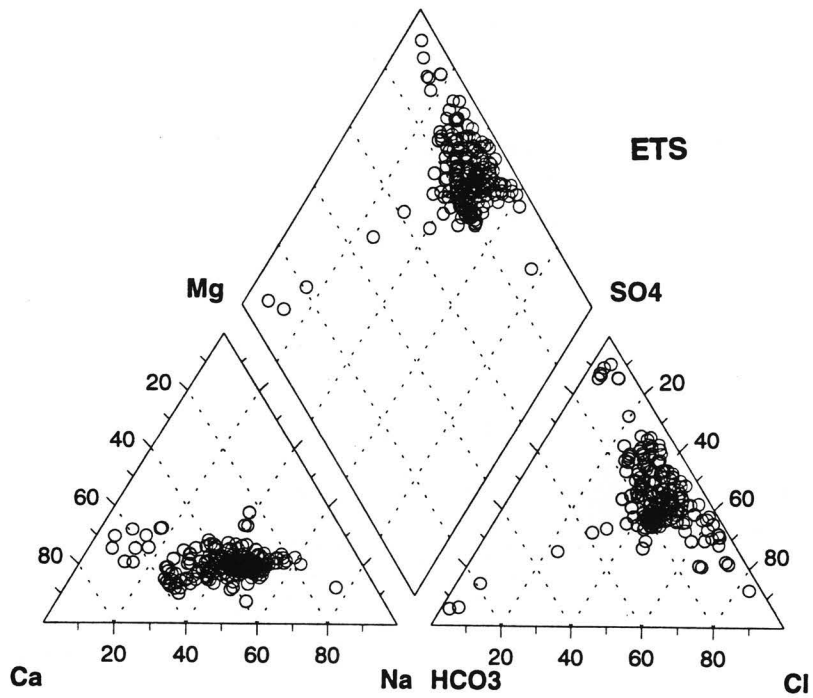
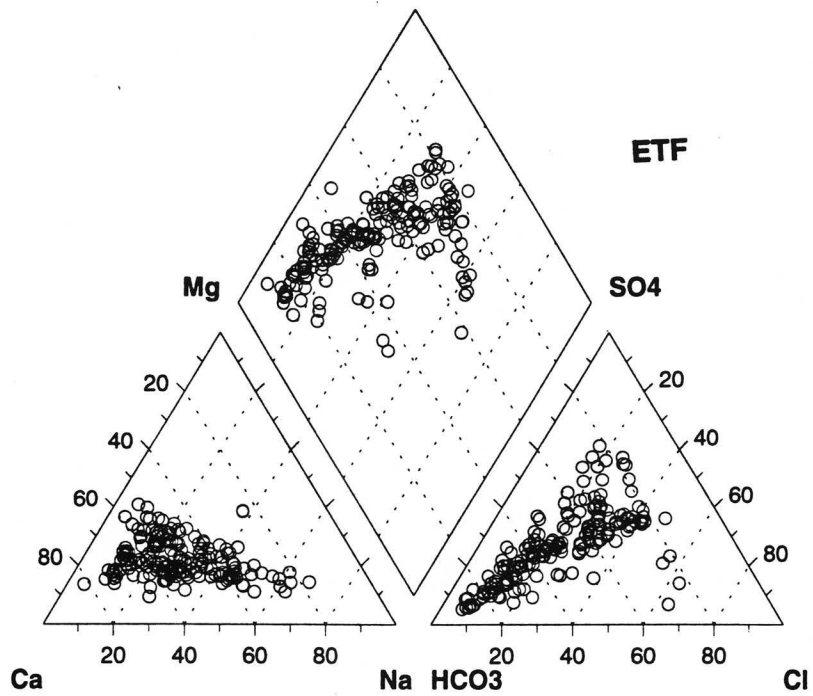


Figure 11. Piper plot showing Edwards-Trinity aquifer water composition

The trough also acts as a barrier for flow from west to east. This reduces the fresh water input east of Fort Stockton meridian.

The water chemistry in the Edwards-Trinity aquifer reflects the local geology, structural controls, and the flow regime. Sulfate and chloride are the dominant ions, with high concentrations of sodium, calcium, and magnesium. Where the aquifer is underlain by the semi-permeable Tecovas Formation, the water is fresh to brackish (TDS<1,500 mg/l). In this region, roughly representing the western, southern, and southeastern Pecos County, the Tecovas keeps the artesian Rustler water from flowing upwards and mixing with Edwards-Trinity waters. East of the trough and in northeastern Pecos County the Tecovas aquitard thins and, farther east, is missing. In this region the Edwards-Trinity water is brackish to saline (TDS=1,500-80,000 mg/l). This is the result of mixing between Rustler water and Edwards-Trinity water. Piper plots of the Edwards-Trinity water chemistry are shown in figure 11.

#### **D. Diamond Y Springs**

Veni (1991) completed the first hydrogeological investigation of the Diamond Y Springs. He mapped the springs, delineated their drainage basin, and provided the first geochemical and hydrogeological description of each of the

springs. This study extends Veni's work and places the springs in a regional context to determine their origin and interactions with the regional flow systems.

Veni stated that the Diamond Y Springs are fed by the Edwards-Trinity aquifer and issue from Cretaceous limestone at the bottom of an alluvial valley. The head-spring, and the largest of the system, is Diamond Y Spring, which rises from a pool on the edge of an alluvial plain. Its discharge flows northeast for 0.8 mi (1.5 km) to meet Leon Creek, and to continue as the Diamond Y Draw (figure 12). Along its path the flow is augmented by smaller springs and seeps. Veni (1991) splits the spring system into upper and a lower segments. The upper segment is fed mainly by the Diamond Y Spring and it flows northwards for almost a mile before sinking into the alluvium. The lower stream segment begins about 1.2 mi (2 km) downstream and flows for another 1.3 mi (2.1 km) before it sinks into the alluvium. From there dry Diamond Y Draw runs north to the confluence with Comanche Creek and finally into Pecos River.

In 1990 The Nature Conservancy of Texas (TNCT) staff established a monitoring network for the Diamond Y Springs system. Their same gauging and sampling network was employed for this study. It includes four springs and

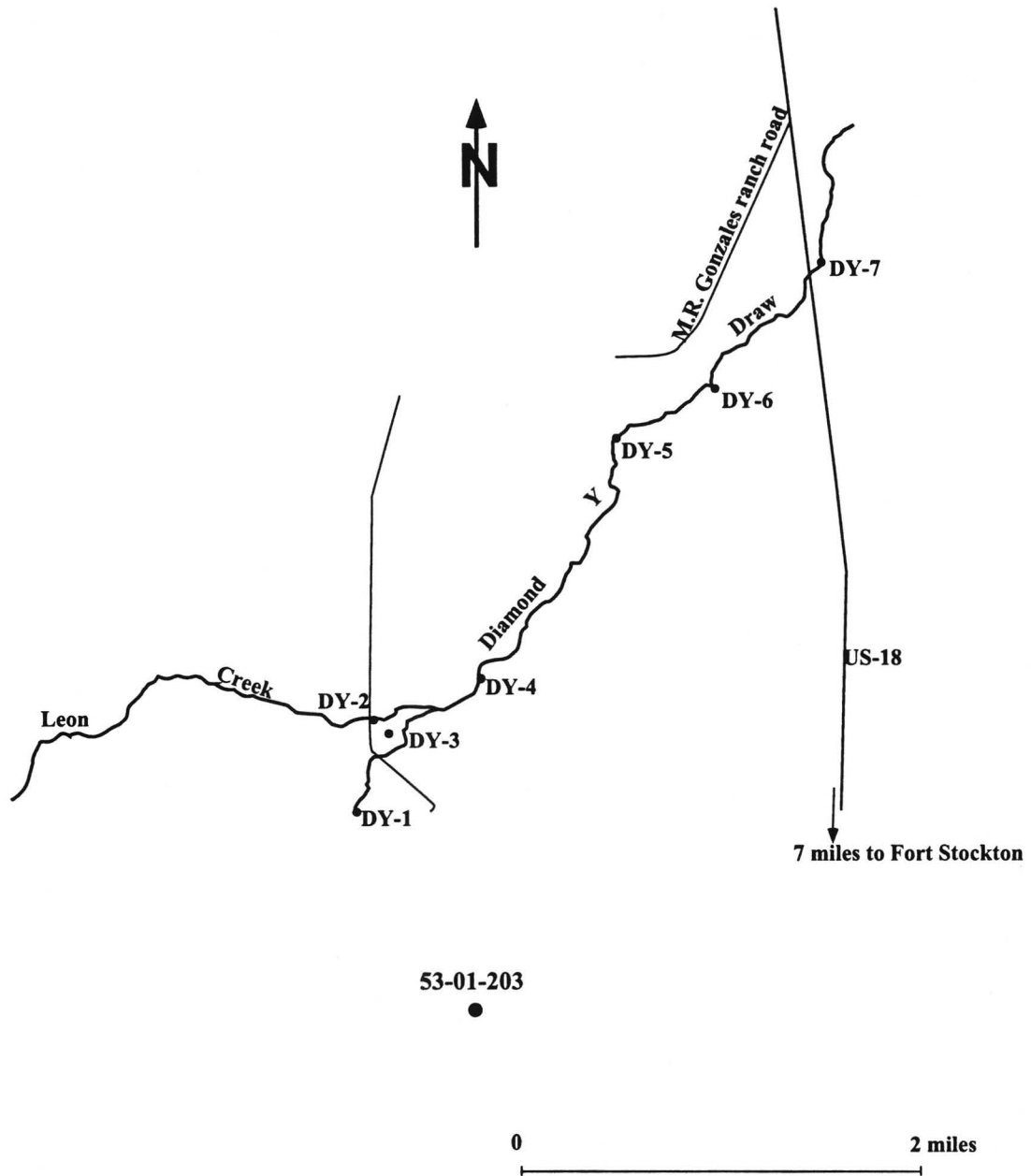


Figure 12. Map showing the Diamond Y springs and sampling locations

three monitoring stations described below as stations DY-1 through DY-7 (figure 12).

Diamond Y Spring, designated as DY-1, rises from the bottom of a 12-ft (3.5 m) deep rectangular pool, measuring roughly 80 ft (24.5 m) long by 46 ft (14 m) wide.

DY-2 designates a gauging station located on Leon Creek, 0.4 mi (640 m) upstream of its confluence with the DY-1 channel. The station measures the flow of a couple of seeps located about 0.3 mi (480 m) upstream. At DY-2 the channel is about 3 ft (1 m) wide and 1 ft (0.3 m) deep.

DY-3 is a tiny seep, positioned 0.2 mi (320 m) southeast of DY-2, almost hidden by vegetation. Like DY-1 it issues at the contact between the Cretaceous limestone and the valley alluvium. The hole is 2 ft (0.6 m) long, 1 ft (0.3 m) wide, and 1.8 ft (0.5 m) deep.

DY-4 is a monitoring location which measures the combined flow from the upper segment of the Diamond Y Springs system. Veni placed this location about 0.3 mi (480 m) downstream of the Diamond Y-Leon Creek confluence. One tenth of a mile (160 m) downstream the discharge of this southern segment sinks into the ground. At DY-4 the channel is 5 ft (1.5 m) wide and less than 1 ft (0.3 m) deep.

DY-5 is the location where the flow resurfaces and re-fills the channel of Diamond Y Creek. The spring measures 2.3 ft (0.5 m) in length, is 1 ft (0.3 m) wide, and 1 ft (0.3 m) deep (Veni, 1991).

DY-6, also called "Euphrasia" or "Monsanto Spring" issues from a shallow, oval pool measuring 27 ft (8 m) in length, 18 ft (5.5 m) in width, and 1 ft (0.3 m) deep. DY-6 has the largest flow in the lower segment of the springs' system.

DY-7 is the gauging station located farthest downstream, where the creek passes under State Highway 18 north of Forth Stockton. It is also the oldest station. It was used for monitoring the Diamond Y Creek between 1986 and 1987. The stream channel at DY-7 is 5 ft (1.5 m) wide and almost 1 ft (0.3 m) deep.

Discharge data for the Diamond Y Springs are sparse: only four measurements were taken in the time period between 1943 and 1987, and then only DY-1 was measured. Measurements from 1990 and 1991, now taken at all stations, provide an insight into the system's internal dynamics. This data confirms the existence of two distinct groups of springs, based on their response to rainfall events (see figure 13). The upper segment includes stations DY-1 through DY-4, which show a swift increase in discharge within 24-48 hours of

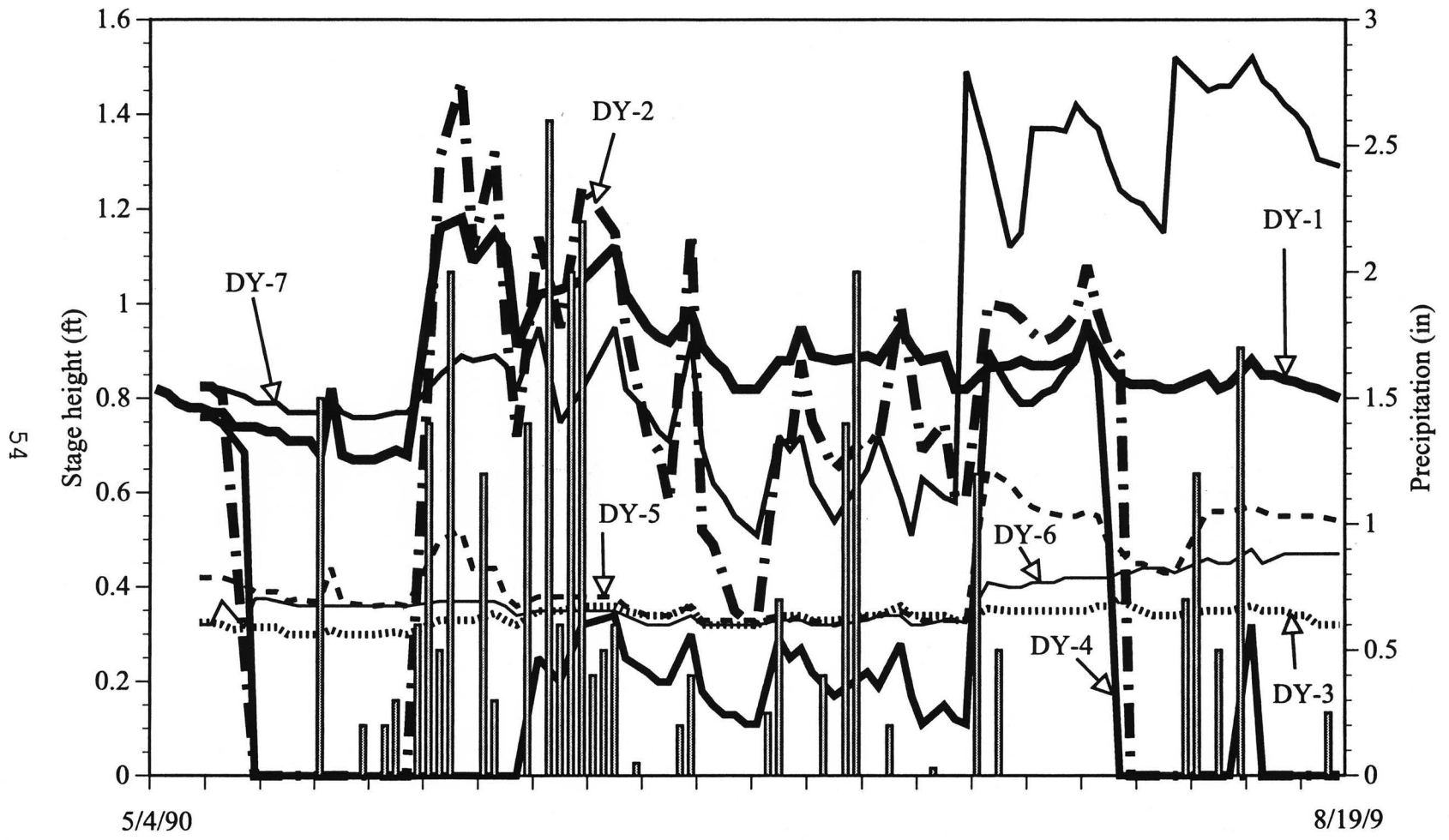


Figure 13. Diamond Y Springs system hydrograph, 4 May 1990 - 18 July 1991  
(Data from Veni, 1991)

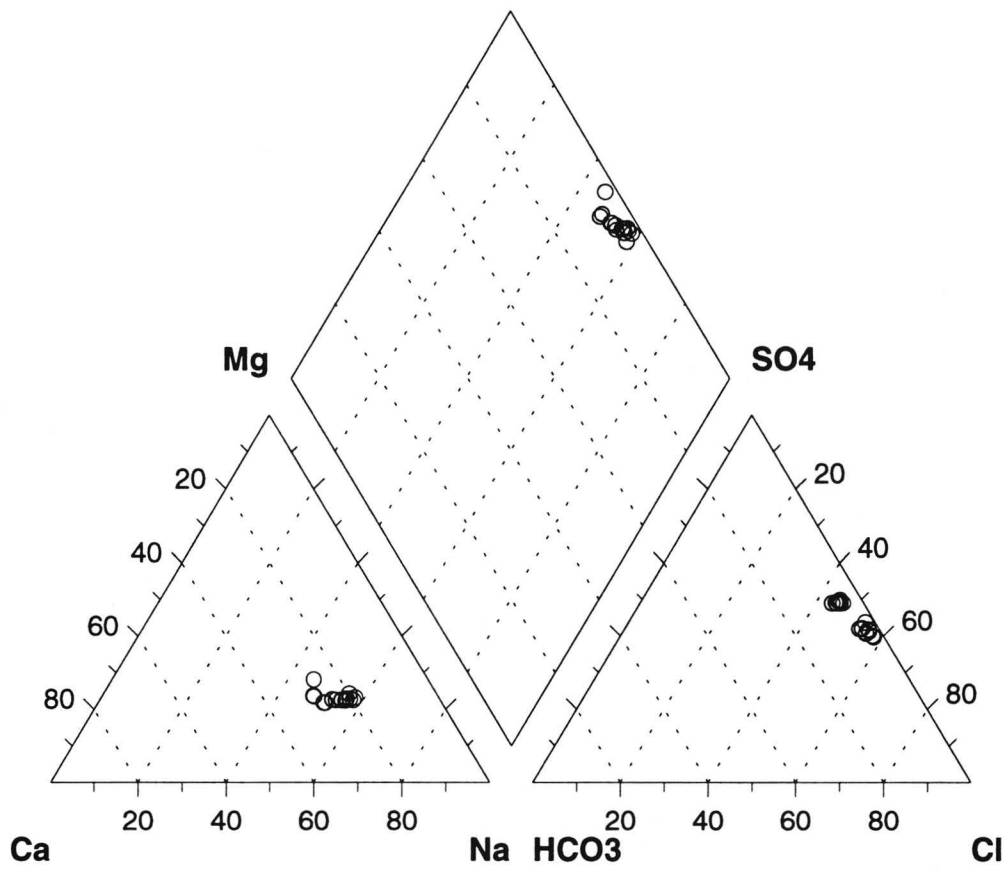


Figure 14. Piper plot showing Diamond Y springwater composition

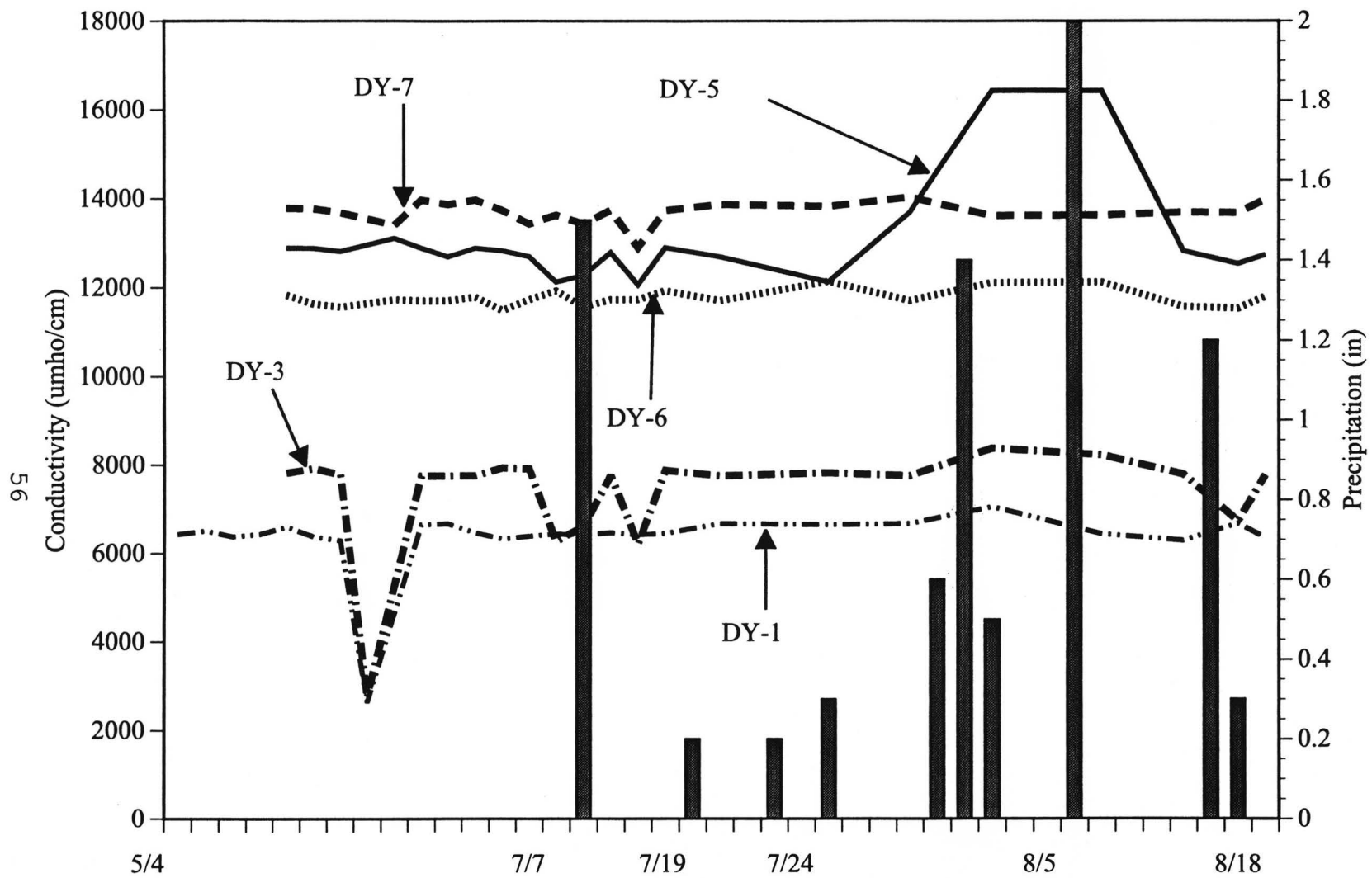


Figure 15. Diamond Y Springs system conductivity, May 4 - August 18, 1990.  
 (Data from Veni, 1991)

rainfall. Their gentle recession curves suggest a strong contribution from diffuse groundwater flow. The lower segment consists of stations DY-5 through DY-7 and shows little fluctuation before recharge. After rain, the response is slow; stage height rises steadily for a period of three months or more, which indicates a largely diffuse-flow aquifer. The springs' general response to recharge suggests slight to moderately extensive flow conduits feeding the Diamond Y Spring system. Figure 13 shows the Diamond Y system hydrographs for the time interval between January and July 1991.

Diamond Y Springs discharge a low to moderately saline Na-Cl-SO<sub>4</sub> type of water (figure 14). The presence of two distinct segments inside the Diamond Y Springs system is substantiated by the springs' baseflow chemistry. The downstream springs (DY-6 and DY-7) show little sensitivity to precipitation events, and maintain consistently higher total dissolved solids (TDS) compared with their upstream counterparts (DY-1 - DY-5, figure 15). The pH readings appear to oscillate randomly, but many of the changes at the upper segment correlate with rainfall events (figure 16). Veni (1991) matches the fluctuations in dissolved oxygen (D.O.) readings with storm events (figure 17). The figure shows a large drop and a rebound in pH for DY-5 and DY-6, even though DY-6's hydrograph shows only a slight change in stage height.

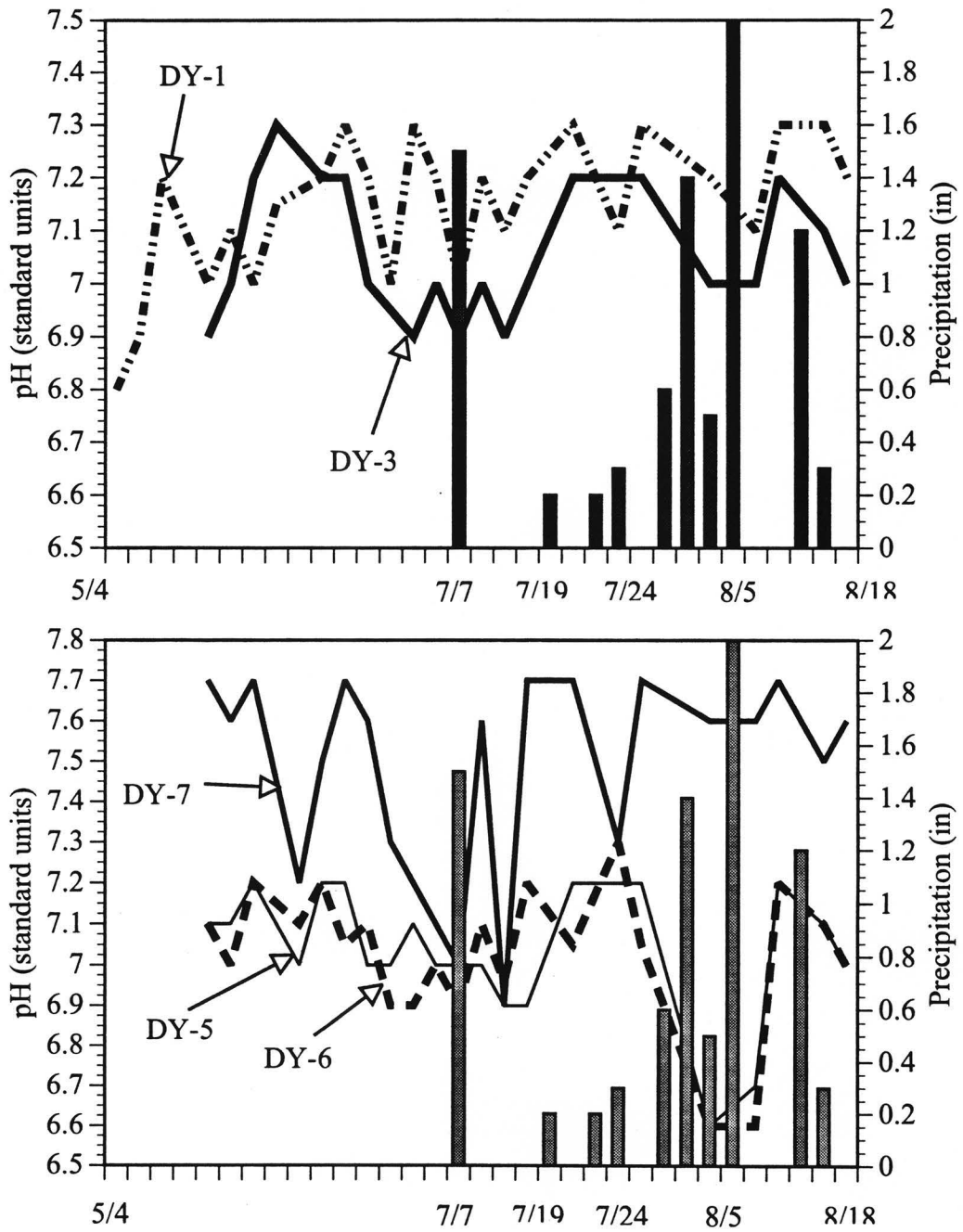


Figure 16. Diamond Y Springs system pH, May 4 - August 18, 1990  
(Data from Veni, 1991)

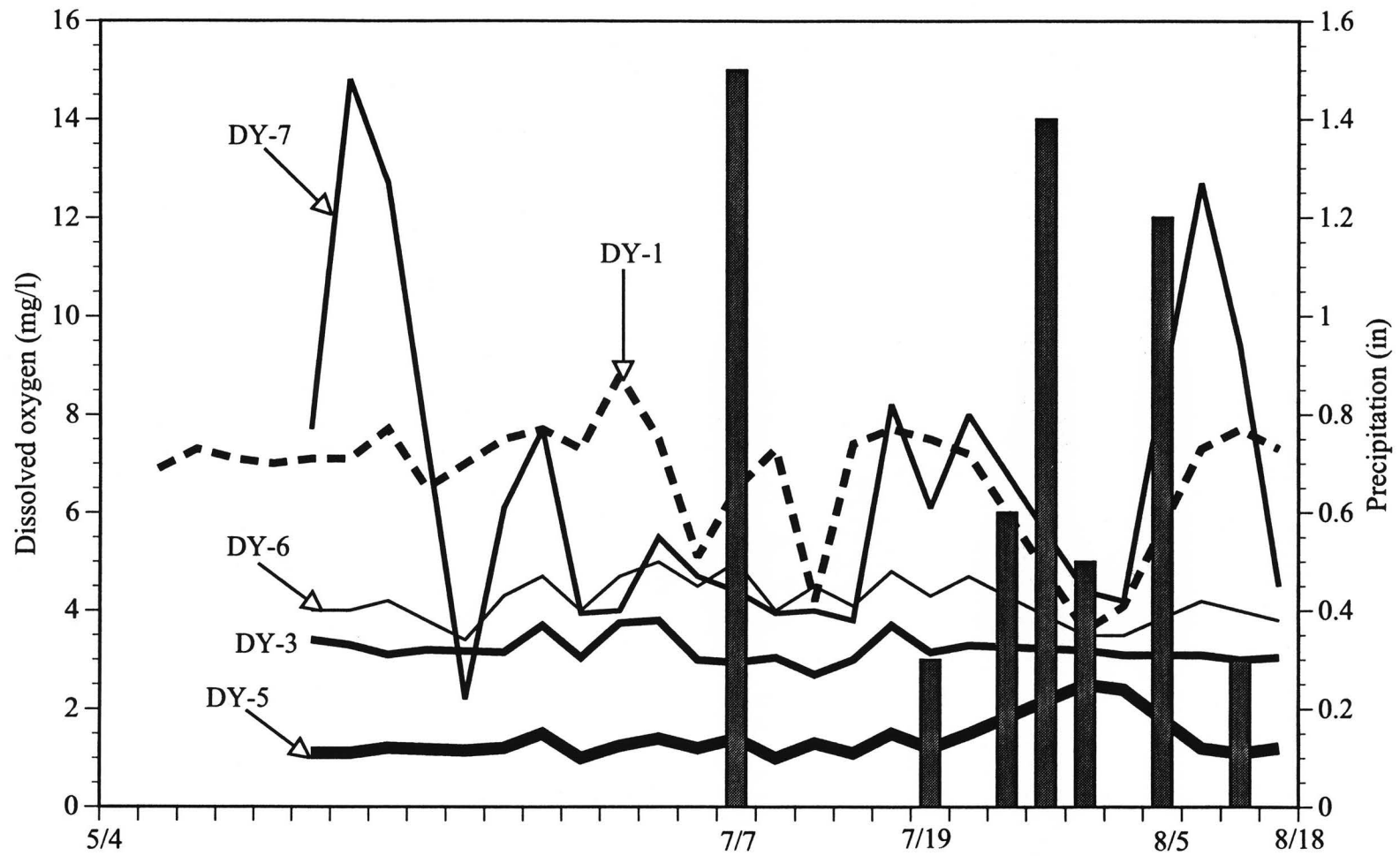


Figure 17. Diamond Y Springs system dissolved oxygen  
 May 4 - August 18, 1990  
 (Data from Veni, 1991)

The steep decline in D.O. at DY-1 coincides with flow cessation at DY-2 (June 1990) and a slight increase in stage at DY-3. Veni (1991) explains this through a "groundwater diversion" process, where low-D.O. waters from DY-2 would actually discharge into the DY-1 pool. In the upper springs' segment the chemistry of DY-1 is "mimicked" by water at the DY-2 and DY-4 locations, whereas water chemistry in the lower segment correlates with DY-6. The TDS increase along the flow channel is caused by saturation excess due to CO<sub>2</sub> degassing (which decreases solubility), and evapotranspiration (which increases concentration). Na/Cl and Ca/Mg ratios are nearly equal to unity, indicating halite dissolution and water passing through a dolomite aquifer. Corroborating this data with geochemical evidence from Balmorhea Springs by Sharp and LaFave (1987), Veni proposes that the Capitan aquifer is the source for the water discharging today at Diamond Y Springs.

## 5. GROUNDWATER CHEMISTRY AND ISOTOPIY

This chapter addresses the issues of Diamond Y springs origin and evolution, and their interactions with the regional flow systems. The hydrochemical and isotopic methods of investigations are described first, followed by the results and data interpretation.

### A. Methods

#### Sample Collection

Four samples were collected from each well or spring, filtered through 0.2  $\mu\text{m}$  filters and stored in Nalgene sample bottles without any head space. One sample was used immediately for alkalinity titration, another was acidified with nitric acid to  $\text{pH} < 2.0$  for cation analysis, and the other two samples were sealed with parafilm, and stored at 4°C for further analyses. Prior to sampling, wells were pumped until temperature, pH, and conductivity stabilized. This purging procedure was not used when sampling active irrigation wells or the springs.

Waters were analyzed for pH, temperature, conductivity, dissolved oxygen, and alkalinity on site. Sample pH was measured with an *Orion* model SA 250 pH meter, and a *Ross* combination electrode with an automatic temperature compensating probe. The measurements' accuracy was 0.05 units.

This probe was also used for temperature measurements to an accuracy of 0.1°C. Conductivity was measured with a *Hanna* model *HI8773C* conductivity meter. Dissolved oxygen levels in samples were measured with a *Chemetrics* 0-12 ppm colorimetric analysis kit to an accuracy of +/-1 ppm. Temperature, pH, and conductivity measurements were made in a flow cell, with electrodes calibrated with buffer solutions that had been equilibrated to sample temperature. Alkalinity titrations were performed on 25 ml filtered samples to a pH of 4.5 using 0.1N HCl as the titrant.

Samples collected for analysis of stable isotopes ( $^2\text{H}$  and  $^{18}\text{O}$ ) and  $^3\text{H}$  were stored at 4°C in 500 ml and 1 l polyethylene bottles, respectively, and sealed with parafilm to avoid contact with the atmosphere.

### **Analysis**

Chemical analyses for selected ions (Na, Ca, Mg, Sr, Si, Ba, Co, Cr, Fe, Ni, Pb, Zn, Mn, F, Cl, NO<sub>2</sub>, Br, NO<sub>3</sub>, HPO<sub>4</sub>, SO<sub>4</sub>) were performed at the chemistry labs of the U.T. Austin Department of Geological Sciences, using inductively-coupled plasma-optical emission spectrometry (ICP-OES) for cations, and single-column ion chromatography for anions.

The  $\delta^{18}\text{O}$  and  $\delta^2\text{H}$  measurements were made by means of gas-source mass spectrometry at the U.T. Austin Department of Geological Sciences

Laboratories, and at Coastal Science Laboratories, Austin, Texas, respectively. The  $\delta$ -values are reported relative to SMOW. The  $^3\text{H}$  activities were measured by low-level proportional counting of samples that had undergone electrolytic enrichment at the University of Miami Tritium Laboratory, Miami, Florida.

The mass-balance modeling program NETPATH (Plummer et al., 1994) was used to test the hypotheses regarding the origin and evolution of Diamond Y Springs. NETPATH is an interactive computer program used to interpret net geochemical mass-balance reactions between an initial and final water along a ground-water flow path. The net geochemical mass-balance reaction consists of the masses of minerals and gasses that must enter or leave the initial water along a flow path to produce the composition of a selected set of chemical and isotopic parameters of the final water. The program is useful for interpreting geochemical reactions, mixing proportions, evaporation and dilution of waters, and mineral mass transfers in the evolution of waters, for a specific set of plausible constraints and phases.

## **B. Results and Interpretation**

Groundwater of the Edwards-Trinity aquifer in the study area is fresh to saline. Total dissolved solids (TDS) concentrations range from 300-1,500 mg/l

in the area west of the trough, to 1,500-80,000 mg/l in northeastern Pecos County. Based on TDS distribution groundwaters have been thus subdivided into two main facies: Edwards-Trinity fresh (ETF) and Edwards-Trinity saline (ETS), each of them covering the areas shown in figure 18. Waters from these regions are chemically distinct, reflecting aquifer lithology, and location within the flow system with respect to recharge, mixing, and discharge.

Figures 11, 14, and 8 show major ion compositions for both ETF (11, upper) and ETS (11 lower), plus major ion compositions for Diamond Y Springs (14) and Rustler aquifer (8). The ETF waters vary from Ca-HCO<sub>3</sub> to a Ca-Na-HCO<sub>3</sub>-Cl-SO<sub>4</sub> facies, with the higher TDS concentration the result of higher concentrations of Cl and SO<sub>4</sub> ions. Most of the ETF brackish water samples (figures 11, 18) are located west of the Pecos trough. The ETS facies data points are much less scattered and are characteristic for Na-Ca-Cl-SO<sub>4</sub> waters. A mixing trend appears to dominate the chemistry of Rustler aquifer in the study area. Waters with a Ca-Mg-HCO<sub>3</sub> signature, issuing from Rustler wells in western Pecos County, are mixing with Na-Cl brines collected from wells near Girvin (figure 2, p. 14). The result is a Na-Ca-Cl-SO<sub>4</sub>-facies water encountered in the Rustler wells around Fort Stockton. The Diamond Y Springs waters are of Na-Ca-Cl-SO<sub>4</sub> type. It is apparent that the DY and Rustler plots coincide with the Rustler water mixture.

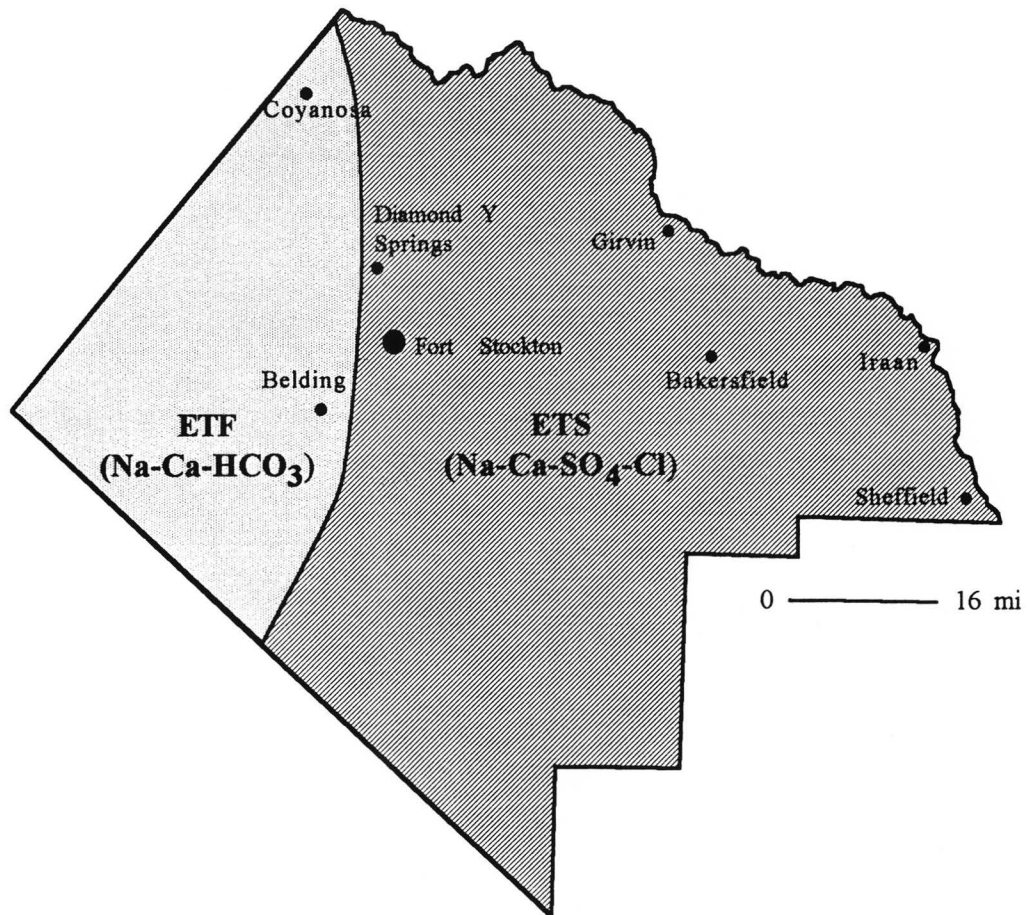


Figure 18. Hydrochemical facies in Edwards-Trinity (Plateau) aquifer, Pecos County

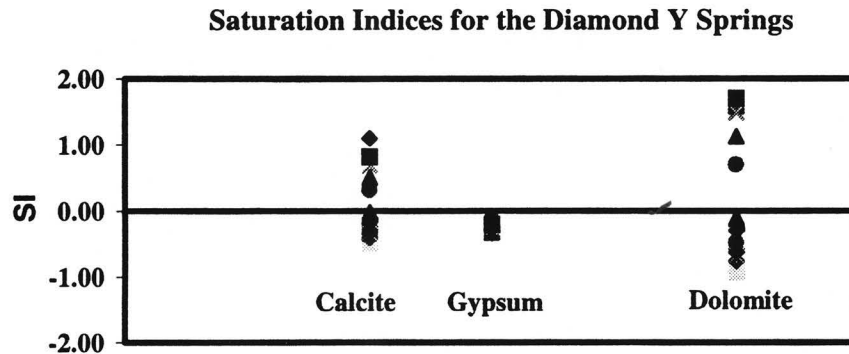


Figure 19. Saturation indices for Diamond Y waters

Calcite, gypsum, and dolomite equilibria are plotted in figure 19. Waters range from slightly undersaturated to supersaturated with respect to calcite and dolomite and are at equilibrium with respect to gypsum. According to Plummer and Busenburg (1982) and Herman and White (1985), dolomite supersaturation is very unusual, many years being required for the aqueous solution to reach near-saturation. Siegel and Anderholm (1994) proposed a hydrochemical model for dolomite-supersaturated groundwaters in the Rustler aquifer in SE New Mexico, whereby supersaturation is due to of  $Mg^{2+}$  input into the solution: (1) solutes are added to the Rustler by dissolution of evaporite minerals; (2) the solubilities of gypsum and calcite increase as the salinity increases; these minerals dissolve as chemical equilibrium is maintained between them and the

groundwater; (3) equilibrium is not maintained between the groundwater and dolomite; sufficient  $Mg^{2+}$  is added by dissolution of polyhalite or carnallite such that the degree of dolomite supersaturation increases with the ionic strength. The scenario above could be applicable to the Diamond Y waters, the source of  $Mg^{2+}$  being the polyhalite-rich "potash district" which underlies Rustler rocks throughout the Delaware Basin (Adams, 1944).

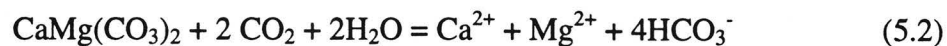
### **Chemical Processes Responsible for the Composition of Diamond Y Springs**

Following are the governing equations for prominent mineral dissolution and precipitation reactions occurring in aqueous systems.

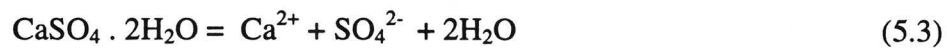
Calcite dissolution and precipitation:



Dolomite dissolution:



Gypsum dissolution:



Halite dissolution:



Ion exchange:

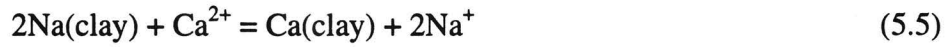


Figure 20 shows the relationship between the concentration of  $\text{Ca}^{2+} + \text{Mg}^{2+}$  versus  $\text{HCO}_3^-$  concentration. If all  $\text{Ca}^{2+} + \text{Mg}^{2+}$  were derived from calcite and dolomite dissolution, then data would plot along a line with slope 1:2, as stated by equation (5.1). Yet, all points are above the 1:2 line, thus indicating an additional source of  $\text{Ca}^{2+}$  and  $\text{Mg}^{2+}$ . A potential source of  $\text{Ca}^{2+}$  is the upper

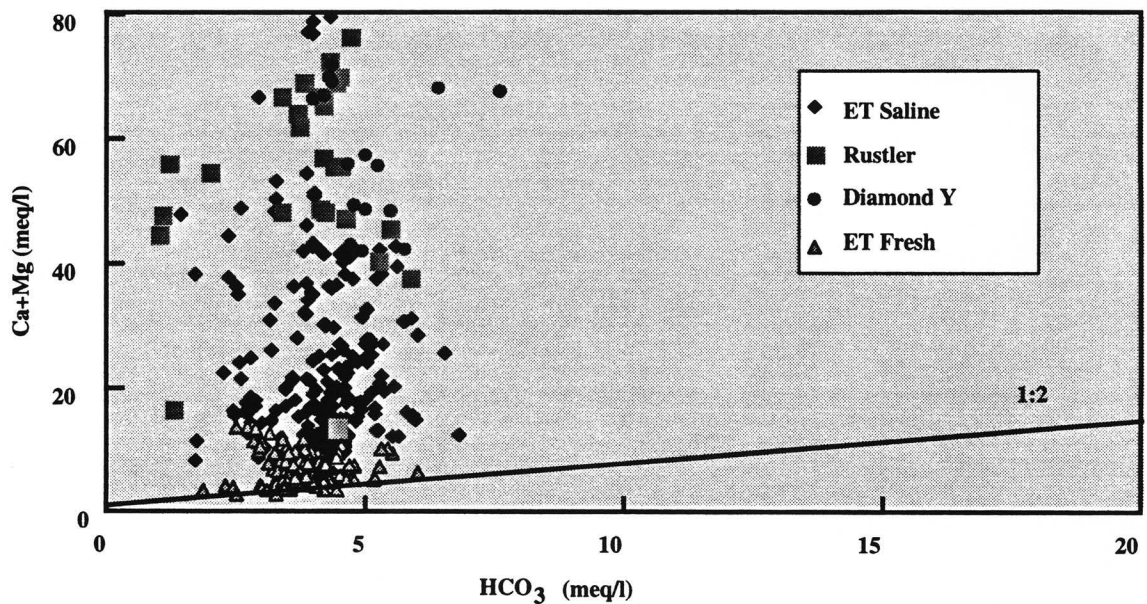


Figure 20. Plot of Ca + Mg versus HCO<sub>3</sub>

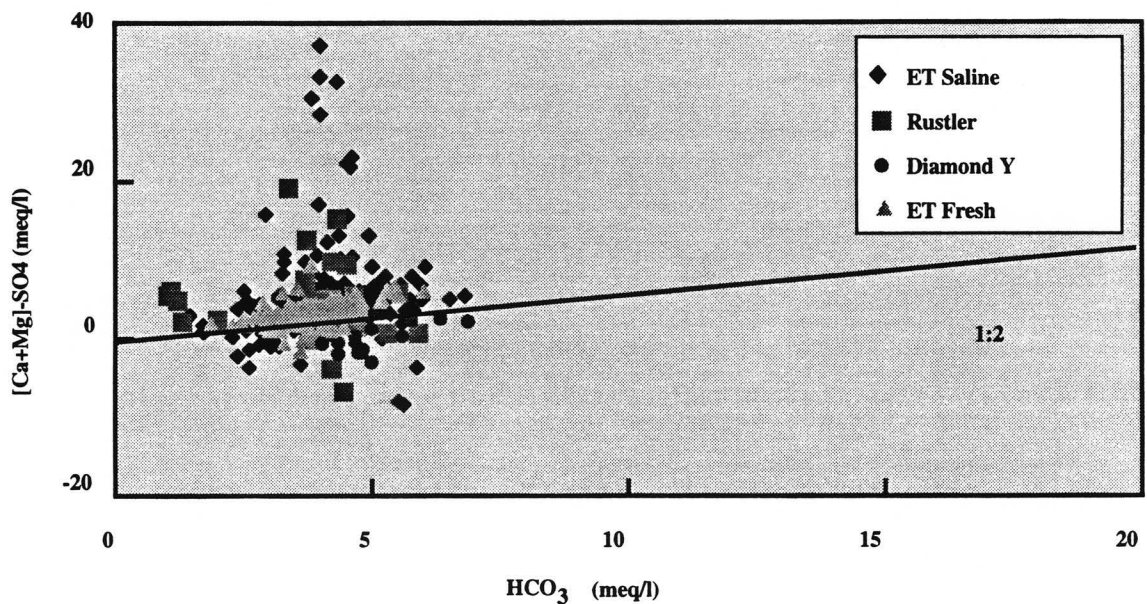


Figure 21. Plot of  $\text{Ca} + \text{Mg} - \text{SO}_4$  versus  $\text{HCO}_3$

Rustler Formation which contains gypsum. To account for the  $\text{Ca}^{2+}$  derived from gypsum dissolution, the  $\text{SO}_4^{2-}$  concentration is subtracted from  $\text{Ca}^{2+} + \text{Mg}^{2+}$ , which concentration is then plotted as a function of  $\text{HCO}_3^-$  (figure 21).

The Diamond Y Springs plot below the 1:2 line, indicating that although carbonate and gypsum dissolution explain much of the variations in  $\text{Ca}^{2+}$ ,  $\text{Mg}^{2+}$ , and  $\text{HCO}_3^-$  concentrations, another process, such as ion exchange between  $\text{Ca}^{2+}$  and/or  $\text{Mg}^{2+}$  and  $\text{Na}^+$  is removing  $\text{Ca}^{2+}$  and/or  $\text{Mg}^{2+}$  from solution. To test this hypothesis the concentration of  $(\text{Na}^+ - \text{Cl}^-)$  is plotted against  $(\text{Ca}^{2+} + \text{Mg}^{2+} - \text{SO}_4^{2-} - 0.5\text{HCO}_3^-)$ . The quantity  $(\text{Na}^+ - \text{Cl}^-)$  represents "excess"  $\text{Na}^+$ , that is,  $\text{Na}^+$  coming from sources other than halite dissolution, assuming all  $\text{Cl}^-$  is derived from halite dissolution. The quantity  $(\text{Ca}^{2+} + \text{Mg}^{2+} - \text{SO}_4^{2-} - 0.5\text{HCO}_3^-)$

represents the  $\text{Ca}^{2+}$  and/or  $\text{Mg}^{2+}$  coming from sources other than gypsum and carbonate dissolution. These two quantities represent the maximum amount of  $\text{Na}^+$  and  $\text{Ca}^{2+} + \text{Mg}^{2+}$  available for ion exchange processes. The data (figure 22) plot on a line with slope close to unity, suggesting cation exchange between  $\text{Ca}^{2+}$ ,  $\text{Mg}^{2+}$ , and  $\text{Na}^+$ .

Figure 23 plots  $\text{Na}^+$  versus  $\text{Cl}^-$  concentrations. The data plots along the 1:1 line, suggesting that halite dissolution is yet another process responsible for the groundwater chemistry in the study area.

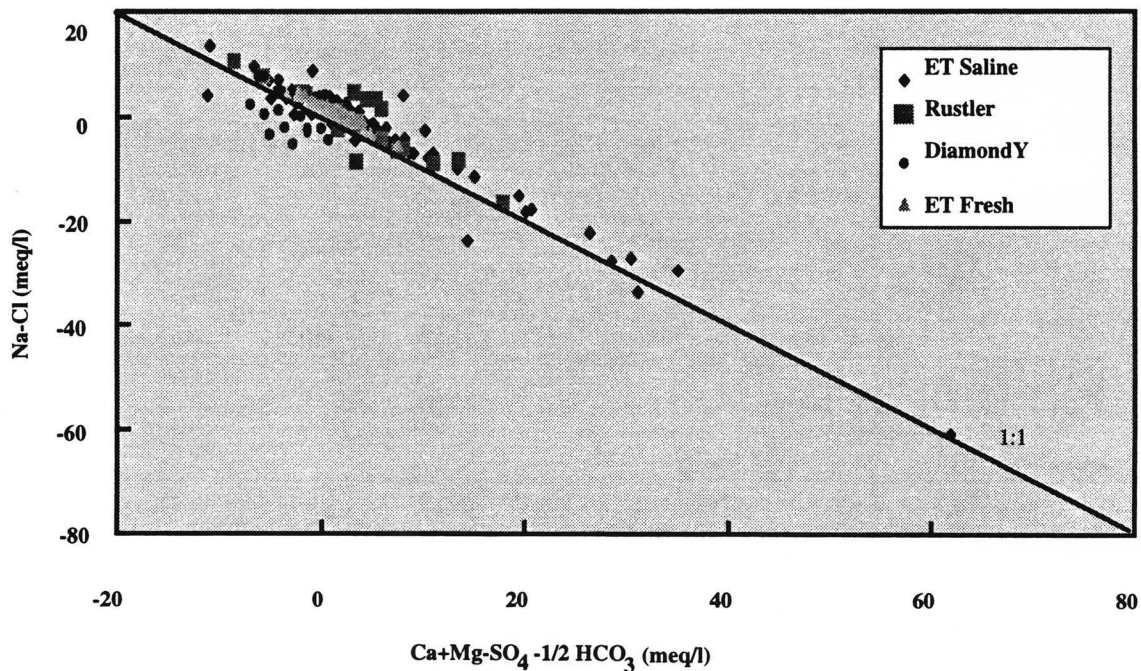


Figure 22. Plot of Na - Cl versus Ca + Mg - SO<sub>4</sub> - 1/2 HCO<sub>3</sub>

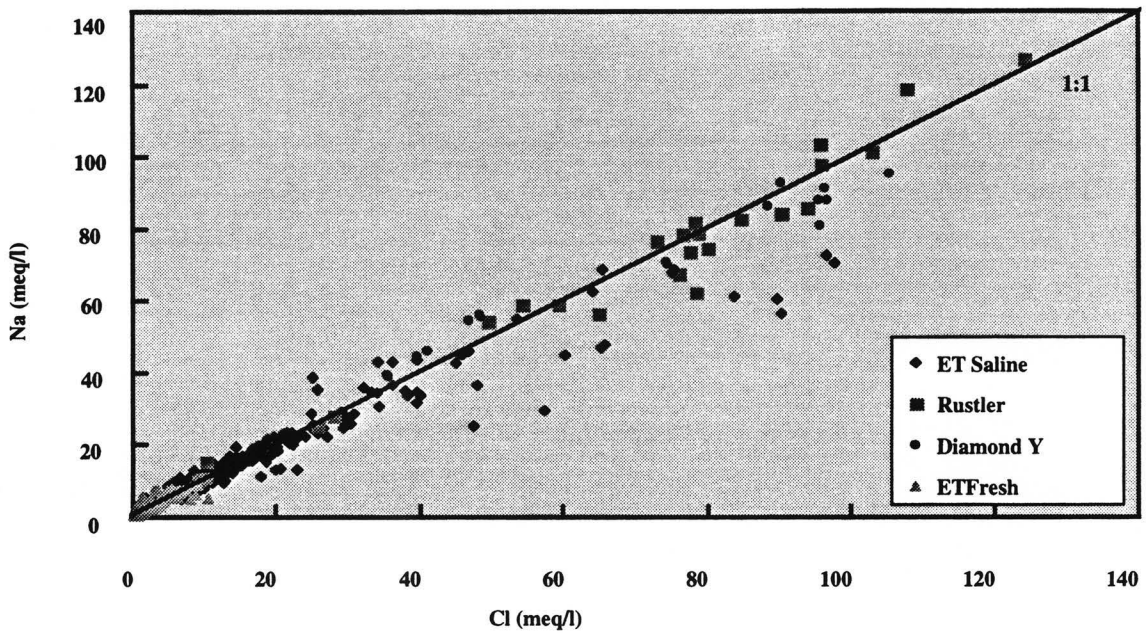


Figure 23. Plot of Na versus Cl

### C. Isotopic Analyses

The results of stable and radiogenic isotope analyses in the Diamond Y Springs suggest that evaporation and water mixing processes are important controls on the springwater chemistry.

#### Application of Stable Isotopes in Hydrologic Studies

The stable isotopes of water, deuterium, and oxygen-18 provide effective means of evaluating the origin, movement, and mixing of natural waters. When used in conjunction with unstable isotopes, such as tritium, they contribute to

understanding the areal distribution and timing of recharge. They also provide insight into the range of temperatures or elevations over which recharge occurs.

The isotopic composition of water is calculated with reference to Standard Mean Ocean Water, or SMOW (Craig, 1961). Measurements are reported as  $\delta$ -values, or per mil ( $\text{‰}$ ) deviations from SMOW.

Water that is depleted in the heavy isotope relative to the composition of the standard has a negative  $\delta$ -value, and water that is enriched in the heavy isotope relative to the standard has a positive  $\delta$ -value. Processes such as evaporation, condensation, and isotope exchange affect the abundances of  $^2\text{H}$  and  $^{18}\text{O}$  in hydrologic systems.

### **Applications of Tritium in Hydrologic Studies**

Tritium was used to delineate recharge areas, trace groundwater flow paths, estimate groundwater ages, and identify areas where mixing occurs between recent and old waters. Tritium has a half life of 12.43 years and is used to identify waters that have been recharged within the last 40 years. Tritium is formed in the upper atmosphere through the interaction of cosmic-ray neutrons and  $^{14}\text{N}$  (Faure, 1986, p.328). It is also produced by nuclear power plants and nuclear-weapons tests (Geyh, 1990, p.183). Above-ground nuclear bomb tests during the 1950's and 1960's increased tritium levels in some areas to more than 2000 TU (Geyh, 1990,

p.334). These elevated levels of bomb tritium provided a spike that allows for identification of waters recharged after 1950 (Geyh, 1990, p.183).

The amount of  $^3\text{H}$  in meteoric waters is measured in tritium units (TU), where 1 TU is 1 atom of  $^3\text{H}$  per  $10^{18}$  hydrogen atoms (Geyh, 1990, p.181). The amount of tritium in meteoric water varies according to natural atmospheric production of  $^3\text{H}$ , the decay of  $^3\text{H}$  to  $^3\text{He}$ , seasonal injection from the stratosphere into the troposphere, and the production of tritium by nuclear reactors and weapon tests (Geyh, 1990).

## **Results and Interpretation**

Stable isotope and tritium data suggest that Diamond Y springwater has a meteoric origin and is the result of mixing with rainwater fallen on the springs' pools. Evaporation also affects the spring's isotopic composition.

### **Stable Isotopes**

Figure 24 shows a plot of  $\delta^2\text{H}$  versus  $\delta^{18}\text{O}$  of waters sampled from the Rustler aquifer, Edwards-Trinity aquifer, the fresh facies (ETF), and from DY-1 through DY-7. Craig's (1961) Global Meteoric Water Line (GMWL) is shown, with the stable isotope composition of rain water in the study area. The data points plot near GMWL, suggesting a meteoric origin for both ETF and Rustler waters. DY data points appear to lie on a line originating in the four Rustler samples, and

extending towards heavier isotope composition below GMWL. This type of data distribution is characteristic for evaporated waters. Samples experiencing lower evaporation rates lay near GMWL towards its lighter end, and tend to preserve the composition of rainwater from which they are derived.

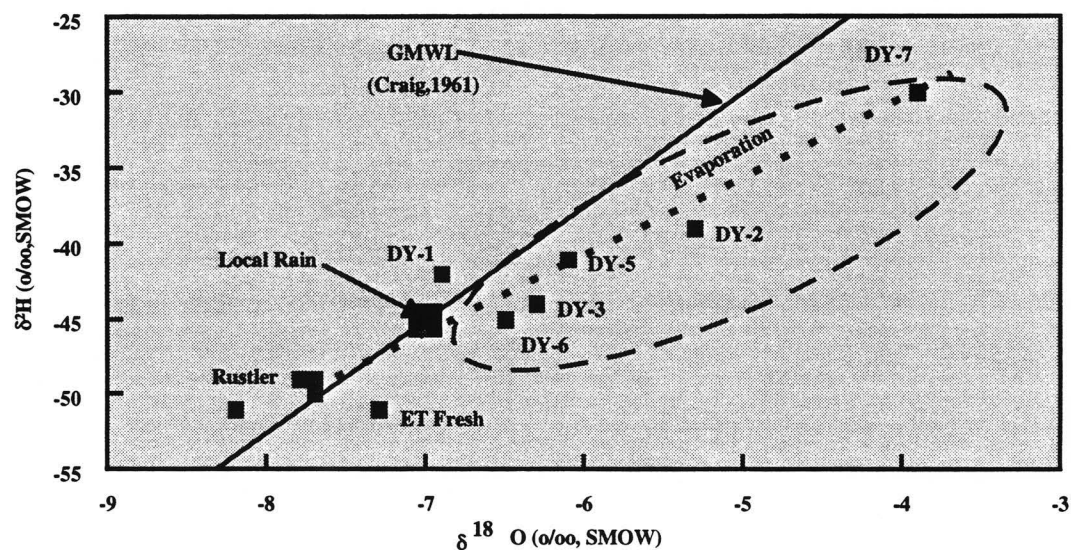


Figure 24. Plot of  $\delta^2\text{H}$  versus  $\delta^{18}\text{O}$

Samples undergoing high evaporation tend to become isotopically heavier, because evaporation removes the lighter isotopes preferentially. Study area data conform to this interpretation. DY-1 has the isotopic composition closest to rainwater, because the spring's larger discharge rate and pool size make evaporation less effective. Waters from DY-2 through DY-7 lay on the evaporation line according to their flow rate and pool size: the larger the discharge and the pool, the closer to DY-1 they plot along the line.

Samples from DY-2 and DY-7, for instance, plot towards the end of the evaporation line, and show the largest departure from GMWL. This is because they have the lowest discharge of all DY locations. Consequently, the water in their pools was most affected by evaporation.

The same  $\delta^2\text{H} / \delta^{18}\text{O}$  plot shows the DY evaporation line originating in the Rustler samples and not in the ETF sample, suggesting that water from the Rustler aquifer might be contributing to the flow at Diamond Y Springs. This hypothesis is tested below in section D, which discusses the origin of the springs.

### **Tritium**

Six water samples were collected for tritium analysis from the Diamond Y Springs and from wells representing the Edwards-Trinity, and Rustler aquifers. The reliability of the Capitan sample is doubtful, because of the chance of contamination by Rustler water through a leaky casing.

Table 4 presents the tritium data:

TABLE 4. RESULTS OF TRITIUM ANALYSES

SAMPLE	TRITIUM (TU)	ACCURACY (eTU)
ETF	0.26	0.09
ETS	0.14	0.09
RUSTLER	-0.10	0.09
DY-1	1.92	0.10
DY-6	4.35	0.10
CAPITAN	0.03	0.09

Four samples (ETF, ETS, Rustler, and Capitan) have virtually no tritium, and two samples (DY-1 and DY-6) show some amounts of tritium. This fact suggests that the DY springwaters are probably a mixture of older (no tritium) and recent (higher tritium) waters. The only source of high tritium water in the region is rainfall which in the Trans-Pecos can show concentrations as high as 24 TU (Mullican and Fisher, 1990). Low-tritium DY-1 and DY-6 groundwater mixes up with rainwater falling directly on the pool and produces the higher-tritium springflow that was sampled here. Rainfall changes only the springs'  $^3\text{H}$  signature; this is confirmed by the low value (0.14 TU) obtained for ETS. This sample is from a shallow well (45-57-803, shown on figure 12) located 0.5 mile west of DY-6. Its water is chemically identical to DY-6. If recharge from rainfall were of significance to areas other than the springs themselves, one might expect

similar tritium concentrations in both the well and the springs. This is not the case.

Water mixing at Diamond Y Springs is also supported by the  $^3\text{H}$  levels in DY-1 (1.92 TU) compared to DY-6 (4.35 TU). Rain falling on the DY-1 pool makes a smaller contribution in the final mixture than rain falling on the DY-6 pool, because of the difference between pool sizes, so that TU numbers are higher for DY-6 than for DY-1.

#### **D. Origin of Solutes**

One issue regarding the origin of Diamond Y Springs is the amount of springflow that might be fed by deep oil-field brines. The Diamond Y Springs Preserve is riddled by a number of oil and gas wells which produce from the Paleozoic Ellenburger Formation. McNeal (1965) reports Ellenburger water with salinities as high as 300,000 mg/l pumped as an oil and gas by-product. The springs' high (4,000 to 8,000 mg/l) TDS concentrations raise the question: do oil-field brines contribute to the springs' discharge ?

One method to differentiate the oil and gas field (deep basin) brines from the halite-dissolution brines is to examine their bromide concentrations, and Cl/Br ratios (Whittemore and Pollock, 1979; Whittemore et al., 1981). Bromide concentrations in brines are governed by the interaction of water with evaporitic

rocks, by the composition of the original formation fluid, or by both. During the evaporation of seawater and precipitation of halite, some bromide is incorporated into the halite crystal, with a distribution coefficient of about 0.0035 (Holser, 1979). Therefore, Cl/Br ratios are higher in halite than in seawater, but lower in the evaporated brine than in seawater. Dissolution of such halite, which has a high Cl/Br ratio by contact with groundwater will increase the chloride concentration in the resulting water to a greater extent than it will increase the bromide concentration in the water. This causes an increase in the Cl/Br ratio of the water. Halite-dissolution brines typically have Cl/Br ratios of more than 400 (Whittemore et al., 1981). In contrast, "connate" formation waters will have Cl/Br ratios similar to or lower than those of seawater (i.e., lower than 500) according to Whittemore et al. (1981).

Figure 25 plots  $\text{Cl}^-$  versus  $\text{Br}^-$  concentrations from Diamond Y Springs and wells in the study area. The Cl/Br = 500 line is the typical ratio for modern seawater. Waters including halite dissolution brines would display a Cl/Br ratio greater than 500, and plot above the line. By contrast, oil-field brines would show an enrichment in Br relative to Cl, and would therefore plot below the seawater line. All of the data but one plot above the line suggesting the source of solutes in spring flow is from halite dissolution, and not from oil field waters (Whittemore *et al.*, 1981).

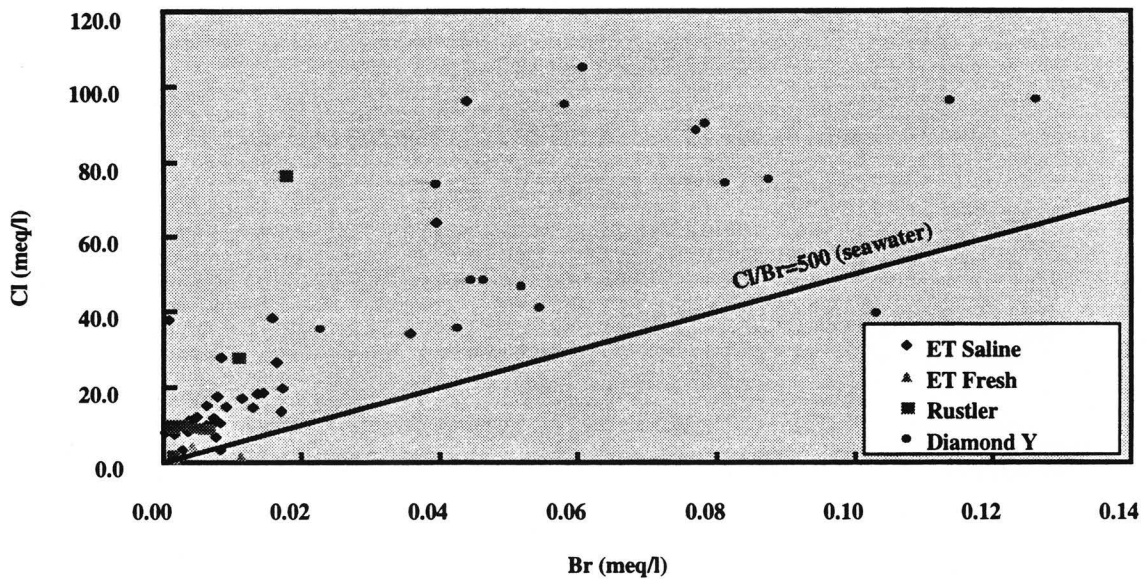


Figure 25. Plot of Cl versus Br

Tracing the origin of the solutes requires evaluation of the chemical processes affecting the Diamond Y Springs chemistry. These are carbonate dissolution and precipitation, gypsum and halite dissolution, and ion exchange. Ascertaining the springwater geochemical evolution also requires consideration of evapotranspiration and mixing.

There are at least two major sources of gypsum and halite under the study area: (1) the Castile and Salado Formations and (2) the Rustler Formation. Only the Rustler is documented to be a permeable unit with the potential for cross-formational flow into the overlying units. Nearly all Rustler wells in the study area are artesian. This includes well 53-01-203 (Sibley) located 0.5 mi

(800 m) south of DY-1 (see figure 12). If conduits such as the Diamond Y fault system are available, Rustler water could flow up into the Edwards-Trinity.

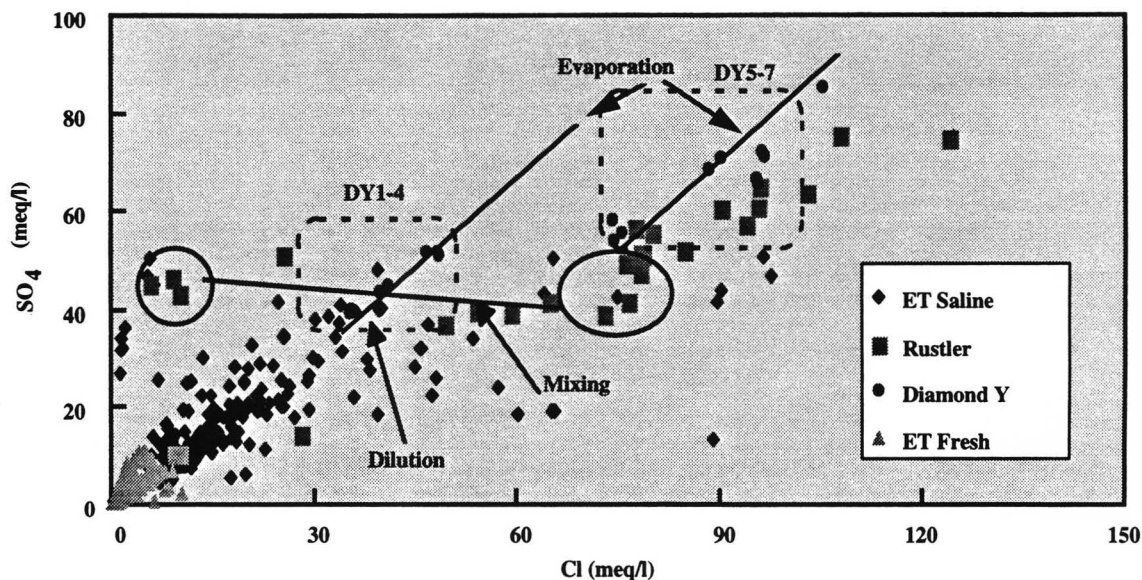


Figure 26. Plot of SO<sub>4</sub> versus Cl

A plot of two conservative ions (figure 26) such as sulfate versus chloride provides further insight into the origins and evolution of the water discharging at Diamond Y Springs. Figure 26 re-confirms Veni's assertion regarding the existence of two distinct groups of springs within the Diamond Y Springs system. Their composition appears to be the result of mixing between two types of Rustler waters: (1) a sulfate-facies, less saline water, characteristic for wells located in, or west of the Pecos trough and, (2) a chloride-facies, more saline water, characteristic for wells located northeast of the study area. The two groups of springs, designated on the plot as DY1-4 and DY5-7, stem from the

same mixing line, at different chloride concentrations, and proceed upwards, along their own evaporation lines. Significantly, from each of the spring groups the ones closest to the "parent" mixing line are DY-1 and DY-6, the locations with the largest flow and, probably, subject to the least evaporation. Actually, DY-1 may be undergoing a slight dilution, because it is below the mixing line. Farther down the stream than from DY-1, water has undergone more evaporative concentration and is encountered at DY-2, DY-3, and DY-4. These data are ordered along the line according to the degree of evaporation. The same reasoning applies to the second spring group (DY-6, DY-5, and DY-7). DY-6 plots closest to the Rustler mixing line, although it is farther away from it than DY-1. DY-6 stems from the chloride-rich Rustler endmember, and follows an evaporative path similar to that of the DY 1-4 group. Most of the points for ETF and ETS waters cluster in the "diluted" area of the chart.

The head distribution in the Rustler aquifer shows that mixing of the two Rustler water facies is physically possible. As shown on figure 7 (p. 40), flow defined on the Rustler potentiometric surface map converge towards Diamond Y area, which would mix sulfate-facies groundwater from the west and chloride-facies groundwater from the northeast. Furthermore, the evaporative salt crust, ubiquitous in the Diamond Y Springs area has been identified as polyhalite by Land (1995, personal communication). The only known source of polyhalite in

the area is the "potash district" north of the Pecos, hosted by rocks immediately adjacent to the Rustler. This suggests that Rustler water from the north may be indeed flowing southwards under the Pecos River to discharge in the study area.

### **Geochemical Modeling**

To further test the hypotheses regarding the origin and evolution of springflow at Diamond Y Springs, the geochemical mass-balance modeling program NETPATH (Plummer et al, 1994) was employed to simulate groundwater mixing between endmember Rustler waters and evaporation of springflow from DY-1 and DY-6. The goal of this modeling exercise was to identify a realistic scenario where (1) saline and dilute Rustler waters would mix and evolve on paths leading to the DY-1 and DY-6 chemical composition, and (2) DY-1 and DY-6 waters would evaporate resulting in waters with the DY-3 and DY-7 chemical composition, respectively.

It is important to stress out that the mass-balance modeling of NETPATH applies only to the case of chemical steady state along a flow path. Some aquifer systems might be in a transient state, where water entering the aquifer today has significantly different chemical and isotopic composition from the recharge that has evolved chemically to the presently observed final water. Using the program in such instances could produce misleading results. Also, in

constructing net geochemical mass-balance reactions, it is necessary to select truly evolutionary initial and final waters, such as waters sampled along a flowpath in a confined regional groundwater system. The program has no means of checking whether waters are evolutionary, and it will consequently always report reactions if it can find them. Hydrogeologic intuition is required to overcome this problem. Another limitation of NETPATH is that it does not consider the uncertainty in the analytical data, and how this uncertainty affects modeling results. Because of analytical errors or failure to analyze for all dissolved species, water analyses rarely are exactly charge-balanced. These errors are then incorporated in the computed masses of one-component phases such as CO<sub>2</sub> gas, N<sub>2</sub> gas, etc. The problem can be acute with high-salinity waters, where even a small percentage of charge imbalance can cause tens of millimoles of CO<sub>2</sub> to be computed erroneously. Also, though not directly pertaining to the Diamond Y springs study, NETPATH does not explicitly account for hydrodynamic dispersion. The mixing effects due to hydrodynamic dispersion cannot be separated from the analytical data and become incorporated into the implied mass transfer.

Ion concentrations for locations DY-1, DY-3, DY-6, DY-7, Belding 26, and 45-42-700 were first entered into the program. All data sets but the last one are representative for samples taken during June 1995. September 1990 data was

used for well 45-42-700 due to the unavailability of a June 1995 analysis. The DY-5 sample displayed a -10% charge imbalance and it was not included in this model. There was suspicion of the DY-2 sample being non-evolutionary (mostly evaporated rainwater), reason for which it was eliminated as well. The NETPATH output files displaying the modeling results are shown in the Appendix.

Groundwaters from Belding well #26 (“dilute Rustler”) and well 45-42-700 (“saline Rustler”) were first mixed in an attempt to obtain a final water with the composition of DY-1. The results indicate that a mixture of 53% “dilute Rustler” and 47% “saline Rustler” waters diluted by a factor of 1.258 could produce water with the chemical composition of DY-1. From the initial solutes contained in 1 kg of Rustler mix, 7.8 mmol of CO<sub>2</sub> gas would be released into the atmosphere, with the dissolution of 6.2 mmol of dolomite, and the exchange of 2.3 mmol of Ca for Na.

The same Rustler endmembers were then mixed with the goal of obtaining a final water with the composition of DY-6. The chosen model predicts that DY-6 water could be produced by mixing 14% “dilute Rustler” and 86% “saline Rustler” waters with the dissolution of 12.5 mmol dolomite, the precipitation of 7.5 mmol polyhalite, and the outgassing of 21.5 mmol CO<sub>2</sub> gas

per 1 kg of Rustler mix. The model also predicts 0.97 mmol Ca would be exchanged for Na, and no evaporation or dilution was considered.

Another model was developed to test the hypothesis of DY-1 water evolving into DY-3 water through evaporation. The results indicated that the solutes in 1 kg of DY-1 water would be concentrated by a factor of 1.219, leaving 820.067 g H<sub>2</sub>O remaining to produce water of composition of DY-3. Or, every kg of DY-3 water has been evaporated on the average from 1.219 kg H<sub>2</sub>O from the DY-1. To the initial solutes in 1 kg of DY-1 water 1.61 mmol of gypsum and 4.09 mmol of halite would be added by dissolution, and 1.48 mmol Ca would be exchanged for Na.

Finally, water with the DY-7 chemical composition was successfully produced by applying a 1.287 evaporation factor to the DY-6 water. The main chemical processes taking place were precipitation of calcite (2.09 mmol/kg H<sub>2</sub>O), polyhalite (0.28 mmol/ kg H<sub>2</sub>O), CO<sub>2</sub> outgassing (0.8 mmol/kg H<sub>2</sub>O), and ion exchange (1.22 mmol Na exchanged for Ca per kg H<sub>2</sub>O).

Keeping in mind the limitations of mass-balance modeling, it could be proposed that NETPATH results support the findings outlined in the preceding section: (1) DY-1 and DY-6 seem to be the products of mixing between two distinct types of Rustler water and, (2) DY-3 and DY-7 could be reasonably well interpreted as products of evaporative concentration of DY-1 and DY-6,

respectively. The main chemical reactions identified through the analysis of ion plots have been successfully reproduced by NETPATH.

The validity of the models depends in part on the selection of phases. The models could be further refined by exactly identifying the constituent in the pools' sediment, task which has not been accomplished yet. Other complicating factors such as diffusion of solutes into the sediment, historical variation in inflow composition could be considered in NETPATH, but their evaluation would require additional data.

In conclusion, the processes controlling the evolution of Diamond Y Springs chemistry are carbonate, gypsum, and halite dissolution/precipitation, ion exchange, evaporation, and water mixing. Water from the Rustler aquifer probably accounts for most of the discharge at the springs.

## **6. FLOW SYSTEM MODELING**

### **A. Methods**

Numerical models provide quantitative analysis of groundwater systems. To develop a numerical model of an aquifer, it is necessary to understand conceptually how that system behaves. Numerical solutions approximate continuous partial differential equations with a set of discrete equations in time and space. These discrete equations are combined to form a system of algebraic equations that must be solved at each time step.

The following two sections provide brief discussions about boundary and initial conditions and finite-difference methods in numerical modeling.

#### **Boundary and Initial Conditions**

In order to obtain a unique solution of a partial differential equation corresponding to a given physical process, additional information about the physical state of the process is required. This information is described by boundary and initial conditions. For steady-state problems only boundary conditions are required, whereas for unsteady-state problems both boundary and initial conditions are required. Mathematically, the boundary conditions include the geometry of the boundary and the values of the dependent variable or its derivative normal to the boundary. In physical terms, for groundwater applications the boundary conditions are generally of three types: (1) specified

head; (2) specified flux; or (3) head-dependent flux. The initial conditions are, in fact, the values of the dependent variable specified everywhere inside the boundary.

### **Finite-Difference Methods**

One numerical approach that has been applied successfully to the groundwater flow equation involves finite-difference approximations. When using finite-difference methods to solve a partial differential equation, a grid is first established throughout the region of interest. For two-dimensional, areal problems, a grid is overlaid on a map view of the aquifer. Associated with the grids are node points that represent the position at which the solution of the unknown (head, for example) is calculated. Each numerical approximation leads to an algebraic equation for each node in the grid system. These algebraic equations for each node point are combined to form a matrix equation, that is, a set of  $N$  equations with  $N$  unknowns, where  $N$  is the number of nodes. The general form of these equations, written in matrix form is:

$$\underline{A} \underline{h} = \underline{d},$$

where  $\underline{A}$  is a matrix containing coefficients related to grid spacing and to aquifer properties, such as transmissivity;  $\underline{h}$  is a vector containing the dependent

variables to be determined, like head values at each node; and  $\underline{d}$  is a vector describing all known information, like pumpage and boundary conditions information. Generally, a matrix equation can be solved numerically by one of two basic ways: (1) direct and (2) iterative. In *direct methods* a sequence of operations is performed only once, providing a solution that is exact, except for computer round-off error. *Iterative methods* such as were used in this study, solve the equations by a process of successive approximation. This involves making a guess at the matrix solution, then improving this guess through an iterative process until an error criterion is reached.

### **B. Groundwater Flow Modeling in the Diamond Y Springs Region**

The U.S. Geological Survey modular flow model MODFLOW (McDonald and Harbaugh, 1988) was used to develop a one-layer, two-dimensional horizontal model for the Edwards-Trinity aquifer. The main purpose of this exercise was to test the validity of the conceptual flow model outlined in section 4.C. The secondary goal was to evaluate qualitatively the impact of groundwater pumping on the flow system.

MODFLOW uses a finite-difference approximation to solve the steady-state, groundwater flow equation:

$$\partial / \partial x (K_x \partial h / \partial x) + \partial / \partial y (K_y \partial h / \partial y) = 0$$

where x and y are cartesian coordinates aligned with the major axes of the flow system, with  $K_x$  and  $K_y$  as the hydraulic conductivities in the x and y directions; and h is hydraulic head.

The fundamental simplifying assumptions used to construct and apply the model include:

- (1). Flow in the aquifer is in accordance with Darcy's law;
- (2). Flow in the aquifer is horizontal; and
- (3). Density of the water is spatially and temporally constant;

### **Model Setup**

The model grid is block-centered, and consists of 52 rows and 46 columns. The cells are squares with the side of 7845 ft (2391 m), for a total of 1866 cells

Boundary conditions were selected to correspond as closely as possible with actual model boundaries (figure 27). A no-flow boundary was established at the northern edge of Glass Mountains, generally recognized as the southern boundary of the Edwards-Trinity aquifer.

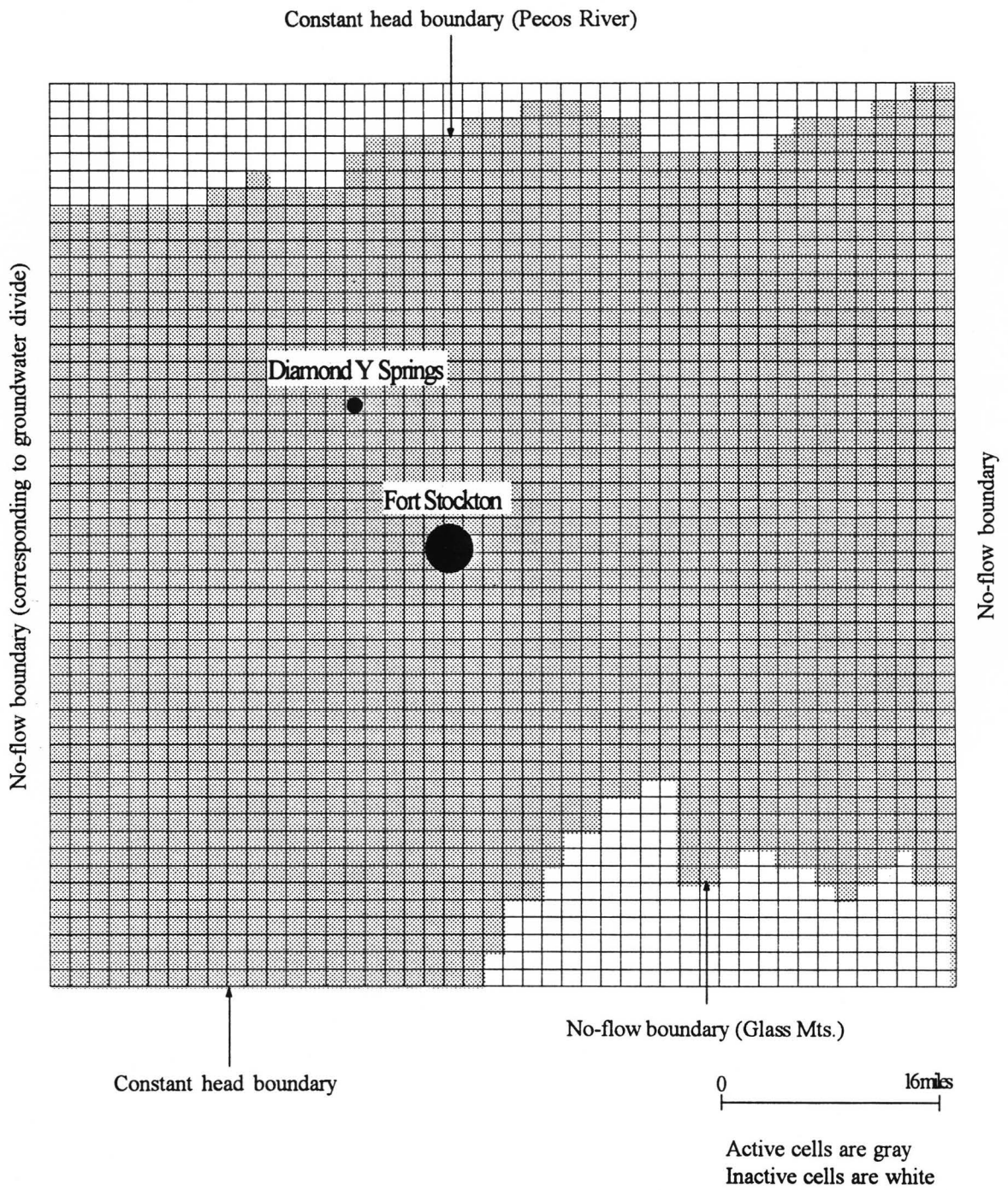


Figure 27. Model grid, boundaries, and active cells

The northern boundary of the model is represented by the Pecos River, and is treated as constant head. A groundwater divide, modeled as a no-flow boundary, is located 4 mi (6.5 km) west of and parallel to Pecos/Reeves county line (LaFave, 1987). A no-flow boundary limits the model domain to the east. This boundary coincides with a presumed groundwater divide (Small and Ozuna, 1993).

The governing equations of the model are solved with the preconditioned conjugated gradient solver package of MODFLOW (Hill, 1990). The model includes a routine that allows cells to rewet during model iteration (McDonald and Harbaugh, 1991). This routine is used because very large head changes during the first few model iterations resulted in the dewatering of an excessive number of cells. As the numerical model begins to converge to an acceptable solution, dry cells must rewet so that the cells are included in the final solution. Dry cells are not allowed to rewet in MODFLOW unless this routine is used.

#### **Definition of Hydraulic Conductivity Zones**

Assigning correct conductivities to grid cells is critical for a realistic flow model. The main sources of accurate conductivity values are pump tests and specific capacity data. The strata are then separated into zones that correlate

with spatial variations of conductivity. The conductivity zones can be refined using lithologic, structural, and geologic descriptions.

The Texas Water Development Board (TWDB) records for Pecos County contain data for only five pump tests, all in wells with partial penetration, yielding conductivity values between 1.4 and 7.2 ft/day ( $5 \cdot 10^{-6}$  and  $2.4 \cdot 10^{-3}$  m/s). Given this scarcity of pump test data, the values for hydraulic conductivity had to be estimated for most of the model's active domain.

Hydraulic conductivities were assigned to correspond with major rock units and structural features as follows: (1) the north-south-crossing Belding-Coyanosa trough, and (2) the Edwards-Trinity aquifer area bounding the trough at west and east.

On the base of published values (Myers, 1969), geological descriptions (Armstrong and McMillion, 1961; Adkins, 1927), and typical permeability values for different types of rocks (Domenico and Schwartz, 1990, p.65), rocks of the Pecos trough were assigned a hydraulic conductivity of 7.2 ft/day ( $2.4 \cdot 10^{-3}$  m/s). The hydraulic gradient is slightly steeper outside the trough (figure 10), suggesting a lower transmissivity for the rocks of the Edwards-Trinity "proper". A conductivity of 1.4 ft/day ( $5 \cdot 10^{-6}$  m/s) was specified for this region, to account for the reduced saturated thickness of the aquifer (Small and Ozuna, 1987). The distribution of conductivities across the model area is shown in figure 28.

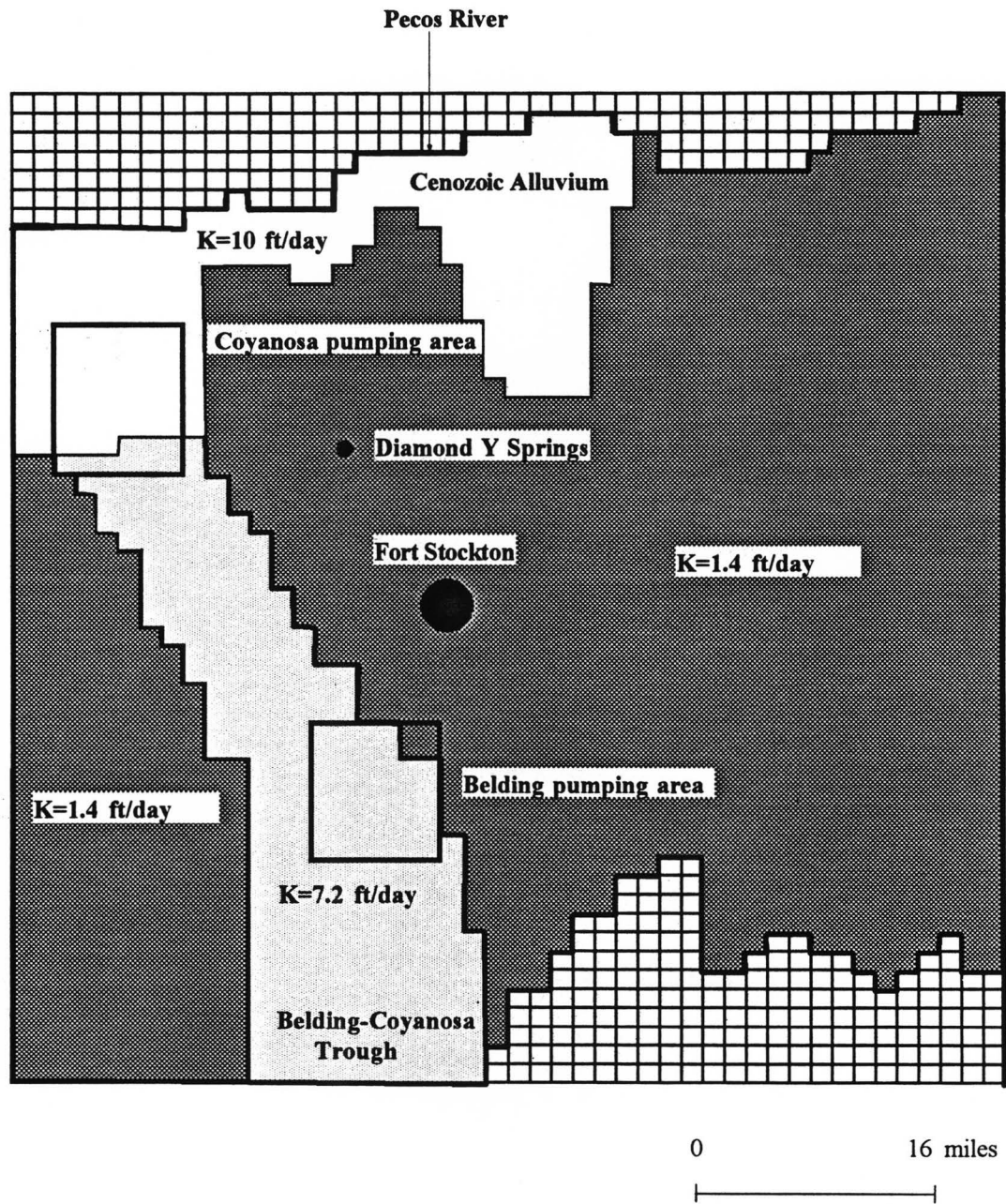


Figure 28. Assigned conductivity domains and pumping cells

## **Recharge and Discharge**

Cross-formational flow from the Rustler aquifer is probably an important mechanism for recharge to the Edwards-Trinity flow system in the study area, although there is no published estimate for its contribution to the water budget. The assigned recharge rates and areas are shown in figure 29. Distributed recharge by rainfall is assumed to be negligible over much of the model domain, and the model prescribes a 0.22 in/yr (5.5 mm/yr) recharge to a 1-mile (1.6 km) wide band around Glass Mountains. The rationale for these assumptions follows:

- (1) In the study region potential evapotranspiration was estimated to be about nine times higher than the precipitation rate (Armstrong and McMillion, 1961).
- (2) In arid environments it is commonly assumed that distributed recharge is negligible over much of the flow system, and that groundwater was recharged either long ago during less arid conditions, or only at the highest elevations of the system where precipitation is more abundant (Hibbs and Darling, 1993).
- (3) Historical and recent water geochemistry and tritium data indicate little modern recharge in this flow system.

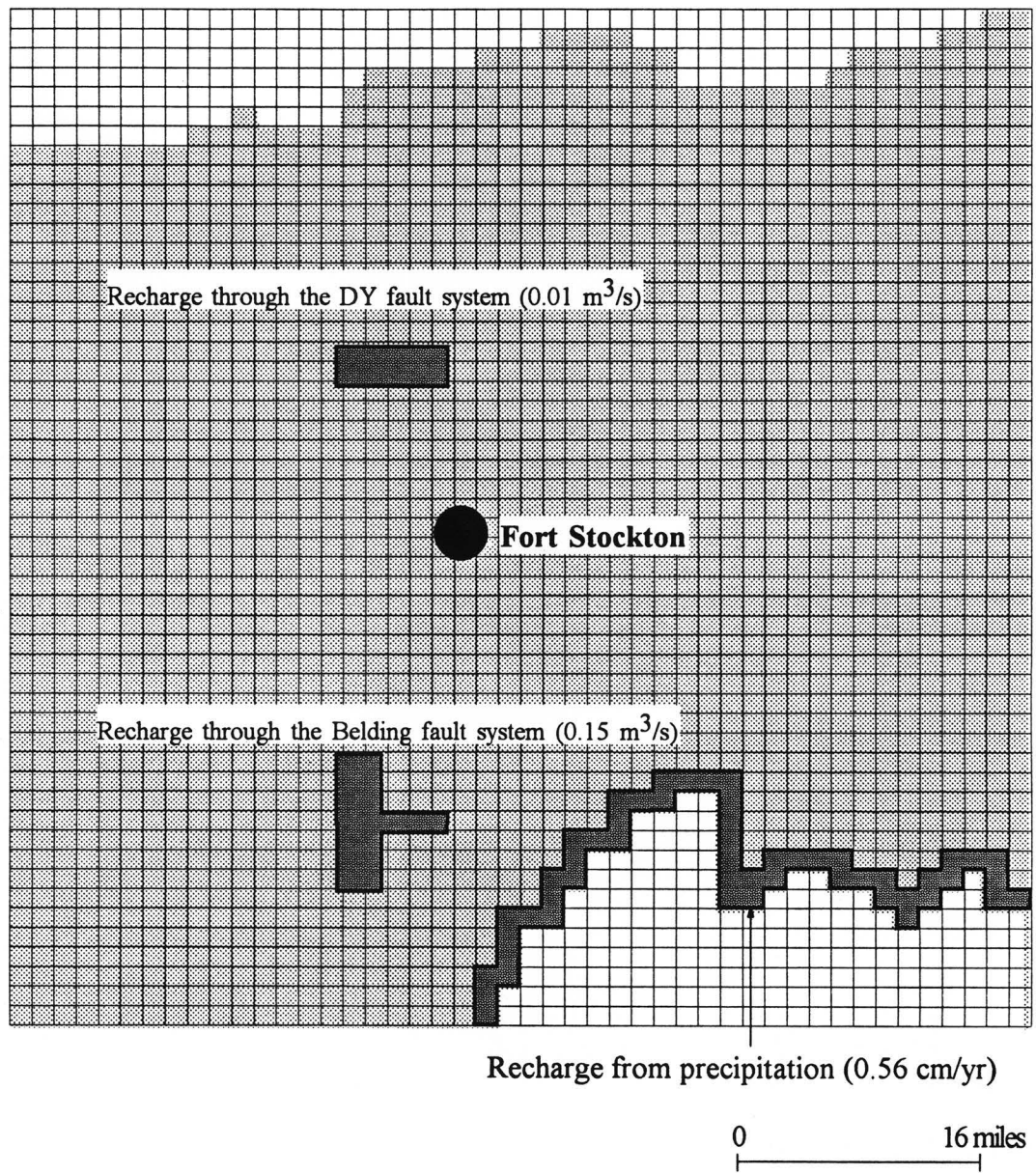


Figure 29. Modeled rates of recharge to the Edwards-Trinity aquifer

Modern discharge occurs mainly by irrigation pumping, about 77,000 acre-ft/yr or 3.01 m<sup>3</sup>/s (Rees and Buckner, 1977), being extracted through two major irrigation areas: Belding and Coyanosa. Before groundwater development began in Pecos County, about 2000 acre-ft/yr or 0.08 m<sup>3</sup>/s (Rees and Buckner, 1977) were discharged by springs, an amount included in the model-calibration runs. An average of 4,000 acre-feet per year are pumped for municipal use across Pecos County (TWDB groundwater database).

### **Calibration**

The model was calibrated by matching the simulated hydraulic heads with the measured hydraulic heads. This was accomplished by varying the amount of cross-formational flow to the Edwards-Trinity aquifer through the Belding and Diamond Y fault systems until a good agreement between the simulated and pre-1940 measured heads was obtained. The upwards flow of deeper water was simulated by assigning a positive flux to the grid cells overlaying the Belding and Diamond Y faulted areas. After repeated trials the head distribution map shown in figure 30 was obtained, which visually matches the steady-state, pre-1940 water level map presented here for comparison. The best match between simulated and measured heads was achieved when the amount of recharge from cross-formational flow through the Belding fault system was set to 3,800 acre-ft/year, (0.15 m<sup>3</sup>/s).

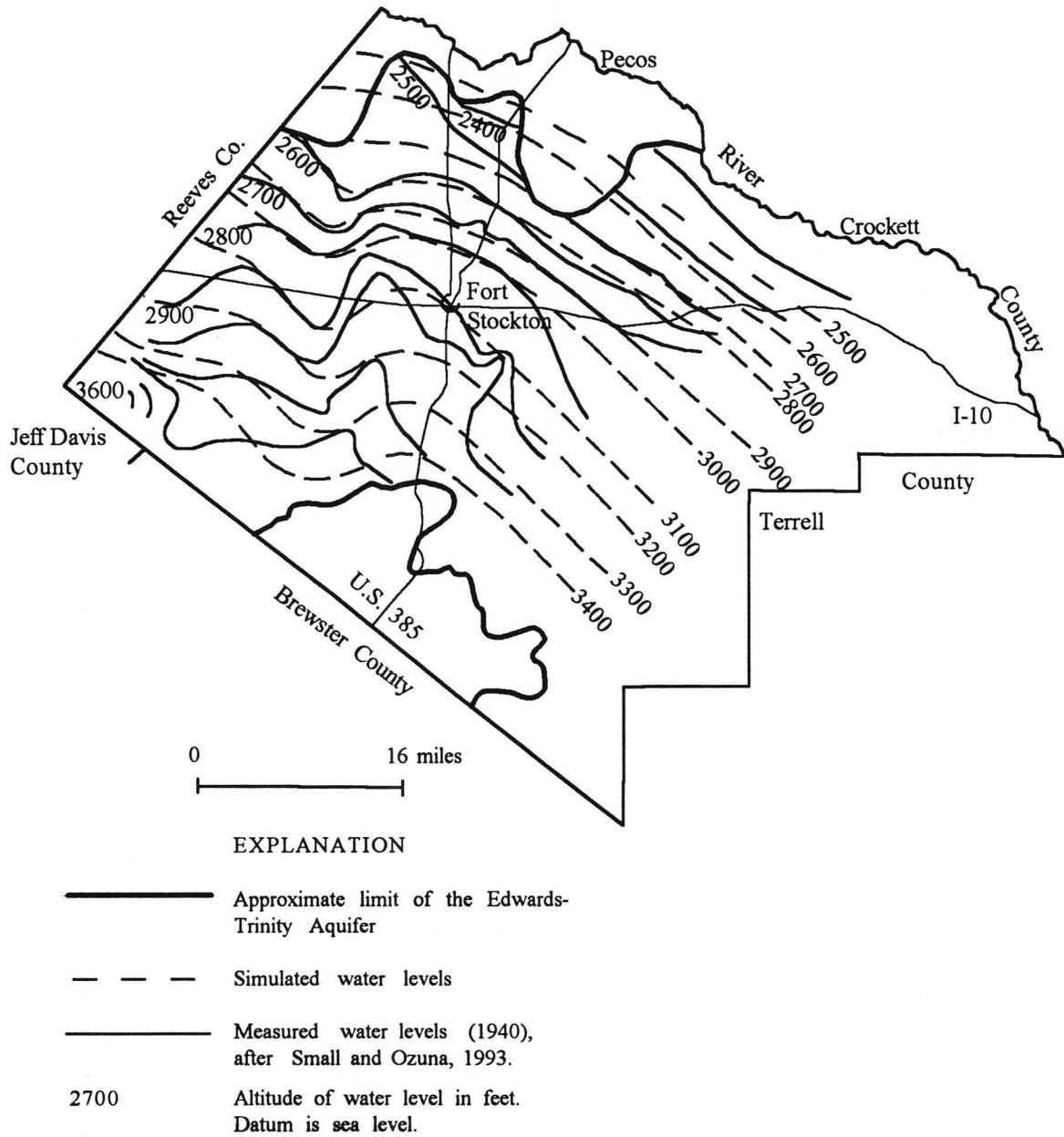


Figure 30. Calibrated and measured water levels in the Edwards-Trinity aquifer

Vertical flow from the Rustler aquifer through the Diamond Y fault system was set at 260 acre-ft/year (0.01 m<sup>3</sup>/s), based on discharge measurements in well 53-01-203.

### Model Results and Discussion

Despite the lack of conductivity data, the calibration runs show that the conceptual flow model is feasible. The simulated head map agrees with the interpreted water table and reproduces its main features: the potentiometric high and steep gradient around Glass Mountains, the low near Pecos River, the flatter gradient and isoline curvature in the Belding-Coyanosa trough. The main controls on the steady-state regional flow pattern are: (1) the permeability contrast between the Belding-Coyanosa trough fill and the Edwards Formation and (2) the amount of cross-formational flow recharging the Edwards-Trinity aquifer through the Belding fault system. Table 5 presents the results of water balance calculations for the whole model domain, as performed by MODFLOW:

Table 5. WATER BALANCE OF THE WHOLE MODEL DOMAIN

(steady-state calibration runs)

FLOW TERM	IN(m <sup>3</sup> /s)	OUT(m <sup>3</sup> /s)	IN-OUT(m <sup>3</sup> /s)
Constant head	0.287	1.059	-0.772
Recharge	0.772	0.000	0.772
SUM	1.059	1.059	0.000

Steady-state simulations are commonly employed during model calibration runs based on the assumption that the pre-development flow system is at steady-state. However, this might not be the case with the Edwards-Trinity aquifer: historical discharge measurements in the Comanche Springs (see appendix) suggest a constant decline in springflow before pumping began in the area.

The secondary goal of this modeling exercise was to evaluate qualitatively the impact of groundwater pumping on the flow system. In a series of transient simulations, pumping stresses were added to the cells covering the irrigation districts at Coyanosa, Belding-Fort Stockton, Bakersfield, and Girvin. The transient model began in 1950 with the calibrated, steady-state head distribution and ran until 2020. This 70-year interval was divided in seven stress periods each of them covering a decade. Each stress period consisted of ten time steps, the model thus being able to calculate heads in yearly time increments. Pumping rates were assumed to be constant within each stress period and were based on published data by the Texas Water Development Board (table 6). Where enough data were available, yearly pumping values were averaged and assigned to the corresponding decade. Where systematic data were lacking, the available one-year pumping figures were assumed to be representative of the

decade they belonged in; for example, 1958 data (Rees, 1980) were assigned for the decade 1950-1960. Future (2000-2020) pumping rates were based on the TWDB water-use projections (1996 Consensus Water Planning).

Table 6. Pumping rates used in the transient flow simulations

PUMPAGE (ACRE-FEET/YEAR) BY IRRIGATION AREA				
STRESS PERIOD	Belding-Ft. Stockton	Coyanosa	Girvin	Bakersfield
1950-1960	122,580	177,304	15,000	18,000
1960-1970	76,545	109,645	9,322	11,365
1970-1980	63,574	50,369		
1980-1990	55,020	14,495		
1990-2000	54,863	16,388		
2000-2010	53,970	16,121		
2010-2020	52,998	15,831		

Figure 31 shows how the simulated head map for 1987 compares to that year's real data (Small and Ozuna, 1993). Modeled heads are generally higher, and the potentiometric surface they define does not show the relief of the field data. There are, however, several important similarities between the modeled and interpreted head maps like lower gradient and line curvature induced by the

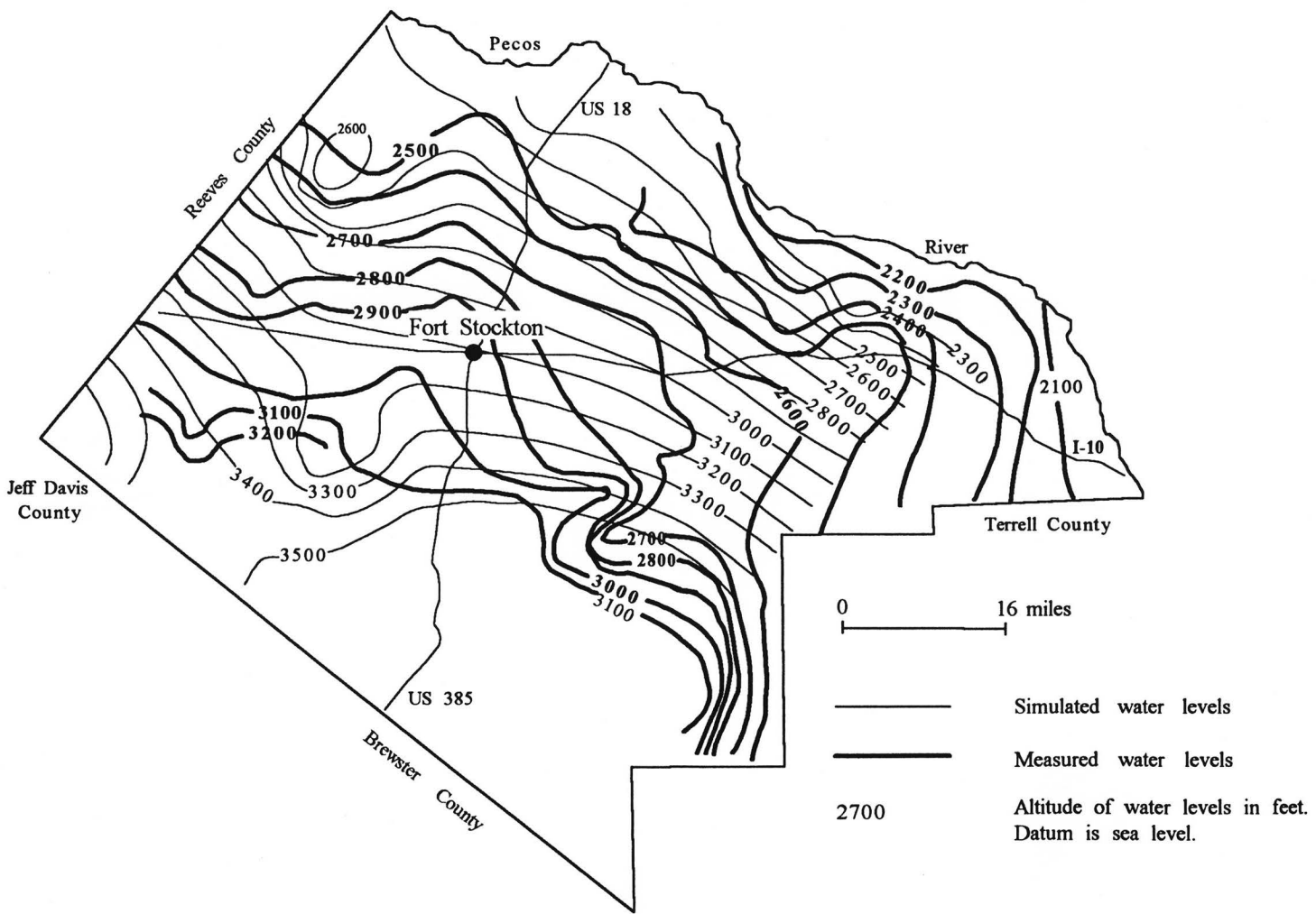


Figure 31. Simulated (after-pumpage) and measured water levels in the Edwards-Trinity aquifer. 1987 head map after Small and Ozuna (1993).

Belding-Coyanosa trough, the steep flow gradient around the Glass Mountains, the change in head due to pumpage in the Coyanosa, Belding-Fort Stockton, Bakersfield, and Girvin areas. The modeled and interpreted water level contours do not match in eastern Pecos County, possibly due to a perched water table intercepted in wells south of Bakersfield. The effects of pumpage are more visible on the simulated head map, possibly because of underestimated conductivities. This could explain the limited areal effect of groundwater withdrawals on the modeled head map, and why inflexions in contours can still be seen in Girvin and Bakersfield areas 20 years after the simulated pumping ceased.

Figure 32 presents the water levels the model predicted for the year 2020. The eastern half of the model area is unchanged, except for the Girvin and Bakersfield areas, which appear to have recovered when compared to the 1987 situation. On the western side irrigation pumping continues to affect the water levels: the Coyanosa cone of depression is somewhat smaller, following big reductions in pumping rates; a new cone of depression develops in the Belding-Fort Stockton district, even if groundwater withdrawal now takes place at diminished rates. Also, the model shows that an area of about 10 mi<sup>2</sup> in the Belding area might go dry altogether (see figure 32).

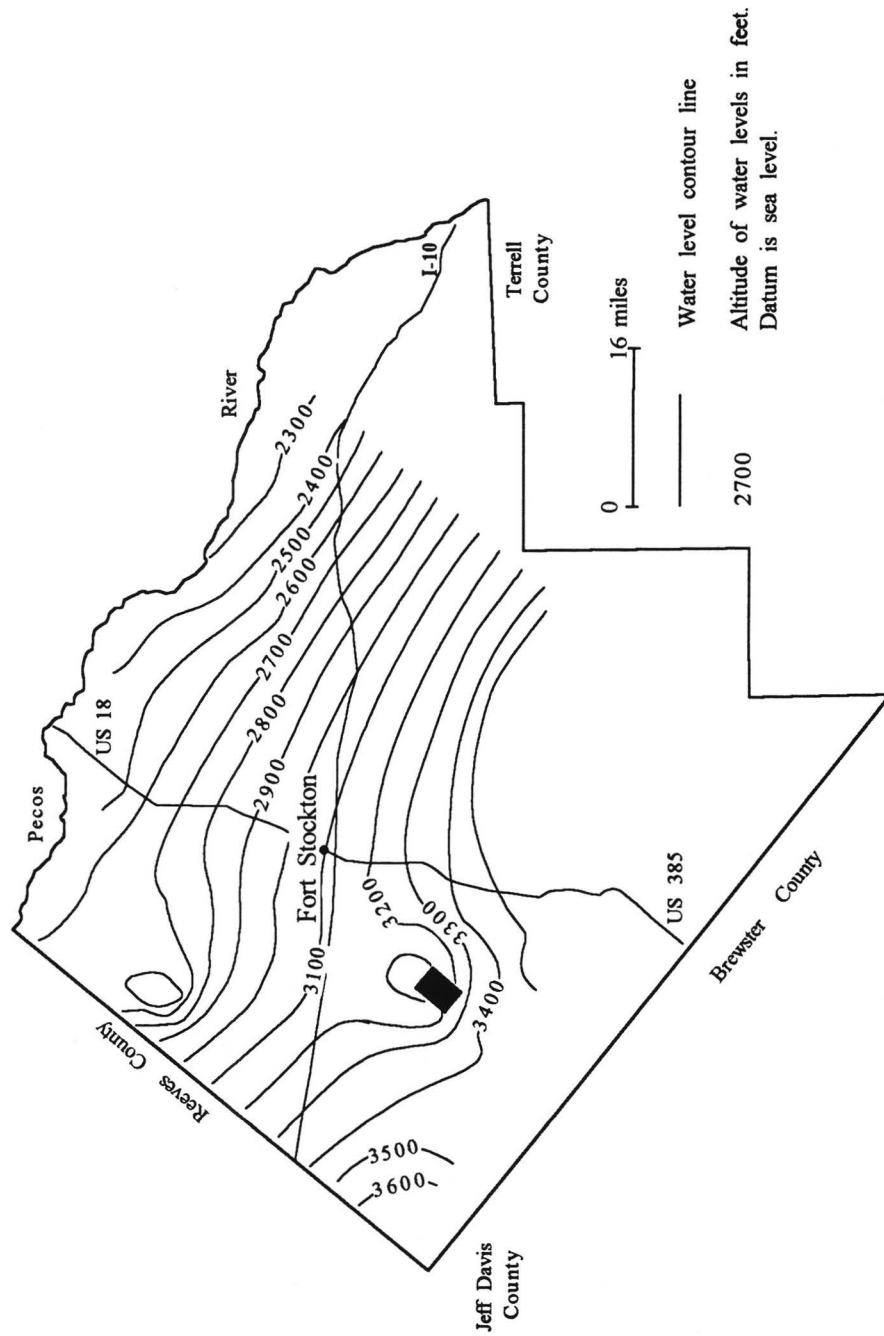


Figure 32. Simulated water level map for the Edwards-Trinity aquifer, year 2020

Obviously, the model scenario does not match the situation in the field. Present-day groundwater withdrawals are 20 percent of what they were three decades ago. Because of this decline in withdrawals, water levels in Belding and Coyoanosa wells started to recover during the 1980's (Small and Ozuna, 1993).

This impasse might be avoided by employing a two-layer flow model. As pumpage lowers the heads in the Edwards-Trinity, an increased amount of cross-formational flow recharges the aquifer through the Belding fault system (due to the larger head difference between the Rustler and the Edwards). A second layer would allow for simulating time-dependent recharge fluxes in the Belding area. Adding a second layer, however, would require detailed information regarding heads in the Rustler and their variation with time, as well as specific yield data. Such knowledge is not yet available and this modeling effort was pursued no further. This clearly illustrates that the results of a computer model are as accurate as the data that go into it, and great precautions should be taken when using groundwater flow modeling as a predicting tool.

#### **Model Limitations**

Overall, the model results agree with the conceptual flow hypothesis formulated in section 4C. The model presents a simplified picture of the hydrostratigraphy of the area, as defined by major structural and geologic features (such as the Belding-Coyoanosa trough). The simulated pre-pumping

hydraulic heads were fairly well matched with the measured heads, but the model's reliability is limited by the lack of information on vertical and horizontal hydraulic conductivity, effective porosity, and hydrostratigraphy. The limiting factors that are pertinent to this modeling effort include:

- (1) the assumption that fractured rock, at large scales, is equivalent to a porous medium.
- (2) the assumption that groundwater flow is restricted to the plane of the planar model.
- (3) the assumption that each of the zones has a constant horizontal hydraulic conductivity and effective porosity.

## 7. CONCLUSIONS

This study presents the results of local hydrogeologic and hydrochemical investigations at Diamond Y Springs and vicinity, and regional groundwater studies in a 660 mi<sup>2</sup> (1710 km<sup>2</sup>) area of north-central Pecos County, Texas.

Diamond Y Springs Preserve is the only remaining natural habitat for the Leon Springs pupfish (*Cyprinodon bovinus*), a federally listed endangered species.

The major aquifers in the area are the Cretaceous Edwards-Trinity (Plateau) aquifer and the Permian Rustler aquifer. These are separated in the western portion of the area by the Triassic Tecovas Formation that is a siltstone/shale aquitard. East of Fort Stockton Cretaceous rocks rest unconformably upon permeable Triassic and Permian rocks. Diamond Y Springs issue from the edge of an alluvial valley at or near the contact with Cretaceous carbonate rocks.

A structural trough runs roughly N-S through western Pecos County. High transmissivities in the trough make it a sink for the flow in the Edwards-Trinity aquifer. Rustler wells in the vicinity of Diamond Y springs are flowing so that an upward potential for Rustler water discharge is present at the springs. The data confirm the hypothesis of Rustler waters as the chief source of flow at Diamond Y Springs today. Dissolution of halite and gypsum, base exchange,

evaporation, and mixing of the two hydrochemical facies of the Rustler with a subsidiary components of recent local waters can explain the water chemistry and isotopic composition. Evapotranspirative concentration of the brackish waters in the alluvial valley raise spring water salinities to levels higher than those found in either the Rustler or Edwards Trinity aquifers.

The groundwater flow model suggests the main controls on regional flow pattern are: (1) the permeability contrast between the Belding-Coyanosa trough fill and the Edwards Formation, (2) the amount of cross-formational flow recharging the Edwards-Trinity (Plateau) aquifer through the Belding fault system, (3) the amount of cross-formational flow recharging the Edwards-Trinity (Plateau) aquifer from the Rustler aquifer, and (4) the amount of groundwater pumped in the Belding-Fort Stockton and Coyanosa irrigation districts.

## 8. REFERENCES

- Adams, J.E. (1944). Upper Permian Ochoa Series of Delaware Basin, West Texas and southeastern New Mexico. *American Association of Petroleum Geologists Bulletin*, v. 28, p.1596-1625.
- Adkins, W.S. (1927). The geology and mineral resources of the Fort Stockton Quadrangle. *Bureau of Economic Geology, University of Texas Bulletin*, 2738, 166p.
- Anderson, R.I., Dean, W.E., Jr., Kirkland, D.W., and Snider, H.I. (1972). Permian Castile varved evaporite sequence, West Texas and New Mexico. *Geological Society of America Bulletin*, v. 83, p.59-85.
- Anderson, R.Y., Kietzke, K.K., and Rhodes, D.J. (1978). Development of dissolution breccias, northern Delaware Basin, New Mexico and Texas, *in* Austin, G.S., ed., *Geology and mineral deposits of Ochoan rocks in Delaware Basin and adjacent areas*. New Mexico Bureau of Mines and Mineral Resources Circular 159, p.47-52.
- Armstrong, C.A., McMillion, L.G. (1961). Geology and ground-water resources of Pecos County, Texas. *Texas Board of Water Engineers Bulletin* 6106, 1, 2, 536p.
- Audsley, G.L. (1956). Reconnaissance of ground-water development in the Fort Stockton area, Pecos County, Texas. USGS open-file report.
- Bachman, G.O. (1984). Regional geology of Ochoan evaporites, northern part of Delaware Basin. *New Mexico Bureau of Mines and Mineral Resources Circular* 184, 24p.
- Barnes, V.E. (1983). Fort Stockton sheet. The University of Texas at Austin, Bureau of Economic Geology. *Geologic atlas of Texas*, scale 1:250,000.
- Brune, G. (1975). Major and historical springs of Texas. *Texas Water Development Board Report*, 189, p.56-99.
- Cummins (1890). The Permian of Texas and its overlying beds. *Geol. Surv. Texas*, 1<sup>st</sup> Ann. Rept., p.189-190.

- Darling, B.K., Hibbs, B.J., and Dutton, A.R. (1993). Ground-water hydrology and hydrochemistry of Eagle Flat and surrounding area. The University of Texas at Austin, Bureau of Economic Geology, Contract Report (92-93)-0910, 137p.
- DeFord, R.K., Riggs, G.D. (1941). Tansill Formation, West Texas and southeastern New Mexico. American Association of Petroleum Geologists Bulletin, v. 25, p.1713-1728.
- Dietrich, J.W., Owen, D.E., and Shelby, C.A. (1983). Van Horn-El Paso sheet. The University of Texas at Austin, Bureau of Economic Geology. Geologic Atlas of Texas, scale 1:250,000.
- Domenico, P.A., Schwartz, F.W. (1990). Physical and Chemical Hydrogeology. John Wiley & Sons, 824p.
- Dougherty, J.P. (1975). Evaporation data in Texas. Compilation report January 1907-December 1970. Texas Water Development Board, Report 192, 237p.
- Eager, G.P. (1983). Core from the lower Dewey Lake, Rustler, and upper Salado formations, Culberson County, Texas *in* Shaw, R.L. and Pollan, B.J., eds., Permian Basin cores - a workshop: Permian Basin Section, Society of Economic Paleontologists and Mineralogists, p.273-283.
- Eifler, G.K. (1976). Pecos sheet. The University of Texas at Austin, Bureau of Economic Geology. Geologic Atlas of Texas, scale 1:250,000.
- Faure, G. (1986). Principles of Isotope Geology. New York, John Wiley & Sons, 589p.
- Gester, G.C., Hawley, H.J. (1929). Yates field, Pecos County, Texas, *in* Structure of typical American oil fields. Tulsa, Oklahoma, American Association of Petroleum Geologists Bulletin, v. 2, p.480-49.
- Geyh, M.A. (1990) Absolute Age Determination-Physical and Chemical Dating Methods and Their Application. New York, Springer, 503p.
- Hall, W.L. (1952). Geology of Maverick area, Culberson and Reeves Counties, Texas. University of Texas, Austin, Master's thesis, 60p.

- Hentz, T.F., Price, J.G., and Gutierrez, N.G. (1989). Geologic occurrence and regional assessment of evaporite-hosted native sulfur, Trans-Pecos, Texas. The University of Texas at Austin, Bureau of Economic Geology, Report of Investigations No. 184, 70p.
- Hills, J.M. (1972). Late Paleozoic sedimentation in West Texas Permian Basin. American Association of Petroleum Geologists Bulletin, v. 56, p.2303-2322.
- Holser, W.T. (1979). Mineralogy of evaporites, *in* Burns, R.G., ed., Marine minerals. Mineralogical Society of America Short Course Notes, v. 6, p.211-286.
- King, P.B. (1930). The geology of Glass Mountains, Texas, part 1, descriptive geology. Austin, University of Texas Bulletin 3038, 167p.
- King, P.B. (1942). Permian of West Texas and Southeastern New Mexico. American Association of Petroleum Geologists Bulletin, v. 26, p.535-763.
- Kroenlein, G.A. (1939). Salt, potash, and anhydrite in Castile Formation of southeast New Mexico. American Association of Petroleum Geologists Bulletin, v. 23, p.1682-1693.
- Lang, W.B. (1935). Upper Permian formation of Delaware Basin of Texas and New Mexico. American Association of Petroleum Geologists Bulletin, v. 19, p.262-270.
- LaFave, J.I. (1987). Groundwater flow delineation in the Toyah Basin of Trans-Pecos Texas. Unpublished Masters Thesis, University of Texas at Austin, 159p.
- LaFave, J.I., Sharp, J.M., Jr. (1987). Origins of groundwater discharging at the springs of Balmorhea. West Texas Geological Society Bulletin, v. 26, p.5-14.
- McDonald, M.G., Harbaugh, A.W. (1988). A modular three-dimensional finite-difference ground-water flow model. U.S.G.S. Open-File Report 88-875.

- McGowen, J.H., Granata, G.E., and Seni, S.J. (1979). Depositional framework of the Lower Dockum Group (Triassic), Texas Panhandle. The University of Texas at Austin, Bureau of Economic Geology Report of Investigations No. 97, 60p.
- McNeal, R.P. (1965). Hydrodynamics of the Permian Basin, *in* Young, A. and Galley, J.E., eds., Fluids in subsurface environments. American Association of Petroleum Geologists Memoir 4, p.308-326.
- McNeal, R.P., Hemenway, G.A. (1972). Geology of Fort Stockton sulphur mine, Pecos County, Texas. American Association of Petroleum Geologists Bulletin, v. 56, p.26-37.
- Mear, C.E., Yarbrough, D.V. (1961). Yates Formation in southern Permian Basin of West Texas. American Association of Petroleum Geologists Bulletin, v. 45, p.1545-1556.
- Page, L.R., Adams, J.E. (1940). Stratigraphy, eastern Midland Basin, Texas. American Association of Petroleum Geologists Bulletin, v. 24, p.52-64.
- Plummer, L.N., Prestemon, E.C., and Parkhurst, D.L. (1991). An interactive code (NETPATH) for modeling net geochemical reactions along a flowpath. U.S. Geological Survey Water Resources Investigation Report 91-4078, 227p.
- Rees, R.W., Buckner, A.W. (1980). Occurrence and quality of water in the Edwards-Trinity (Plateau) aquifer in the Trans-Pecos region of Texas. Texas Department of Water Resources, R255, 40p.
- Rees, R.W. (1987). Records of wells, water levels, pumpage, and chemical analyses from selected wells in parts of the Trans-Pecos region, Texas, 1968-1980. Texas Water Development Board, R301, 256p.
- Richardson, G.B. (1904). Report of a reconnaissance in Trans-Pecos Texas north of the Texas and Pacific railway. University of Texas, Austin, Bull. 23, 119p.
- Rives, J.L. (1980). Soil survey of Pecos County, Texas. United States Department of Agriculture, Soil Conservation Service, 97p.

- Richey, S.F., Wells, J.G., and Stephens, K.T. (1985) Geohydrology of the Delaware Basin and vicinity, Texas and New Mexico. U.S. Geological Survey Water Resources Investigations, Report 84-4077, 99p.
- Siegel, M.D., Anderholm, S. (1994). Geochemical evolution of groundwater in the Culebra Dolomite near the Waste Isolation Pilot Plant, southeastern New Mexico, USA. *Geochimica et Cosmochimica Acta*, Vol. 58, No. 10, p. 2299-2323.
- Small, T.A., Ozuna G.B. (1993). Ground-water conditions in Pecos County, Texas. USGS Water-Resources Investigations, Report 92-4190, 63p.
- Snider, H.I. (1966). Stratigraphy and associated tectonics of the Upper Permian Castile-Salado-Rustler evaporite complex, West Texas and southeastern New Mexico. The University of New Mexico, Ph.D. dissertation, 196p.
- Tait, D.B., Ahlen, J.L., Gordon, A., Scott G.L., Motts, W.S., and Spitler, M.E. (1962). Artesia Group of New Mexico and Texas. *American Association of Petroleum Geologists Bulletin*, v. 46, p.504-517.
- Tunnell, B.S. (1952). Geology of Antelope area, Culberson and Reeves Counties, Texas. University of Texas, Austin, Master's thesis, 54p.
- Veni G. (1991). Delineation and preliminary hydrogeologic investigation of the Diamond Y Spring, Pecos County, Texas. Unpublished report, George Veni & Associates, San Antonio, Texas, 111p.
- Whittemore, D.O, Basel, C.L, Galle, O.K., and Vaugh, T.C. (1981). Geochemical identification of saltwater sources in the Smoky Hill River Valley, McPherson, Saline, and Dickinson Counties, Kansas, Lawrence. University of Kansas, Kansas Geological Survey, 78p.
- Whittemore, D.O, Pollock, L.M. (1979). Determination of salinity sources in water resources of Kansas by minor alkali metal and halide chemistry. Contribution No. 208, Manhattan, Kansas, Kansas Water Research Institute, 28p.

## APPENDIX

1) Analyses of water from wells and springs in Pecos County sampled during 1994 and 1995. Ion concentrations are reported in mg/L, temperature measurements in degrees Celsius.

Well	Date	Temp.	pH	Na	Ca	Mg	Sr	Si	Ba	Co	Cr	Fe	Ni	Pb
DY-1	Dec-94	19.1	6.68	876.3	447.0	224.3	9.3	12.3	0.0	0.3	0.2	0.0	0.2	0.5
DY-1	Mar-95	20.5	7.85	906.7	459.4	232.2	9.6	11.8	0.0	0.3	0.2	0.1	0.2	0.6
DY-1	Jun-95	26.8	7.01	899.5	459.3	233.4	9.2	11.4	0.0	0.1	0.1	0.1	0.1	0.2
DY-2	Mar-95	15.0	7.85	1982.0	613.7	453.9	16.1	15.0	0.1	0.4	0.3	0.2	0.3	0.7
DY-2	Jun-95	22.4	7.68	2131.0	609.4	451.8	14.8	13.7	0.0	0.1	0.1	0.1	0.1	0.2
DY-3	Dec-94	20.8	6.64	1275.0	513.0	286.4	11.7	16.1	0.0	0.3	0.2	0.1	0.3	0.5
DY-3	Mar-95	18.6	6.98	1254.0	505.1	283.8	11.4	14.8	0.0	0.3	0.2	0.1	0.2	0.6
DY-3	Jun-95	29.2	6.96	1292.0	496.9	284.2	10.7	14.4	0.0	0.1	0.1	0.1	0.1	0.2
DY-4	Dec-94	18.4	6.78	1024.0	464.6	228.3	9.6	12.4	0.0	0.3	0.2	0.1	0.3	0.5
DY-4	Mar-95	18.4	6.85	1059.0	472.2	234.9	9.8	12.6	0.0	0.3	0.2	0.1	0.3	0.5
DY-5	Dec-94	19.0	6.65	2094.0	690.2	451.8	18.9	19.1	0.0	0.4	0.3	0.1	0.3	0.7
DY-5	Mar-95	18.5	6.74	2022.0	663.7	435.2	18.1	18.3	0.1	0.4	0.3	0.2	0.3	0.7
DY-5	Jun-95	29.0	7.50	2191.0	656.0	448.5	16.6	11.8	0.0	0.1	0.1	0.2	0.1	0.2
DY-6	Dec-94	19.6	6.77	1580.0	557.6	339.8	13.9	15.5	0.0	0.3	0.3	0.1	0.3	0.6
DY-6	Mar-95	20.1	6.78	1611.0	573.0	348.3	14.2	14.1	0.0	0.4	0.3	0.1	0.3	0.5
DY-6	Jun-95	28.4	6.96	1627.0	550.0	340.8	12.8	13.5	0.0	0.1	0.1	0.1	0.1	0.1
DY-7	Mar-95	12.1	8.21	1297.0	637.9	419.9	16.8	10.9	0.0	0.4	0.3	0.1	0.3	0.6
DY-7	Jun-95	29.7	7.95	2019.0	632.8	429.0	15.7	8.3	0.0	0.1	0.1	0.1	0.1	0.1
Calhoun	Dec-94	20.7	6.86	394.9	331.6	104.7	8.8	12.9	0.0	0.2	0.0	0.0	0.0	0.4
Calhoun	Jun-95	30.9	7.04	510.7	377.1	132.7	9.0	10.8	0.0	0.0	0.0	0.1	0.1	0.1
Church	Dec-94	21.0	6.74	805.9	557.0	174.2	14.1	12.4	0.0	0.3	0.1	0.0	0.2	0.7
Church	Jun-95	29.3	6.98	780.2	498.3	161.6	12.0	9.3	0.0	0.1	0.0	0.0	0.1	0.1
Ed Sullivan	Dec-94	20.0	6.54	636.0	391.9	146.2	7.7	11.8	0.0	0.3	0.1	0.0	0.2	0.6
Gomez #2	Dec-94	20.9	6.96	332.8	192.1	71.1	4.0	6.1	0.0	0.2	0.0	0.0	0.1	0.4
Jimmy	Dec-94	21.3	7.17	208.9	135.5	37.2	2.5	5.7	0.0	0.1	0.0	0.0	0.0	0.3
Jimmy	Jun-95	24.0	7.31	275.4	125.9	34.5	2.3	5.1	0.0	0.0	0.0	0.1	0.0	0.1
Menendez	Dec-94	22.0	7.09	181.4	130.3	37.6	2.7	5.4	0.0	0.1	0.0	0.0	0.0	0.2
Menendez	Jun-95	28.5	7.41	271.2	118.6	34.7	2.4	5.0	0.0	0.0	0.0	0.5	0.0	0.1
Tytex1	Dec-94	22.5	7.19	148.4	113.9	42.9	2.8	4.4	0.0	0.1	0.0	0.0	0.0	0.3
Tytex1	Jun-95	22.0	7.57	258.7	107.3	40.8	2.3	3.7	0.0	0.0	0.0	0.1	0.0	0.0
45-57-901	Dec-94	22.2	6.93	232.6	158.5	55.6	3.3	4.8	0.0	0.1	0.0	0.0	0.0	0.3
52-01-206	Dec-94	20.6	7.01	200.4	142.9	44.7	2.9	4.8	0.0	0.1	0.0	0.0	0.0	0.3
53-01-103	Dec-94	21.6	7.01	176.3	137.4	44.8	3.1	4.9	0.0	0.1	0.0	0.0	0.0	0.2
53-01-208	Dec-94	22.2	6.78	332.3	193.6	70.7	4.0	6.1	0.0	0.2	0.0	0.0	0.1	0.3
53-01-402	Dec-94	20.3	6.95	422.2	264.0	104.8	5.2	5.6	0.0	0.2	0.1	0.0	0.1	0.4
Balmorhea	Mar-95			534.6	169.0	91.6	3.8	7.5	0.0	0.2	0.1	0.0	0.2	0.3
Belding 25	Jun-95			255.1	184.5	49.8	2.7	9.0	0.0	0.1	0.0	0.1	0.0	0.2
Belding 26	Jun-95			247.8	194.2	50.7	2.5	8.4	0.0	0.0	0.0	0.3	0.0	0.2
CW #1	Jun-95	26.9	7.29	307.5	156.0	54.0	2.4	9.7	0.0	0.0	0.0	0.0	0.0	0.1
CW #5	Jun-95	26.4	7.21	271.6	144.6	50.6	2.2	9.4	0.0	0.0	0.0	0.0	0.0	0.1
CW #6	Jun-95	26.7	7.35	296.1	133.7	45.8	2.0	9.7	0.0	0.0	0.0	0.0	0.0	0.1
CW #902	Jun-95	29.2	7.17	451.7	307.6	118.5	6.3	9.4	0.0	0.0	0.0	0.2	0.0	0.1
45-57-602	Jun-95	23.9	7.37	306.7	137.5	46.0	2.5	4.4	0.0	0.0	0.0	0.1	0.0	0.0
53-01-203	Jun-95			348.1	603.0	219.6	9.6	5.5	0.0	0.0	0.1	0.2	0.1	0.1
53-102-205	Jun-95	23.4	7.51	309.3	136.4	43.3	2.4	4.3	0.0	0.0	0.0	0.1	0.0	0.0

Well	Date	Zn	F	Cl	NO2	Br	NO3	HPO4	SO4	HCO3	TDS
DY-1	Dec-94	0.0	0.0	1250.0	0.0	4.3	36.2	0.2	1845.3	294.6	2272.0
DY-1	Mar-95	0.0	0.0	1255.9	0.0	1.8	28.8	0.3	1880.6	301.7	3340.8
DY-1	Jun-95	0.0	0.0	1262.9	0.0	3.4	29.5	0.3	1912.9	351.5	4102.4
DY-2	Mar-95	0.0	0.2	3136.0	0.2	6.1	15.8	0.8	3283.7	391.5	4883.2
DY-2	Jun-95	0.0	0.2	3200.6	0.2	6.2	5.8	0.8	3395.2	463.8	6592.0
DY-3	Dec-94	0.0	0.0	1714.9	0.0	3.5	8.0	0.3	2446.0	292.9	2956.8
DY-3	Mar-95	0.0	0.1	1657.0	0.1	4.1	0.1	0.4	2479.7	304.4	3411.2
DY-3	Jun-95	0.0	3.1	1713.6	0.1	3.7	13.0	0.5	2477.9	334.4	5363.2
DY-4	Dec-94	0.0	0.0	1403.1	0.0	8.2	39.5	0.3	2084.5	296.1	2240.0
DY-4	Mar-95	0.0	0.1	1455.8	0.1	4.3	43.7	0.4	2148.3	288.7	3353.6
DY-5	Dec-94	0.0	0.2	3414.6	0.2	9.0	0.2	0.8	3466.6	266.3	9300.0
DY-5	Mar-95	0.0	0.2	3425.2	0.2	10.0	0.2	0.8	3407.9	265.8	5075.2
DY-5	Jun-95	0.0	4.8	3734.9	0.2	4.8	6.2	0.8	4089.9	261.2	3507.2
DY-6	Dec-94	0.0	0.1	2676.3	0.1	6.9	28.9	0.5	2665.8	285.1	5696.0
DY-6	Mar-95	0.0	0.1	2638.7	0.1	6.4	47.3	0.5	2594.9	304.9	2956.8
DY-6	Jun-95	0.0	0.2	2633.7	0.2	3.1	42.6	0.6	2782.5	319.7	4019.2
DY-7	Mar-95	0.0	0.2	3394.1	0.2	0.3	0.2	0.8	3151.0	243.8	5708.8
DY-7	Jun-95	0.0	2.5	3384.3	0.2	4.6	2.4	0.8	3188.4	256.3	7205.1
Calhoun	Dec-94	0.1	0.0	476.0	0.0	1.4	48.9	0.0	1069.3	251.1	3200.0
Calhoun	Jun-95	0.0	0.0	696.8	0.0	1.4	61.0	0.2	1209.9	268.3	2720.0
Church	Dec-94	0.0	0.0	1340.8	0.0	0.0	41.0	0.2	1434.9	251.1	1561.6
Church	Jun-95	0.0	0.0	1356.7	0.0	1.2	30.2	0.3	1331.6	280.5	3884.8
Ed Sullivan	Dec-94	1.2	0.0	939.3	0.0	0.3	27.3	0.2	1210.3	336.3	608.0
Gomez #2	Dec-94	0.0	1.6	524.1	0.0	0.7	4.4	0.2	521.0	267.7	2880.0
Jimmy	Dec-94	0.3	1.4	288.7	0.0	0.3	0.0	0.0	294.5	234.0	960.0
Jimmy	Jun-95	0.0	0.5	315.4	0.0	0.6	1.0	0.2	287.3	256.2	
Menendez	Dec-94	0.0	1.6	276.9	0.0	0.0	0.0	0.0	276.4	237.9	953.6
Menendez	Jun-95	0.0	2.3	306.4	0.0	0.0	1605.7	1.6	267.8	261.1	2411.0
Tytex1	Dec-94	1.0	1.3	258.8	0.0	0.1	0.0	0.0	215.3	227.7	787.2
Tytex1	Jun-95	0.0	0.0	288.8	0.0	0.3	1.8	0.0	253.4	239.9	710.4
45-57-901	Dec-94	0.0	0.0	365.0	0.0	0.7	0.0	0.0	366.5	232.3	1600.0
52-01-206	Dec-94	0.0	0.0	315.5	0.0	0.0	0.0	0.0	315.1	217.4	
53-01-103	Dec-94	0.0	1.3	302.6	0.0	0.5	0.0	0.0	284.4	266.7	1088.0
53-01-208	Dec-94	0.0	1.0	531.7	0.0	0.5	8.9	0.2	513.6	264.8	1152.0
53-01-402	Dec-94	0.0	0.0	602.2	0.0	0.9	0.0	0.2	857.8	219.1	691.2
Balmoreha	Mar-95	0.0	0.0	726.5	0.0	0.0	0.0	0.2	704.5		
Belding 25	Jun-95	0.0	1.2	357.0	0.0	0.2	0.0	0.0	501.5		
Belding 26	Jun-95	0.0	0.0	331.4	0.0	0.4	0.8	0.0	491.6		
CW #1	Jun-95	0.3	0.8	423.6	0.2	0.4	2.2	0.2	410.9	344.1	1817.6
CW #5	Jun-95	0.0	0.4	388.7	0.0	0.3	5.6	0.2	375.5	266.0	1414.4
CW #6	Jun-95	0.0	0.8	390.0	0.0	0.3	1.8	0.2	380.1	280.6	1664.0
CW #902	Jun-95	0.0	0.0	620.7	0.3	0.6	25.7	0.2	983.8	290.4	2387.2
45-57-602	Jun-95	0.0	4.9	363.6	0.0	0.8	0.4	0.2	327.1	260.6	
53-01-203	Jun-95	0.0	0.0	359.2	0.0	0.0	0.0	0.2	2067.0		
53-102-205	Jun-95	0.0	1.1	350.5	0.3	0.4	1.7	0.2	318.3	500.7	

2) Historical discharge at the Comanche Springs (in ft<sup>3</sup>/s) and rainfall totals (in inches) by water years. Data are from Brune (1975) and from the archives of the Annie Riggs Museum, Fort Stockton.

Water Years	Discharge	Rainfall	Water Years	Discharge	Rainfall
1899	66.0		1943	43.0	13.81
1904	64.0	15.97	1944	43.0	15.18
1919	45.0	20.09	1945	43.0	14.55
1922	46.0	12.18	1946	44.0	14.05
1923	42.0	18.83	1947	42.0	8.97
1924	47.0		1948	37.0	6.38
1925	49.0	20.43	1949	38.0	16.85
1932	42.0	24.61	1950	34.0	12.10
1933	47.0	14.35	1951	27.0	7.20
1934	46.0	6.87	1952	26.0	11.50
1935	44.0	10.12	1953	20.0	5.60
1936	42.0	12.75	1954	26.0	7.98
1937	44.0	17.76	1955	17.0	7.98
1938	43.0	13.69	1956	13.0	4.70
1939	42.0	11.52	1957	4.0	14.38
1940	42.0	16.16	1958	1.8	17.28
1941	43.0	29.29	1959	0.8	11.75
1942	44.0	8.69	1961	1.5	11.48
			1962	0.0	9.63

3) Stable isotope composition of water from wells and springs in Pecos County. Samples taken during 1994 and 1995. Values are reported relative to SMOW.

Sample	$\delta^{18}\text{O}$	$\delta^2\text{H}$
DY-1	-6.9	-42
DY-2	-5.3	-39
DY-3	-6.3	-44
DY-5	-6.1	-41
DY-6	-6.5	-45
DY-7	-3.9	-30
5301908	-8.2	-51
5216904	-7.3	-51
5216612	-7.7	-49
5216613	-7.8	-49
5301203	-7.7	-50

4) NETPATH output files showing the chosen model for each run

Initial Well 1 : RUSTLER DILUTE(BELDING 26, JUNE'95)  
 Initial Well 2 : SALINE RUSTLER(4542700, SEP'90)  
 Final well : DY-1(june'95)

	Final	Initial 1	Initial 2
C	6.6372	5.1622	2.1675
NA	39.3311	10.7959	83.3594
CA	11.5196	4.8530	17.1630
CL	35.8085	9.3625	85.4355
MG	9.6505	2.0887	10.3303

EXCHANGE CA -1.0000 NA 2.0000 MG 0.0000  
 CALCITE CA 1.0000 C 1.0000 RS 4.0000 I1 0.0000 I2 0.0000  
 GYPSUM CA 1.0000 S 1.0000 RS 6.0000 I3 22.0000  
 NaCl NA 1.0000 CL 1.0000  
 CO2 GAS C 1.0000 RS 4.0000 I1 -25.0000 I2 100.0000  
 DOLOMITE CA 1.0000 MG 1.0000 C 2.0000 RS 8.0000 I1 0.0000  
 I2 0.0000  
 POLYHALI K 2.0000 MG 1.0000 CA 2.0000

35 models checked  
 8 models found

MODEL 2

Init 1 + F	0.53107
Init 2 + F	0.46893
EXCHANGE	2.32132
NaCl	0.00000
CO2 GAS	-7.77797
DOLOMITE +	6.18374
Dilution factor:	1.258 1.258kg H2O remain

Initial Well 1 : RUSTLER DILUTE(BELDING 26, JUNE'  
 Initial Well 2 : SALINE RUSTLER(4542700,SEP'90)  
 Final well : DY-6(JUNE'95)

	Final	Initial 1	Initial 2
C	6.0721	5.1622	2.1675
NA	71.3678	10.7959	83.3594
CA	13.8384	4.8530	17.1630
CL	74.9141	9.3625	85.4355
MG	14.1361	2.0887	10.3303

EXCHANGE CA -1.0000 NA 2.0000 MG 0.0000  
 CALCITE CA 1.0000 C 1.0000 RS 4.0000 I1 0.0000 I2 0.0000  
 GYPSUM CA 1.0000 S 1.0000 RS 6.0000 I3 22.0000  
 NaCl NA 1.0000 CL 1.0000  
 CO2 GAS C 1.0000 RS 4.0000 I1 -25.0000 I2 100.0000  
 DOLOMITE CA 1.0000 MG 1.0000 C 2.0000 RS 8.0000 I1 0.0000  
 I2 0.0000  
 POLYHALI K 2.0000 MG 1.0000 CA 2.0000

35 models checked  
3 models found

MODEL 3

Init 1 +F 0.13831  
Init 2 +F 0.86169  
EXCHANGE - 0.97776  
CO2 GAS - -21.49167  
DOLOMITE + 12.49102  
POLYHALI -7.54542

Initial Well : DY-6(JUNE'95)  
Final Well : DY-7(JUNE'95)

	Final	Initial
C	4.0814	6.0721
MG	17.8228	14.1361
NA	88.7037	71.3678
CA	15.9470	13.8384
CL	96.4176	74.9141

EXCHANGE CA -1.0000 NA 2.0000 MG 0.0000  
CALCITE CA 1.0000 C 1.0000 RS 4.0000 I1 0.0000 I2 0.0000  
GYPSUM CA 1.0000 S 1.0000 RS 6.0000 I3 22.0000  
NaCl NA 1.0000 CL 1.0000  
CO2 GAS C 1.0000 RS 4.0000 I1 -25.0000 I2 100.0000  
POLYHALI K 2.0000 MG 1.0000 CA 2.0000

15 models checked  
12 models found

MODEL 5

EXCHANGE -1.22364  
CALCITE -2.09525  
CO2 GAS -0.80568  
POLYHALI -0.28817  
Evaporation factor: 1.287 776.975g H2O remain

Initial Well : DY-1(june'95)  
Final Well : DY-3(JUNE'95)

	Final	Initial
C	6.3682	6.6372
MG	11.7679	9.6505
NA	56.5750	39.3311
CA	12.4807	11.5196
CL	48.6579	35.8085

EXCHANGE CA -1.0000 NA 2.0000 MG 0.0000  
CALCITE CA 1.0000 C 1.0000 RS 4.0000 I1 0.0000 I2 0.0000  
DOLOMITE CA 1.0000 MG 1.0000 C 2.0000 RS 8.0000 I1 0.0000  
I2 0.0000  
GYPSUM CA 1.0000 S 1.0000 RS 6.0000 I3 22.0000  
NaCl NA 1.0000 CL 1.0000  
CO2 GAS C 1.0000 RS 4.0000 I1 -25.0000 I2 100.0000

15 models checked  
12 models found

MODEL 4  
EXCHANGE 1.48496  
CALCITE -1.41486  
GYPSUM 1.61518  
NaCl 4.09430  
Evaporation factor: 1.219 820.067g H2O remain

The vita has been removed from the digitized version of this document.